WATER SOLUBLE CALIXARENES, CALIXPYRROLES AND RESORCINARENES

Master's thesis
University of Jyväskylä
Department of Chemistry
22.4.2023
Julia Naulapää

Abstract

Calixarenes, resorcinarenes and calixpyrroles are macrocyclic molecules that can act as a host for various guests, from ions to more complex and biologically active compounds. Water-solubilizing these molecules is important since aqueous environments are a significant research subject.

The literature review of this master's thesis concerns the water-solubilization of tetrameric calixarenes, resorcinarenes and calixpyrroles. The synthesis, properties, and applications of selected molecules are discussed.

In the experimental part the aim was to synthesize potentially water-soluble calix[4]pyrroles. The calixpyrroles bear polyethylene glycol -functionalizations, which resulted in the partial water-solubility of one of the compounds. The synthesized compounds were used in co-micellization with the surfactants Triton X-100 and Triton X-114. Properties of the micelles (hydrodynamic diameter, morphology, and cloud point phenomenon) were investigated.

Tiivistelmä

Kaliksareenit, resorsinareenit ja kalikspyrrolit ovat makrosyklisiä isäntämolekyylejä, jotka voivat sitoa kemiallisia vieraita sisäänsä. Vieraat voivat olla yksinkertaisia ioneja tai monimutkaisempia, biologisesti aktiivisia molekyylejä. On tärkeää syntetisoida vesiliukoisia isäntämolekyylejä, sillä vesiympäristöt ovat merkittäviä sovellutuskohteita useilla tutkimusaloilla.

Tämä *pro gradu* käsittelee kirjallisuusosiossaan vesiliukoisten tetrameeristen kaliksareenien, resorsinareenien ja kalikspyrroleiden syntetisointia. Tutkielma käsittelee synteesien lisäksi valikoitujen isäntämolekyylien ominaisuuksia ja mahdollisia sovellutuksia.

Kokeellisessa osassa esitellään mahdollisesti vesiliukoisten kaliksareenien synteesiä. Kalikspyrroleihin lisätiin polyetyleeniglykolihäntiä, mikä johti yhden isäntämolekyylin osittaiseen vesiliukoisuuteen. Synteesituotteita käytettiin yhdessä tensidien Triton X-100 ja Triton X-114 kanssa misellien muodostukseen. Misellien ominaisuuksia, kuten hydrodynaamista halkaisijaa ja samepisteominaisuutta tutkittiin.

Foreword

This master's thesis was done in the University of Jyväskylä, chemistry department. Experimental work was conducted in the Nanoscience center of the University, between 9.5.2022-9.10.2022. The thesis was written until the end of March 2023. The idea for the thesis began from interest in water-soluble calixpyrroles, but due to limitation in the amount of previous research the thesis was expanded into calixarenes and resorcinarenes. The literature was searched via JykDok, Google Scholar and Reaxys.

The work was instructed by Dr. Kaisa Helttunen and MSc. Malgorzata Pamula, to whom I owe my greatest thanks. I have worked in the Helttunen group (in addition to this thesis) for my bachelor's and as a research assistant. The group has given me invaluable opportunities through the years to form as a scientist and has helped me form my thinking and working skills.

In addition to the Helttunen group, I'd like to thank MSc. Johanna Schirmer for helping with the AFM, Dr. Kosti Tapio for instruction on DLS, Dr. Anniina Kiesilä for measuring mass spectra and MSc. Esa Haapaniemi for measuring NMR spectra.

Writing this thesis has been a long yet rewarding process. As with my bachelor's thesis, my partner and friends have been a great help. They grounded me and cheered me on when things seemed complicated. Writing this thesis in the library with friends around has been the best part about this, and the support network I had during writing was awesome.

Table of contents

Abstract iii

Tiivistelmä iv

Foreword v

Table of contents vi

Abbreviations viii

LITERATURE PART 1

1 Introduction 1

1.1 Calixarenes and resorcinarenes 2

1.2 Calixpyrroles 4

2 Synthesis of calixarenes and resorcinarenes 5

2.1 Synthesis of calixarenes 5

2.2 Synthesis of resorcinarenes 7

3 Synthesis of calixpyrroles 9

4 Supramolecular chemistry of macrocyclic hosts 10

5 Host-guest systems in water 13

5.1 Solubilization of C4As and resorcinarenes and their applications 13

5.2 Solubilization of C4Ps and their applications 31

6 Conclusions 39

EXPERIMENTAL PART 42

1 Introduction and aim of work 42

2 Materials and instrumental methods 45

2.1 Reagents, solvents, and instruments used 45

2.2 Micelle solution preparations 46

2.3 Cloud point method, DLS measurements and AFM sample preparation 47

3 Synthetic methods and reaction schemes 48

4 Syntheses 50

4.1 Four-walled *αααα*-4-hydroxyphenyl-C4P, 1^{63} 50

4.2 mPEG4-Ts, 5[65] 53
4.3 mPEG4-ylated C4P, 2 55
4.3.1 First synthesis 55
4.3.2 Second synthesis 56
4.4 PEGylated C4P, 3 58
4.5 mPEG2-ylated C4P, 4 60
4.6 mPEG2-ylated two-armed C4P, 6 60
4.6.1 In dimethyl formamide 60
4.6.2 In acetonitrile 61
5 Cloud point observations 62
6 DLS measurements 64
7 Atomic force microscopy 68
8 Conclusions 70
8.1 Syntheses 70
8.2 Cloud point and micelle studies 71
9 References 73
10 Appendices 80

Abbreviations

Ad-Vio	*N*-methyl-*N*'-adamantane carbomethyl-4,4'-dipyridinium
AFM	atomic force microscopy
C4A	calix[4]arene
C4P	calix[4]pyrrole
CD	cyclodextrin
CPC	cetylpyridinium chloride
CTAB	cetyltrimethylammonium bromide
DLS	dynamic light scattering
DMSO-d6	deuterated dimethyl sulfoxide
DOX	Doxorubicin
ESI-MS	electrospray-ionization mass spectrometry
IR	infrared
ITC	isothermal calorimetry
MeOD	deuterated methanol
mPEG2/4	polyethylene glycol monomethyl ether
NMR	nuclear magnetic resonance
PDI	polydispersity index
PEG	polyethylene glycol
SEM	scanning electron microscopy
TBA	tetrabutyl ammonium
TEM	transmission electron microscopy
UV-vis titration	ultraviolet-visible light titration

LITERATURE PART

1 Introduction

Macrocycles are cyclic molecules that are formed by at least 12 atoms, which can either be carbon or heteroatoms like oxygen.[1] Calixarenes, calixpyrroles and resorcinarenes are the result of condensation reactions of phenol, resorcinol, and pyrrole, respectively. The condensation reactions between phenolic compounds and aldehydes that create calixarenes and resorcinarenes (Figure 1) were discovered by Adolf von Baeyer in 1872.[2,3] In 1886, he reported a similar condensation reaction between pyrrole and acetone which created calixpyrroles (Figure 1).[4] The compounds were of no significant interest for a long time until the ion and molecule binding abilities of calixarenes were revealed in the 1970s by Gutsche.[5a]

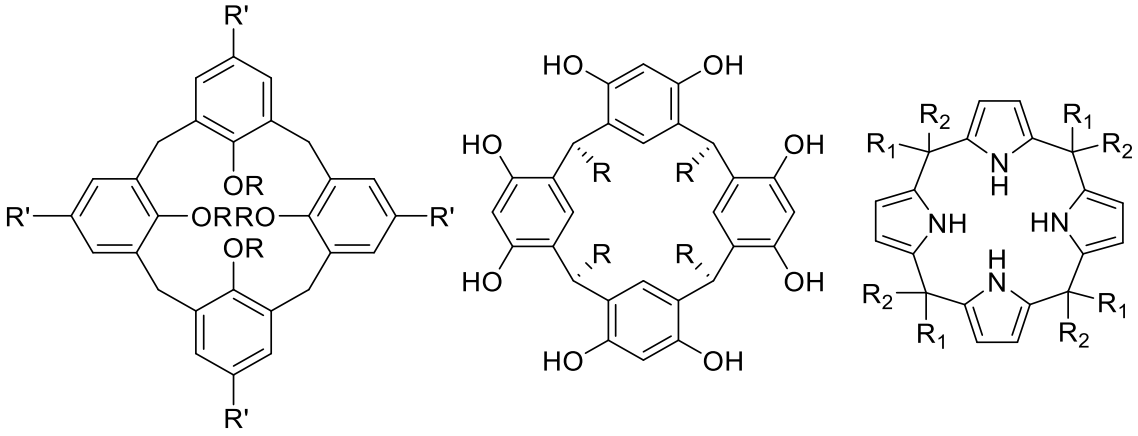

Figure 1. The general structures of tetrameric calixarenes (left), resorcinarenes (middle) and calixpyrroles (right).

All three of these compounds can form supramolecular complexes with suitable guests in solution through the formation of weak bonds like hydrogen bonds or π-ion-interactions. This can be exploited in the controlled transfer of the guest, for example in the selective extraction of a desired analyte[6] or the transport of a drug to the site that needs it[7]. The formation of the assemblies is a phenomenon which depends on the properties of the host, like its functionalization. A host can be fine-tuned to become more selective towards a specific guest. For example, inserting additional positively charged groups onto the cavity of a calixpyrrole can make it more selective towards the pyrophosphate anion.[8]

The solvent the host-guest-complex formation happens has a big effect on the binding. In this thesis, the focus is on the aqueous environment. Water environments are immensely important in research and applications, as biological life almost exclusively happens in the aquatic phase. None of the classes of molecules (calixarenes, resorcinarenes of calixpyrroles) are inherently water-soluble, so special functionalizations must take place in order to solubilize them. Binding guests in the aquatic phase is also difficult due to the binding sites of both the host and its guests being solvated by the water molecules. These are the difficulties that must be overcome to achieve reliable host-guest chemistry in water.

This thesis concerns the synthesis and applications of water-soluble calixarenes, calixpyrroles and resorcinarenes through the years. Of these macrocycles, only the tetramers of each of the compounds are considered. The general syntheses of the calixpyrroles, calixarenes and resorcinarenes will be introduced in addition to their host-guest chemistry.

After the outlining of the molecules the different efforts to solubilize them in water in a variety of methods are considered. The methods range from the choice of reagents in the synthesis of the macrocycles to functionalization post-cyclization. The co-micellization of some compounds of interest with amphiphiles is also considered. The possible applications of the successfully solubilized molecules are simultaneously discussed.

1.1 Calixarenes and resorcinarenes

Calixarenes are a class of macrocycles comprised of phenolic units connected by alkyl bridges. Often the *para*-positions on the subunits are functionalized. The tetrameric calix[4]arene (C4A) can exist in different conformers depending on the direction the *p*-R-groups point in. They are known as cone, partial cone, 1,2-alternate and 1,3-alternate (Figure 2). At first it was thought that the different conformers were not interchangeable after synthesis. Later NMR-studies revealed that in a solvated state the OH-group can move through the annulus (the hole in the middle of the tetramer) resulting in a change in conformation.[9] In the cone conformation, the R-groups of the calixarene are known as the upper rim. The OH- (or OR-) functionalized rim is known as the lower rim.

In general, the cone conformation is the most stable due to formation of stabilizing interactions between the OH-groups. The conformation of C4As is also solvent dependent. In a polar

solvent the molecule favors the cone conformation which is due to the conformation being the most polar.[5a] The functionalization of OH to a bulkier group restricts the conversion between conformers due to steric hindrance, since a larger group cannot move through the annulus.[9]

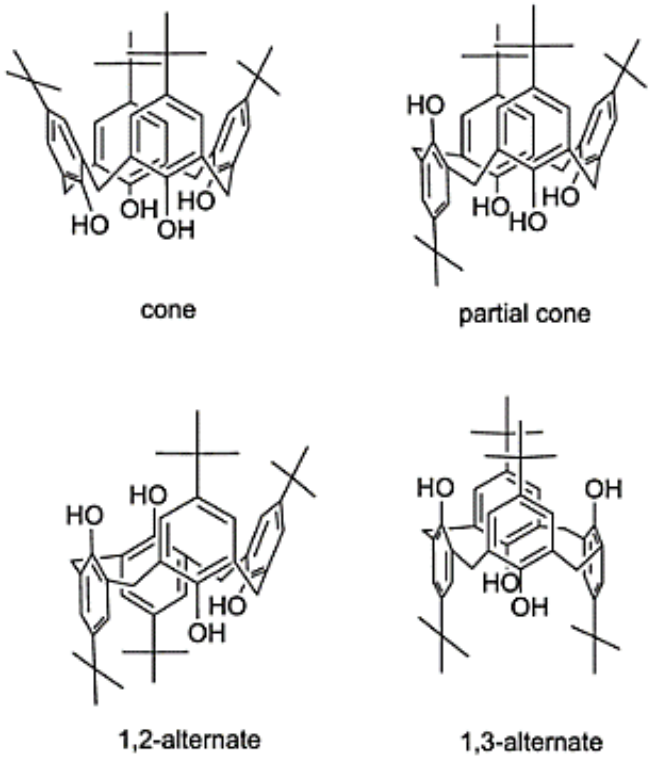

Figure 2. The different conformations of C4As.[10]

C4As can act as hosts for many different classes of molecules, but they are most used in the binding of cationic or partially cationic guests. The guests can be bound to either the upper rim cup or the lower rim. Smaller cations bind to the lower rim via ion-dipole interaction between the OR-groups on the rim, for example when a C4A binds Na^+. Larger cations (like Ag^+) can bind to the upper rim via cation-π-interactions.[5a]

Resorcinarenes are a class of macrocycles that are closely related to calixarenes. They are characterized by an aromatic cavity and two OH- or OR-groups attached to each of the subunits. The tetrameric resorcinarene, which will be in focus in this thesis, can exist in multiple conformations (Figure 3) which differ slightly from C4As in their nomenclature. The boat conformations of the resorcinarene interconvert rapidly in solvated state to give the average conformation of crown.[11] The crown (or cone) conformation of resorcinarenes is stabilized by the interactions between the OH- or OR-groups of the upper rim. It is also the conformation in which resorcinarenes most often exhibit guest-binding.[5b]

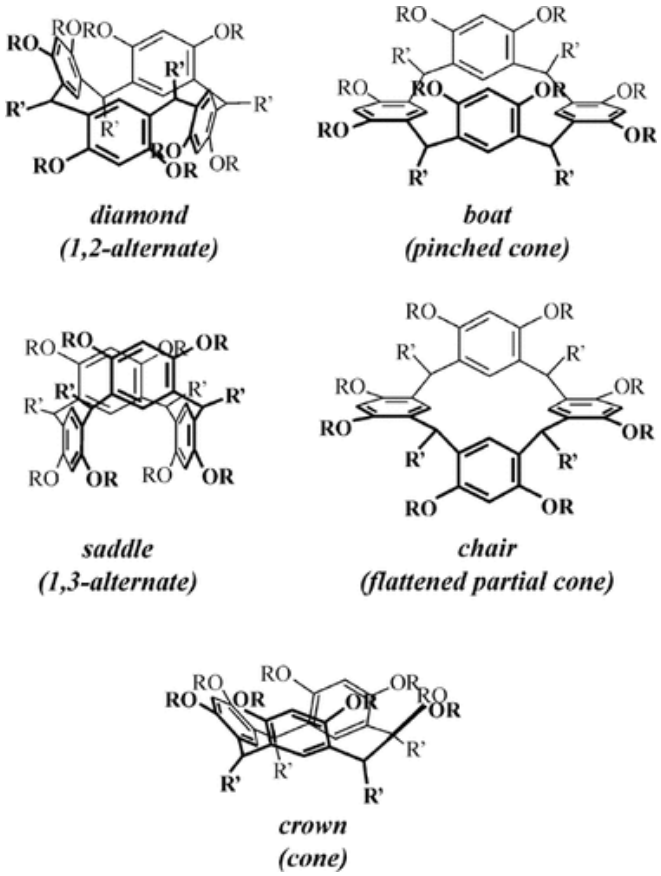

Figure 3. The conformations of resorcinarenes.[11]

1.2 Calixpyrroles

Calix[4]pyrroles (C4Ps) are a class of porphyrinogens, which are comprised of four pyrrole units connected by fully functionalized alkyl bridges.[4] The simplest C4P is the *meso*-octamethylC4P **1** (Figure 4). Like C4As, C4Ps have the different conformations (cone, partial cone, 1,3-alternate and 1,2-alternate) in solution.[12]

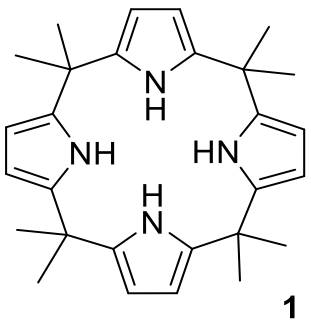

Figure 4. *meso*-octamethylC4P **1**.

As can be seen in Figure 1, C4Ps can have two different substituents in its *meso*-position (R_1 and R_2). These positions can be functionalized by either the choice of the ketone used in the synthesis (see 2.2.1) or by modification post-macrocyclization. The pyrrole-ring can also have substituents in so-called *β*-position (which is on the pyrrole backbone), but this kind of functionalization is not considered in this thesis.[12]

A C4P can have, in addition to different conformations different configurational isomers depending on the stereoisomerism of the groups in the *meso*-positions. These isomers are seen in Figure 5. This isomerism influences the properties of the C4P, namely the solubility and binding properties of the compound.[12]

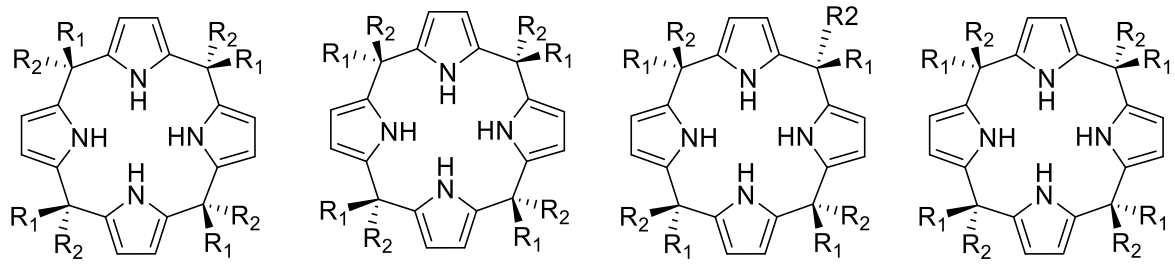

Figure 5. The configurational isomers (from left to right): *αααα*, *ααaβ*, *ααββ* and *αβαβ*.

2 Synthesis of calixarenes and resorcinarenes

2.1 Synthesis of calixarenes

At first, the synthesis of calixarenes was performed by creating a linear precursor, the ends of which would then be joined to form the macrocycle. The method was developed into the more popular fragment condensation. In the synthesis, larger fragments are joined together, the size of which can vary. For example, in Scheme 1 is shown the 2+2 fragment condensation in which two dimers bearing unique functional groups are joined together. The resulting method thus allows each of the units on the upper rim to be functionalized with different groups.[2]

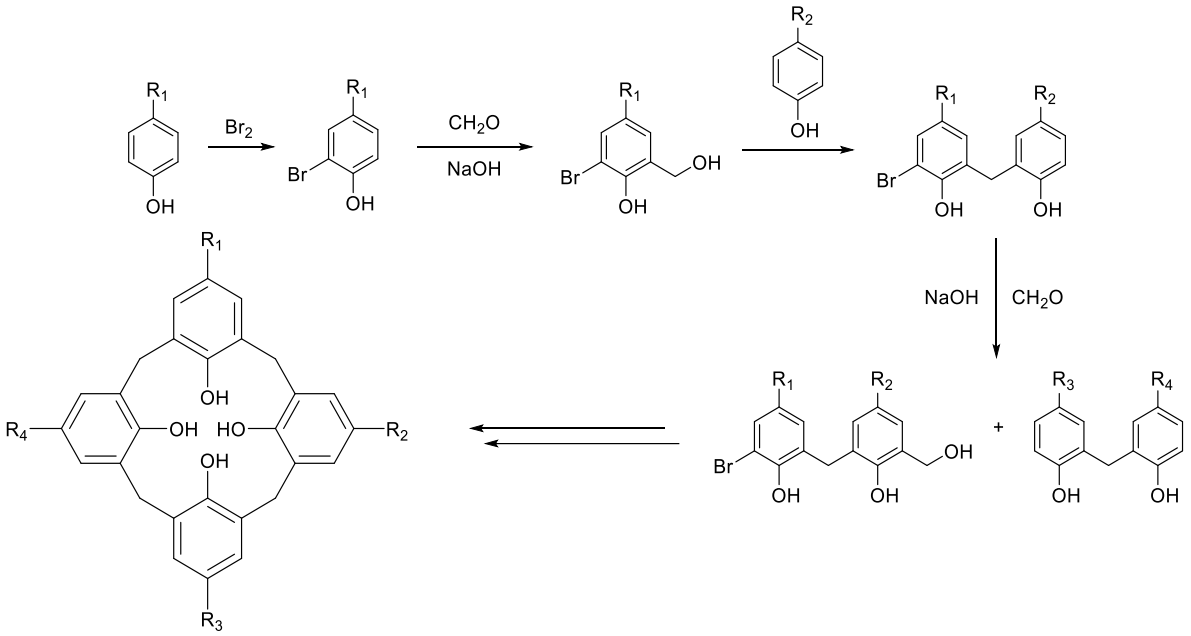

Scheme 1. Synthesis of a general C[4]P via 2+2 fragment condensation.

Calixarenes can also be synthesized in one-pot reactions, which are much simpler but lack the option to individually tune the functionalization on the upper rim. The single-step synthesis can be performed in either acidic or basic conditions. The reaction conditions (choice of solvent and the catalyst in the reaction) in general influence the polymerization and number of monomers in the cycle, and they can be tuned to favor the formation of a specific sized calixarene. This has extensively been done to polymerization of *p-tert*-butylphenyl (Scheme 2, Table 1) to create calixarenes **2a-2e**.[2] The use of formaldehyde as reagent, NaOH as catalyst and diphenyl ether as the solvent are the favorable conditions to synthesize the tetrameric calixarene in fairly high yields (49 %).

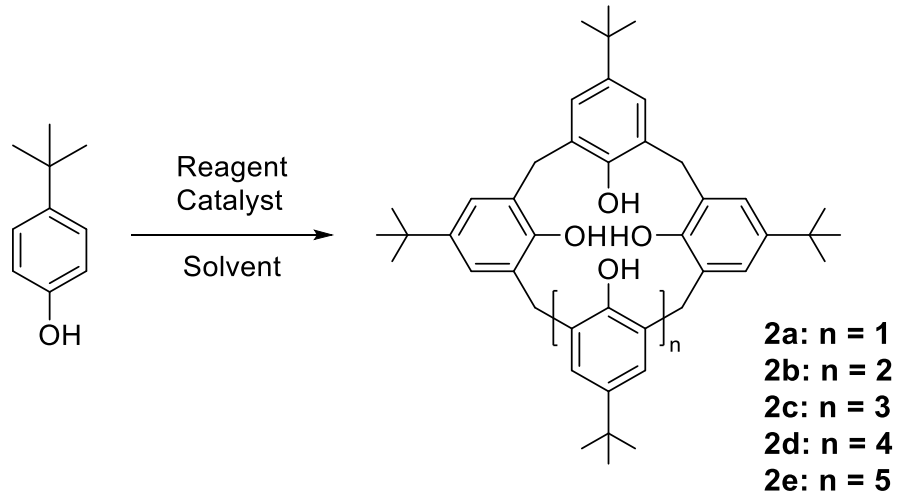

Scheme 2. The synthesis of different sized calixarenes.

Table 1. The effect of solvents, catalysts and reagents on calixarene synthesis

Calixarene	Reagent	Catalyst	Solvent	Yield / %
2a[13]	formaldehyde	NaOH	diphenyl ether	49
2b[14]	formaldehyde	KOH	tetrahydronaphthalene	15 – 20
2c[15]	formaldehyde	KOH	xylene	80 – 85
2d[16]	*s*-trioxane	*p*-TsOH	chloroform	26
2e[17]	formaldehyde	NaOH	xylene	62 – 65

For some applications and functionalizations, a calixarene with no substituents on the upper rim is required. There is no one-pot method to synthesize these kinds of molecules, so dealkylation of *p-tert*-butyl calixarene can be used to achieve it. The *p-tert*-butylcalixarene of the desired size is treated with aluminum(III) chloride, which causes the debutylation of the compound.[18] As an example the debutylation of **2a** to create **3** is shown.

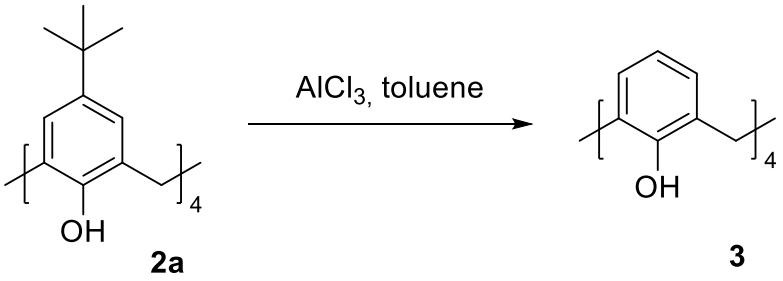

Scheme 3. Debutylation of *p-tert*-butylcalixarenes.

The tetramers, C4As, are the most explored macrocycles in the calixarene family when it comes to the post-synthetic functionalization at the upper and lower rims. Especially the lower rim has been functionalized selectively post-macrocyclization.[9]

2.2 Synthesis of resorcinarenes

Resorcinarenes, like calixarenes, are formed by a condensation reaction. The reaction (Scheme 4) is acid catalyzed and happens between a resorcinol-derivative and an aldehyde other than formaldehyde. The functionalization on the aldehyde determines the groups (R) in the alkyl bridges between the aromatic units.[5b]

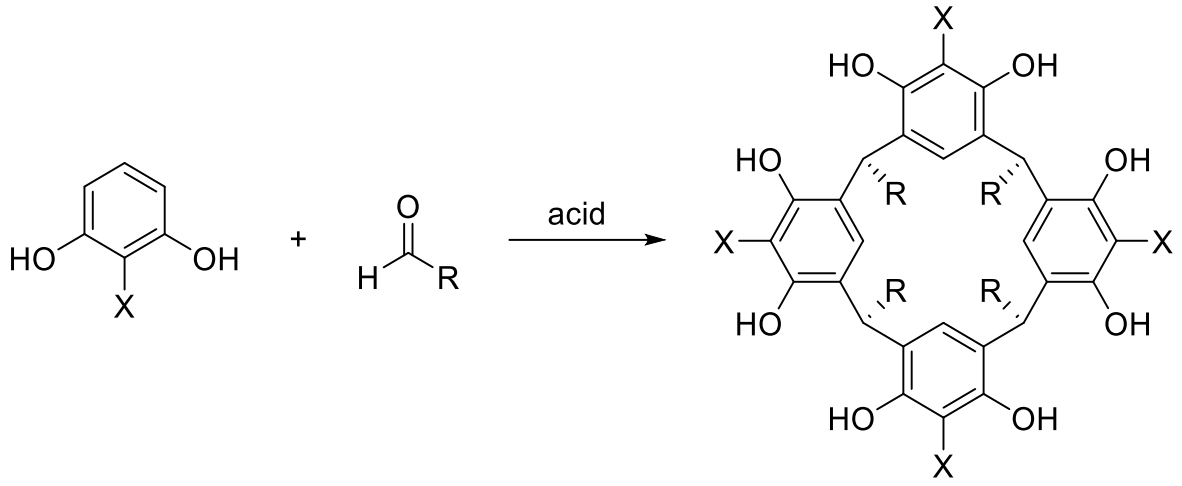

Scheme 4. The general synthetic route to form resorcinarenes.

Resorcinarenes can be functionalized on the upper rim (X-group in Scheme 4) via either the choice of the resorcinol-derivative used in the synthesis or modification after macrocyclization. The OH-groups on the upper rim can be functionalized via standard reactions, for example they can be alkylated. This alkylation has been taken further, and the groups have been bridged together with various units, from simple alkyl bridges to quinoxaline-functionalizations. The resulting cage-like compound is called a cavitand. As an example, in (Scheme 5) the alcohol-groups have been bridged together using CH_2-bridges using an alkylation of both groups with CH_2ClBr. This makes the structure of the resorcinarene rigid and locks it permanently into the crown conformation.[3]

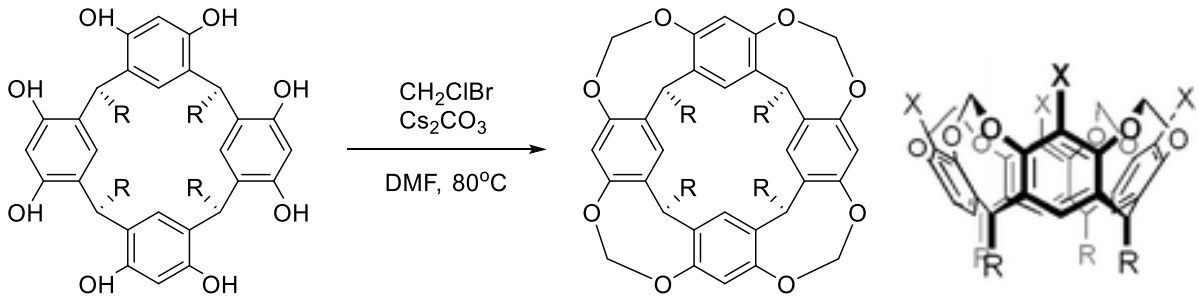

Scheme 5. The synthesis (left) of a general resorcinarene cavitand. The three-dimensional stucture of it (right). Reproduced from ref. 19 with permission from the Royal Society of Chemistry.

3 Synthesis of calixpyrroles

C4Ps are formed *via* the acid-catalyzed condensation reaction between a ketone and pyrrole. A general reaction is shown in Scheme 6. The ketone which is used in the synthesis can have a range of functional groups, from aromatic to aliphatic. This functionalization on the ketone forms the *meso*-positions of the C4P (groups R_1 and R_2).[4] The use of an asymmetrical ketone results in a range of isomers being formed, which were seen in Figure 5. Since the isomers differ in their dipole moment and by extension their solubility, they can sometimes be separated with the use chromatographic methods.[12]

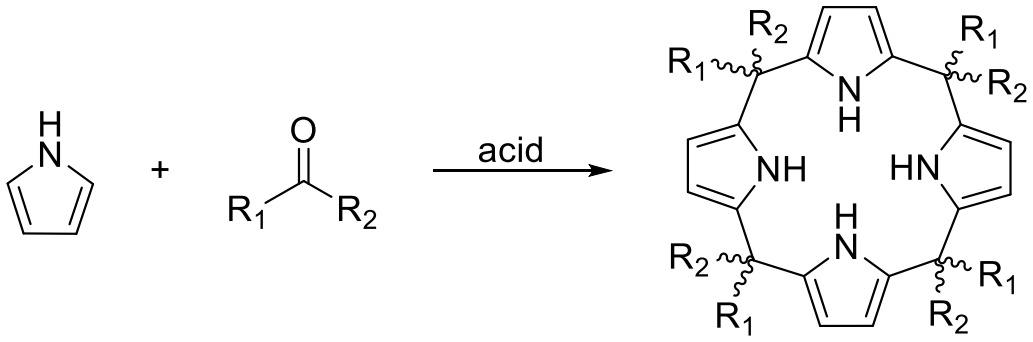

Scheme 6. The general reaction to form C4Ps.

Even though the synthesis of C4Ps is relatively easy (the macrocyclization being a one pot reaction) the syntheses suffer from low yields. Between the competition with polymerization and general difficulties in macrocycle-forming reactions, different methods to increase yields have been employed. Jain *et al.*[20] have used the assistance of microwave irradiation in synthesizing C4Ps more efficiently. The use of microwave in the synthesis of calixpyrroles **4a** and **4b** (Scheme 7) cut the reaction time from 6-8 hours down to 10-12 minutes.

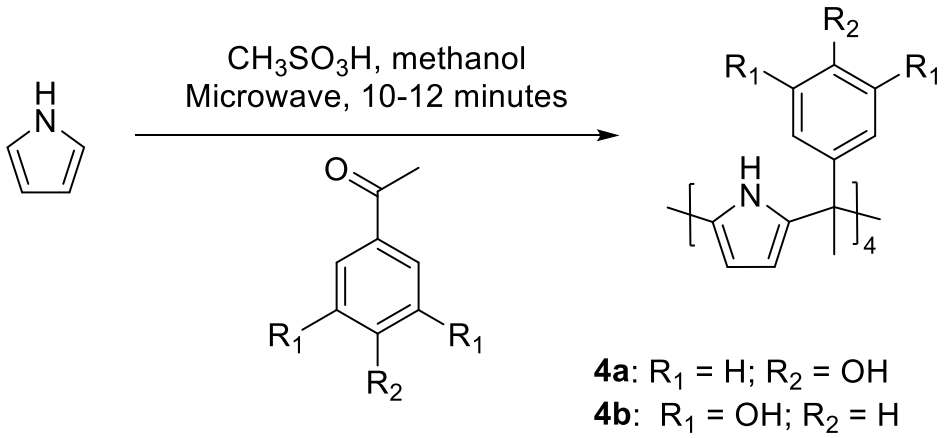

Scheme 7. Microwave assisted synthesis of phenyl-functionalized C4Ps.

4 Supramolecular chemistry of macrocyclic hosts

A phenomenon that connects all three macrocycles is that they partake in the supramolecular binding of guests. The bonds formed between a supramolecular host and the guest are not covalent or ionic bonds, but weaker non-covalent bonds such as hydrogen bonds and π-cation bonds. Since the bonds being formed are non-covalent, the bonding is also reversible.[5c]

As an example of hydrogen-bond based complex, the hydrogen on the nitrogen of a C4P possesses a partial positive charge. This hydrogen can associate with anionic guests such as the chloride anion or neutral and partially negatively charged compounds like dimethyl formamide.[4] This can be seen in Figure 6 in which the C4P **1** is in the cone conformation, with the hydrogens on the nitrogen of the pyrrole subunits pointing towards the chloride anion.

In addition to the anion, calixpyrroles can also bind the counter cation of an ionic compound in what is termed ion-pair binding. The aforementioned binding of the anion causes the calixpyrrole to switch into the cone-conformation. This aligns the electron-rich areas of the pyrrole rings and allows the cation to bind to the aromatic cavity that is present in the cone-conformation (Figure 6).[21] This binding is similar to those exhibited by C4As, which usually bind cationic guests via their π-electrons in the hydrophobic cavity.[5a]

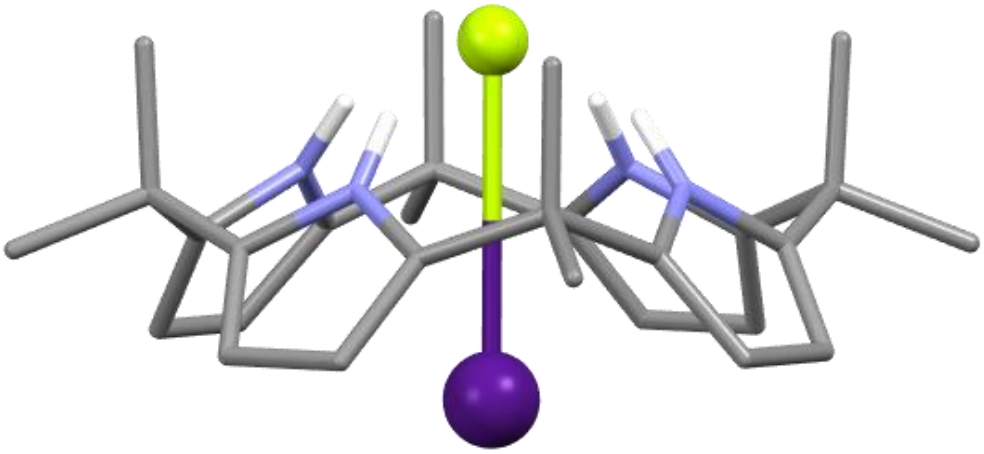

Figure 6. CsF binding to **1** (all hydrogens except NH are omitted). The fluoride (lime) is bound to the NH of the pyrrole units, and the caesium (purple) is bound to the π-area of the pyrrole units.

Quite similar to ion-pair binding exhibited by C4Ps, C4As can bind a cation and a neutral molecule at the same time. Bott *et al.*[22] found out that an O-methylated *p-tert*-butyl C4A in addition to binding a sodium cation on the lower rim also binds toluene in the aromatic cavity. The binding of the sodium causes the C4A to flip to the cone-conformation, which opens the π-electron rich cavity to which the neutral guest can then go into.

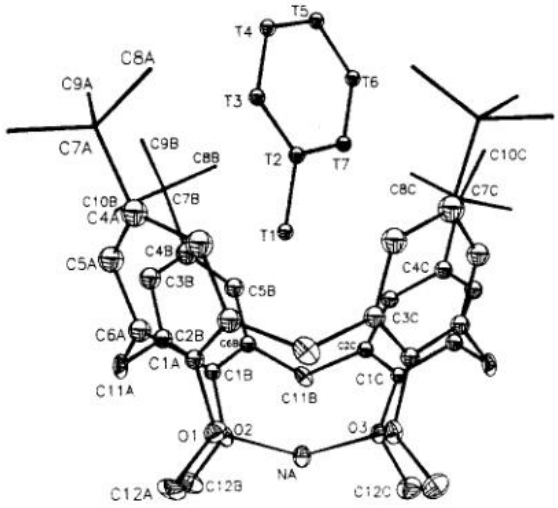

Figure 7. The O-methylated C4A binding to sodium and toluene. Reprinted with permission from 22. Copyright 1986 American Chemical Society.

The association between a host and its guest can be quantified by the determination of binding or association constant K_a. For a 1:1 host/guest complex the phenomenon of binding can be expressed as

$$\mathrm{G(S)_n + H \rightleftharpoons GH + nS} \qquad (1)$$

where G is the guest solvated by n molecules of solvent S and H is the host.[5c]

From this the binding constant can be derived as

$$K_\mathrm{a} = \frac{[\mathrm{GH}]}{[\mathrm{G}][\mathrm{H}]} \qquad (2)$$

where [GH] is the concentration of complex, and [G] and [H] are the concentrations of the free guest and host, respectively. When the association between the host and the guest is large, there is more complex formed and its concentration is thus larger. This means that the binding

constant is bigger. From equation 2 we can also see that the unit for binding constant is M^{-1}. Values for binding constants are often obtained through an NMR titration where the change in the hosts or guests chemical shifts due to weak bond formation are recorded as the concentration of the other is varied. A similar approach can be taken with UV-vis or fluorescence titration, where changes in the absorption or emission of the host or the guest upon complex formation as a function of their concentration are recorded.[5c]

The strength of this association between the host and its guest depends on a variety of factors. The chelate effect is an effect in which a multidentate ligand (in the case of C4A, C4P and resorcinarene chemistry, the host) binds to a guest with higher stability than multiple monodentate ligands. The phenomenon is due to the desolvation of the binding sites of the host and guest resulting in an increase in the entropy of the system.[23]

In addition to the chelate effect, a phenomenon called the macrocyclic effect aids in the complexation between a macrocyclic host and its guest. Before complexation the host is already in the same general shape as it is in the supramolecular complex. This results in all the binding sites of the host to be more easily accessible to the guest. In other words, the high preorganization of the host results in the complexation to be more energetically favorable in the case of cyclical hosts compared to non-cyclical hosts with the same binding sites.[5c]

The solvent that the guest and host are solvated in plays a role in the interaction between them. Essentially the solvent competes for the binding sites of both the guest and the host. As can be seen in eq. 1, the guest (and the binding sites of the host) is first solvated, but after binding the solvent molecules end up in the bulk of the solution.[24] The energetics of the desolvation must be favorable for this to happen.[25]

The tetrabutylammonium (TBA) salt of chloride has been introduced to **1** (Figure 4) in multiple organic solvents: DMSO, acetonitrile, nitromethane, 1,2-dichloroethane, and dichloromethane. The binding affinities between the chloride and **1** were measured using NMR (Table 2).[26] The choice of the solvent plays a huge role on the strength of the association, as the bonding in dichloromethane is a thousand times weaker than it is in acetonitrile.

Table 2. Binding affinities between TBA-Cl and **1**

Solvent	Binding affinity / M^{-1}
DMSO	$2.2 \cdot 10^3$
acetonitrile	$2.5 \cdot 10^5$
nitromethane	$2.4 \cdot 10^4$
1,2-dichloroethane	$1.5 \cdot 10^4$
dichloromethane	$4.3 \cdot 10^2$

5 Host-guest systems in water

The C4As, CAPs and resorcinarenes discussed previously are not soluble in water. This is a problem, since it means that the host-guest systems cannot be investigated in aqueous systems. For example, for applications regarding biological systems (e.g., the human body) the solvent of choice is water. The macrocycles thus need to be functionalized in a specific way to achieve solubility.

As discussed earlier, the solvent where the supramolecular system is formed in influences the binding affinity between the host and the guest. A problem with studying supramolecular systems in water is that water is very efficient at solvating polar and ionic compounds. The energy needed to desolvate the host and the guest is high. This has been solved by hiding the binding sites of the host in a deeper hydrophobic cavity where water tends not to go to. The water prefers to stay in the bulk of the solvent and the binding sites are not solvated.[27]

5.1 Solubilization of C4As and resorcinarenes and their applications

Calixarenes have been made water soluble using many kinds of functionalizations through the years. The earliest examples of this date to the 1980s, when Arduini *et al.*[28] functionalized the lower rim of **2a** with a carboxylic acid (Scheme 8). The resulting C4A **5b** is soluble in neutral aqueous environments as either ammonium (NH_4^+) or alkali (K^+, Li^+, Na^+ or Cs^+) salts. Additionally, due to the sterically large substituents on the lower rim, the conformation of **5b** is permanently locked into the cone-conformation.

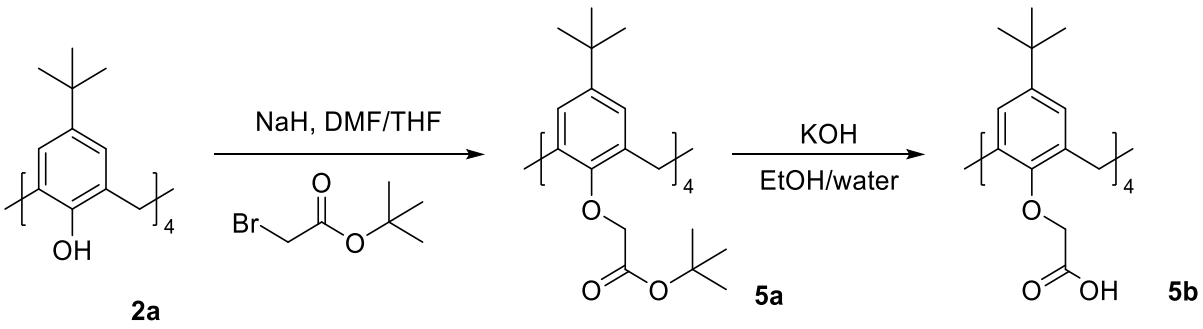

Scheme 8. Synthesis of a carboxylic acid-derivative C4A **5b**.

Later this C4A was further derived by introducing different groups into the lower rim bearing the carboxyl-group (Figure 8). All the compounds, like their predecessor **5b**, are locked into the cone-conformation. The extraction efficiency of Na^+ and K^+ picrate from water to dichloromethane were investigated (Table 3). None of the C4As **5a**-**5p** extracted K^+ efficiently and the extraction percentage was always less than 9 %. In the case of Na^+ some of the C4As (**5d**, **5e**, **5c**, **5l**, **5n** and **5o**) resulted in moderate extraction. The best C4A for the extraction of Na^+ was **5a**.[29]

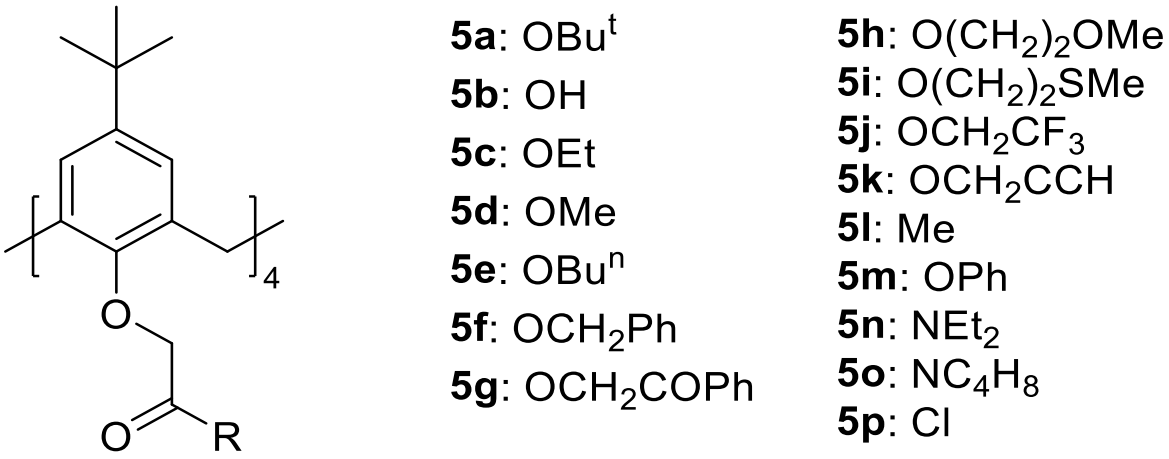

Figure 8. The further functionalizations of carboxylated C4P.

Table 3. The extraction of sodium and potassium cations by **5a-5p**

Calixarene	Extraction percentage (%)	
	Na^+	K^+
5a	29	5
5b	15	3
5c	25	2
5d	56	9
5e	18	2
5f	11	4
5g	11	2
5h	14	1
5i	11	1
5j	2	2
5k	5	2
5l	31	9
5m	22	2
5n	0	0
5o	51	6
5p	51	6

Similar carbonyl-containing functionalization on resorcinarenes have been investigated by Morozova *et al.*[30]. A resorcinarene bearing eight aromatic carboxylic acid groups on its upper rim and four methoxyphenyl groups on its lower rim (**6**, Figure 9) was synthetized. The resorcinarene **6** is highly soluble in water and insoluble in organic solvents. **6** is also not cytotoxic to human red blood cells.

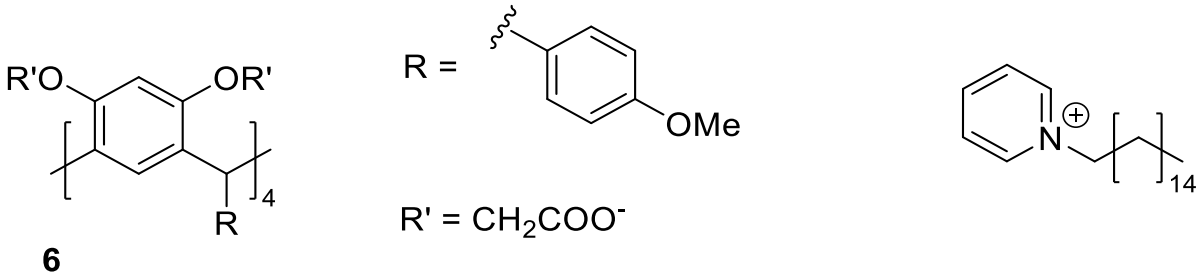

6

Figure 9. A resorcinarene bearing acid-groups **6** (left) and CPC (right).

The association between **6** and cetylpyridinium chloride (CPC, Figure 9) was investigated. It was found that **6** associates with the pyridinium-end of the CPC. The CPC forms micelles, and in aqueous solution the pyridinium ends point outward. **6** can bind to the pyridinium end of multiple CPC-molecules, which causes multiple micelles to be attached to each other forming supramolecular nanoparticles with sizes around 142-164 nm, as seen in Scheme 9. The size of the assemblies depends on the pH of the solution in the range of pH values of 3-8, as lowering pH increased the size of the particles. At pH of 2-3 the micelles precipitated out of the solution. The constructions are also stable up to 50 °C.[30]

The micelles constructed from **6** and CPC were used in the solubilization of the water-insoluble dye methyl yellow. The micelles were successful in the solubilization, but the addition of **6** into the CPC micelle reduced the solubilization of the dye compared to micelles constructed from only CPC. The capturing of a cationic and water-soluble dye rhodamine 6G was also investigated. It turns out, that the addition of **6** into the CPC micelles increased the binding of rhodamine G6 compared to CPC on itself. **6** binds the dye and causes its fluorescence intensity to become quenched.[30]

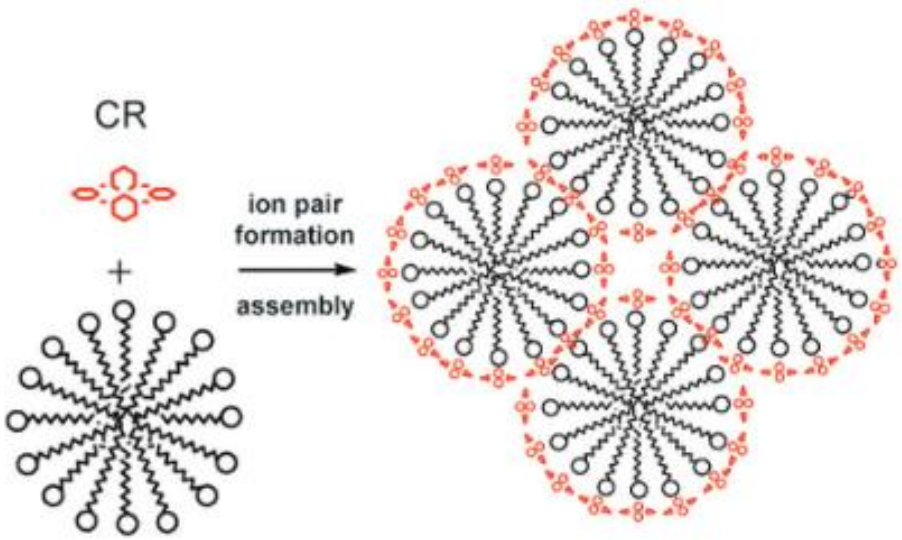

Scheme 9. The supramolecular particles formed by the resorcinarene (CR in the image) and CPC micelles. Reproduced from ref. 30 with permission from the Royal Society of Chemistry.

In addition to these lower rim functionalizations, the functionalization of C4A with sulfonato-groups in their upper rim (**7a**) has been investigated extensively. The functionalization can be achieved through many different synthetic routes (Scheme 10). The different routes are used

for different C4As; for example, the sulfonation using H_2SO_4 might not be suitable for C4As which bear acid-sensitive groups in their lower rim.[31]

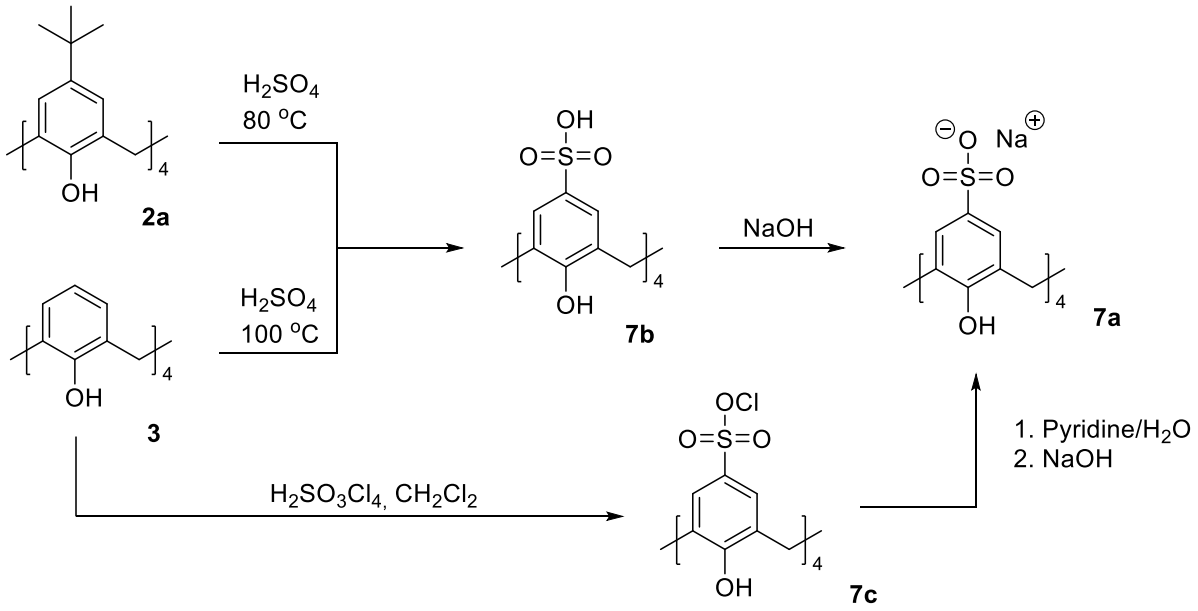

Scheme 10. The upper rim sulfonation of C4A.

7a forms dimers in the solution state when introduced to crown ether (Figure 10). When the Na-18-crown-6-H_2O is added to an aqueous solution of **7a** the sodium of the crown-system is dehydrated and subsequently it bonds to the SO_3^- -groups of **7a**. This formation of a crown ether-C4A system has utility in purification of diaza-crown ethers. After synthesizing diaza-18-crown-6, **7a** is introduced into the reaction mixture alongside a lanthanide. The complex is formed and crystallized from the solution. By adding NaOH to achieve pH 8 the complex dissociates, and the crown ether is released. The diaza-18-crown-6 can be extracted with organic solvents from the aqueous solution.[32]

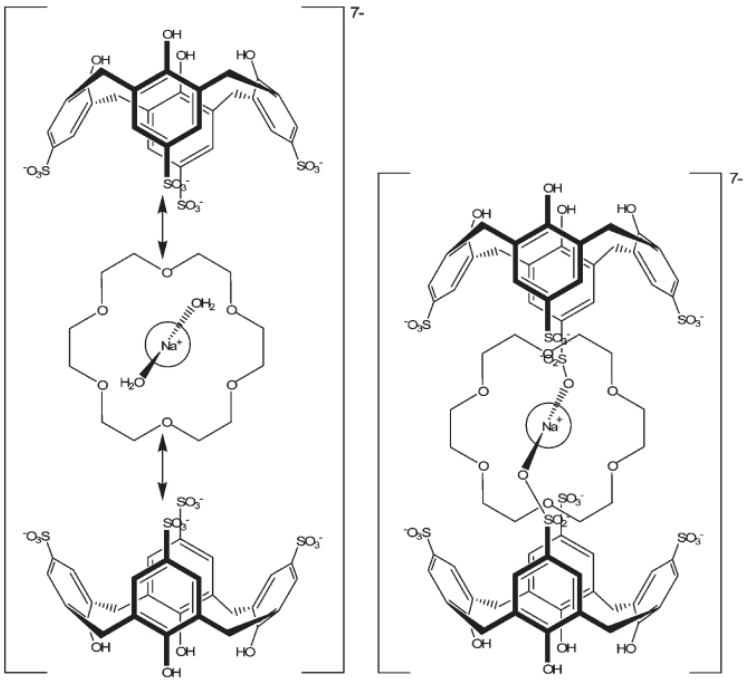

Figure 10. The dimer formed by **7a** and crown ether. Reproduced from ref. 32 with permission from the Royal Society of Chemistry

Since sulfonated C4As have been explored widely, many of their biological interactions have been recorded. For example, **7b** binds multiple different quaternary amines including acetylcholine, which is an important neurotransmitter. **7b** binds acetylcholine with a very strong stability constant of $5.0 \bullet 10^4\ M^{-1}$.[33]

In order to advance the use of supramolecular hosts in applications concerning the human body Silva *et al.*[34] have investigated the hemolytic properties of multiple different water-soluble sulfonated C4As. Upper-rim sulfonated C4As were selectively functionalized in one lower rim position with different functional groups, seen in Scheme 11. The substitution of only one OH-group on the lower rim was achieved via the use of one equivalent of corresponding alkyl bromide.[35]

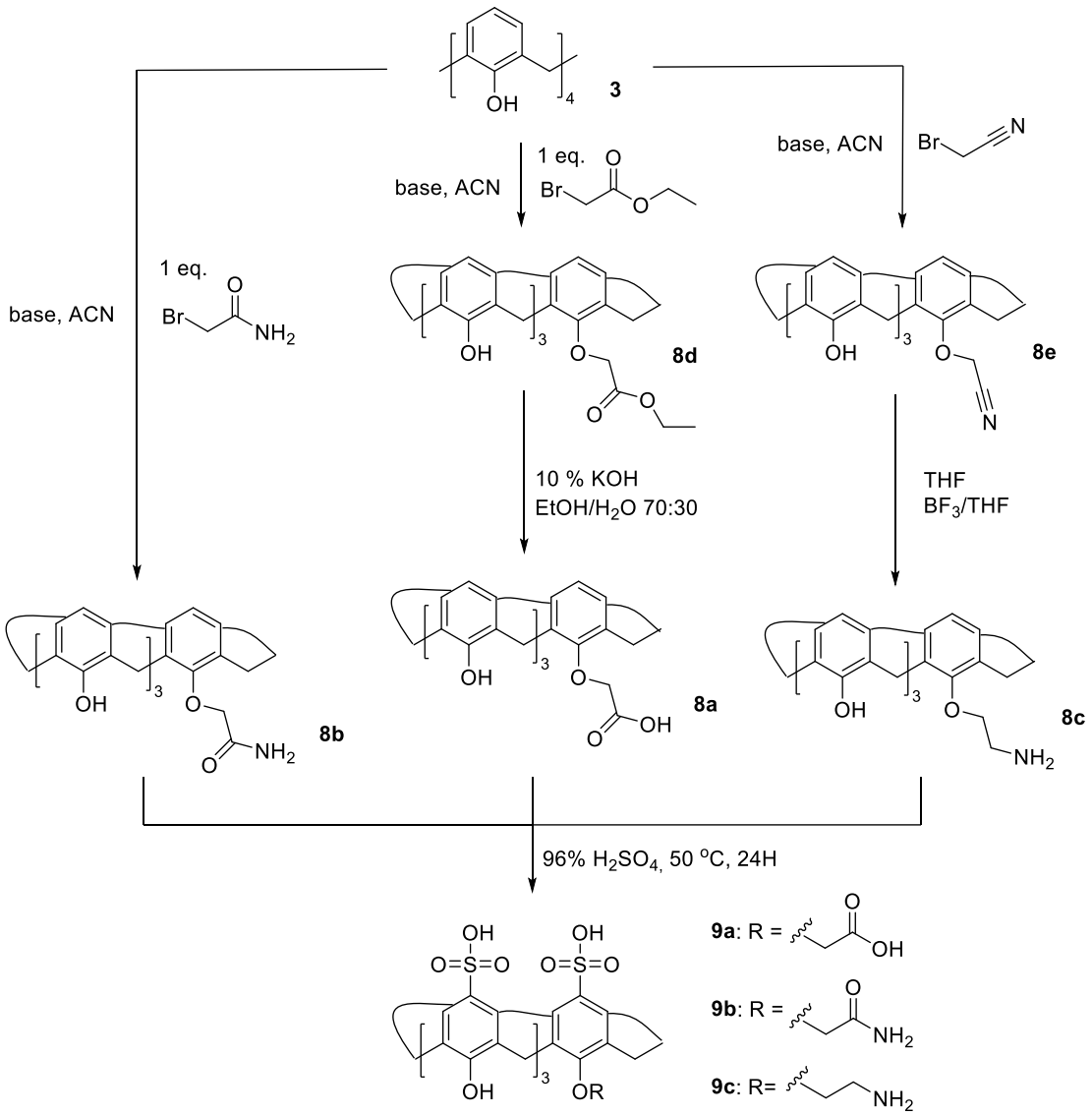

Scheme 11. Synthesis of monofunctionalized sulfonated C4As.

Human erythrocytes were introduced to various sulfonated C4As (**7b, 9a-c**) and the percentage of hemolysis of the cells was recorded using spectrophotometry. While **7b** is only slightly hemolytic (0.5 % at 200 mM), the introduction of a carboxylic acid group (**9b**) to the lower rim further decreased the hemolytic properties of the C4A to 0.1 % at the same concentration.[34]

Zhao *et al.*[36] have joined two sulfonato-C4As together to form a bis-C4A structure. The C4As were joined through an alkyl bridge on one of their OH-groups on the lower rim forming **10a**. The dimer can then be sulfonated on the upper rim of both the moieties resulting in sulfonated C4A dimer **10b** (Scheme 12). Like previously discussed sulfonated C4As, this compound is also water-soluble.

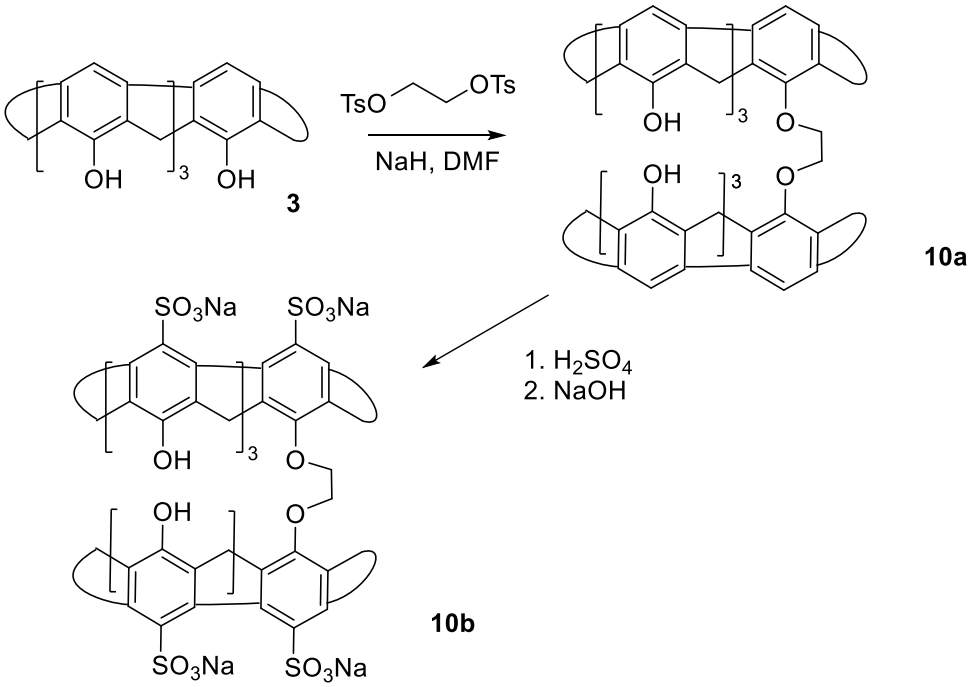

Scheme 12. Synthesis of *bis*-sulfonatoC[4]A **10b**.[37]

10b was used to construct a supramolecular polymer with another host, bis-cyclodextrin (bis-CD), and a guest, *N*-methyl-*N'*-adamantane carbomethyl-4,4'-bipyridinium (Ad-Vio). The two different ends of Ad-Vio (seen in Figure 11) each selectively bind to CD and **10b**. The aromatic bipyridine end of the guest is bound to the aromatic cavity of **10b** while the adamantane end preferentially associates with the CD. This results in a chain in which Ad-Vio connects a bis-CD to **10b** (Figure 11). The binding ratios of 1:2 (host:guest) for the association between the guest and both hosts were individually obtained using isothermal titration calorimetry (ITC).[36]

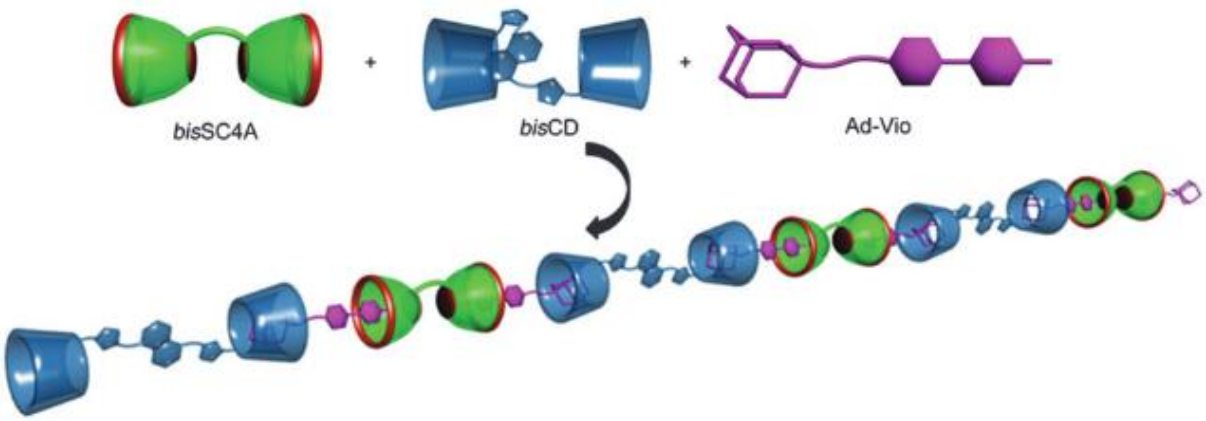

Figure 11. The structure formed by bis-**10b**, guest (Ad-Vio) and the bis-CD. Reproduced from ref. 36 with permission from the Royal Society of Chemistry.

The hydrodynamic diameter of this supramolecular polymer was investigated using dynamic light scattering (DLS). At 0.1 mM concentration of **10b** the average diameter was 409 nm, while at 0.04 mM the diameter was 179 nm. The size of the structure was thus dependent on the concentration. In addition to DLS measurements, the polymers were visualized with atomic force microscopy (AFM). Linear structures with widths comparable to the rims of the CD-units were seen. The lengths of the polymer fibers were over a micrometer long.[36]

The lower rim of a resorcinarene has been functionalized by a sulfonato-group by Pham and Wenzel[38]. The water-soluble compounds **12a-f** bore different chiral groups derived from proline and pipecolic acid on their upper rim (Scheme 13). Due to chiral functionalization the synthesized resorcinarenes were also chiral. These resorcinarenes were then used to resolve chiral guests in aqueous solution.

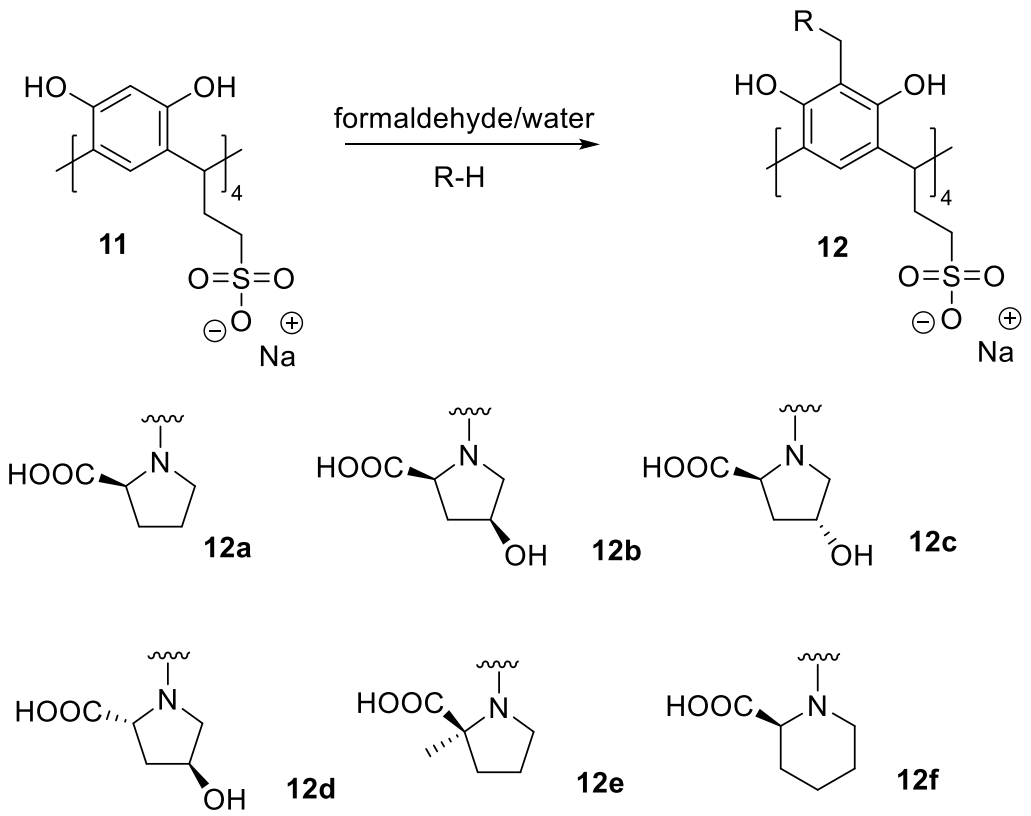

Scheme 13. Synthesis of water-soluble resorcinarenes with proline (**12a-e**) and pipecolic acid (**12f**) groups.

The nuclear magnetic resonance (NMR) spectra of enantiomers are the same, so the amounts of enantiomers in a mixture cannot be determined purely from the spectrum. To obtain this knowledge a chiral derivatizing or solvating agent must be used. The chiral resolving reagent

and guest form a diastereomeric complex, for which the NMR peaks are different. The sizes of the peaks correspond to the amount of each enantiomer in the mixture.[39]

Resorcinarenes **12a-12f** were dissolved into deuterium oxide and 20 different chiral guests (examples in Figure 12) as mixtures of their enantiomers were added. The enantiomeric discrimination of each substrate was investigated by comparing the chemical shifts of the enantiomers. The bigger the difference between the shifts of the enantiomers, the better the enantiomeric discrimination ability of the resorcinarene. The largest enantiomeric discrimination was exhibited by resorcinarene **12f**.[38]

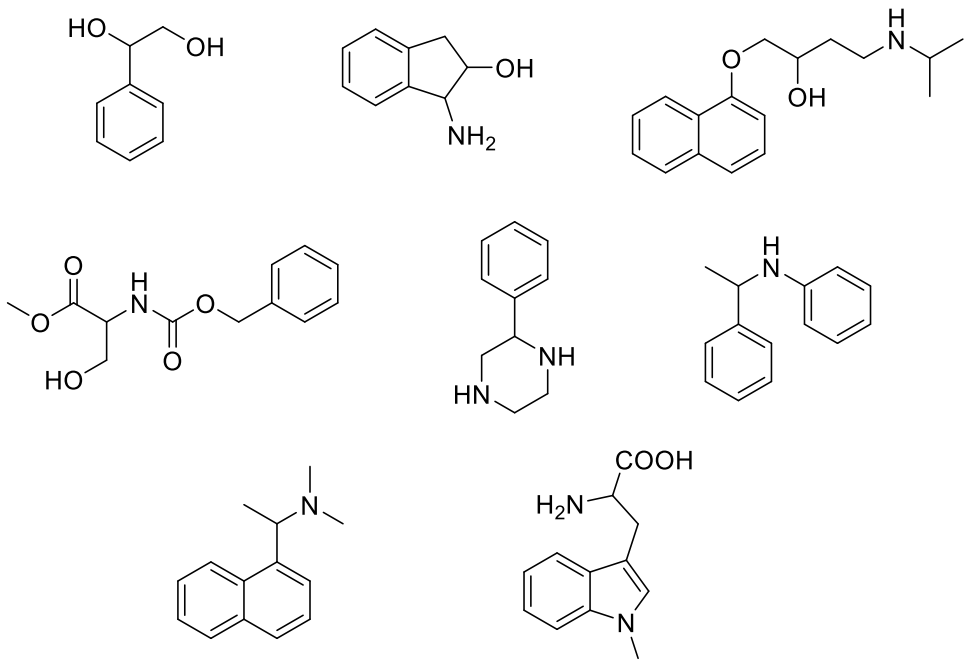

Figure 12. Some of the chiral guests used in the study of the chiral resorcinarenes.

The sulfonato-group has also been added to the X-position of a resorcinarene by Mustafina *et al.*[6]. The sulfonated resorcinarene **14** was formed by the reaction between the standard resorcinarene **13** (formed by reaction in Scheme 4 where X is H and R is a methyl group), formaldehyde and sodium sulfite. **14** is highly soluble in water, at a range of different pH values[40], and it forms 1:1 complexes with lanthanides.[6]

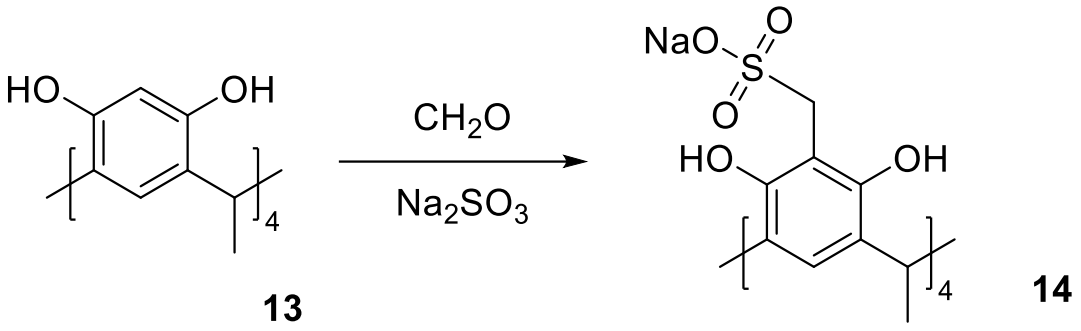

13 **14**

Scheme 14. Sulfonation of a resorcinarene in the X-position.

Cloud point extraction is an extraction method that is based on the aggregation of micelles. Micelles formed by an amphiphile grab the desired analyte, in the case of supramolecular chemistry, via a host-guest interaction. A raise in temperature to a temperature called cloud point causes these micelles to aggregate and separate into their own phase, causing turbidity in the solution. The solution can then be centrifuged which causes the aggregates to form a mass at the bottom. This precipitate can be collected and analyzed.[41]

14 was used in the cloud point extraction of lanthanide(III) cations (lanthanum, gadolinium and ytterbium) from aqueous solution in the presence of an amphiphile called Triton X-100 (Figure 13). The cloud point of an aqueous Triton X-100/**14** is 73-75 °C. To solutions of the lanthanides Triton X-100 and **14** were added. The solutions were heated to the cloud point temperature and the analyte was collected and analyzed spectrophotometrically. The cloud point extraction procedure was also performed for a solution of Triton X-100 and lanthanide without **14**. It turned out, that addition of **14** raised the extraction efficiency by Triton X-100 in the case of La(III) from 0 % to 22 %, and for Gd(III) from 2.2 % to 17 %. In the case of Yb(III) the extraction efficiency was nearly the same with or without **14**.[6] The host grabs onto the guest and are included somehow in the micelles formed by the Triton.

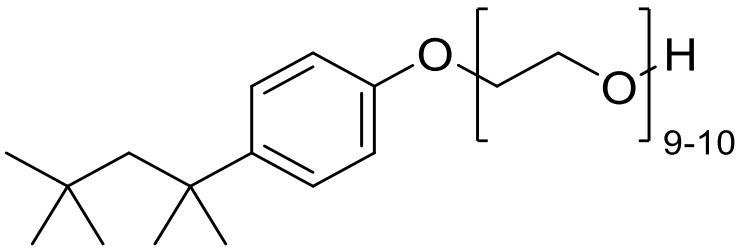

Figure 13. Triton X-100.

Heavy metals are a major pollutant which become biomagnified in aqueous ecosystems. Finding ways to detect and subsequently remove them from waterways is thus important. Sanabria *et al.*[42] synthesized sulfonated resorcinarenes in a similar manner (Scheme 15) as the resorcinarene by Mustafina *et al.*. The resorcinarenes **16a** and **16b** were used in the detection of heavy metals from aqueous solution. The complexation of Cu^+, Pb^+, Cd^+ and Hg^+ were investigated using conductometry and the results were confirmed using atomic absorption and ion-selective potentiometry. The heavy cations were used with perchlorate as their counter cation. It was found that **16a** binds Cu^+ in 1:1 stoichiometry and Pb^+ in 1:2 stoichiometry (**16a**:Pb^+), while it does not bind Hg^+ or Cd^+. In contrast, **16b** binds Hg^+ in 1:1 stoichiometry while not binding any of the other cations. **16b** is thus selective for the mercury out of the investigated cations.

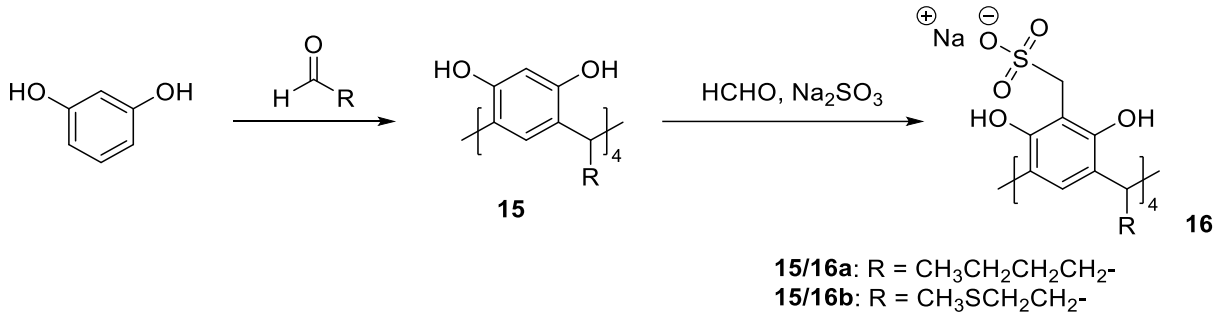

Scheme 15. Sulfonated resorcinarenes **16a** and **16b**.[42]

Resorcinarenes have (in addition to X-position and R-position seen in Scheme 4) been functionalized in the hydroxyl-groups on the upper rim. A sulfonato-group was added into the hydroxyl-groups of an alkylated resorcinarene **17a** (Scheme 16) which was previously synthesized via the acid-catalyzed reaction between hexanal and 3-methoxyphenol. The resulting resorcinarene **17b** is soluble in water and amphiphilic due to the pentyl-chains and the sulfonato-groups. **17b** forms micelles, for which the critical aggregation concentration is 0.3 mM.[43] The critical aggregation concentration is the lowest concentration at which an amphiphile forms micelles.[44]

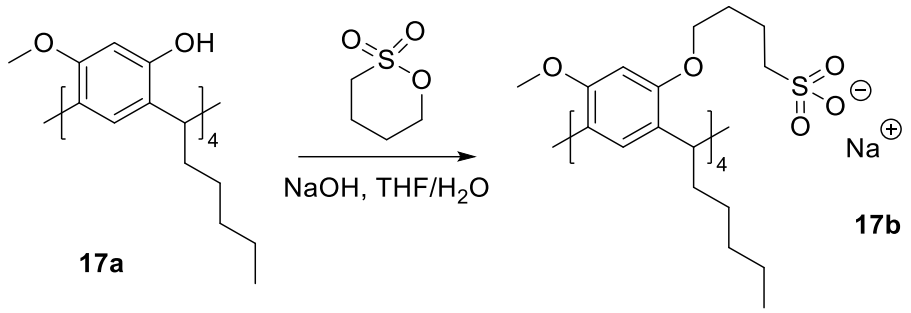

Scheme 16. Synthesis of a resorcinarene functionalized with *n*-pentyl and sulfonato-groups.

17b was used in binding studies with quaternary ammonium cations **18a-i** (Figure 14) in water. The cavity of the resorcinarene has a significant partial negative charge due to the π-electrons resulting in it readily binding the cations. All the guests were shown to interact with the host in 1:1 ratio using NMR titration. The binding geometries were also investigated using NMR.[43] The proposed geometries are in Figure 15.

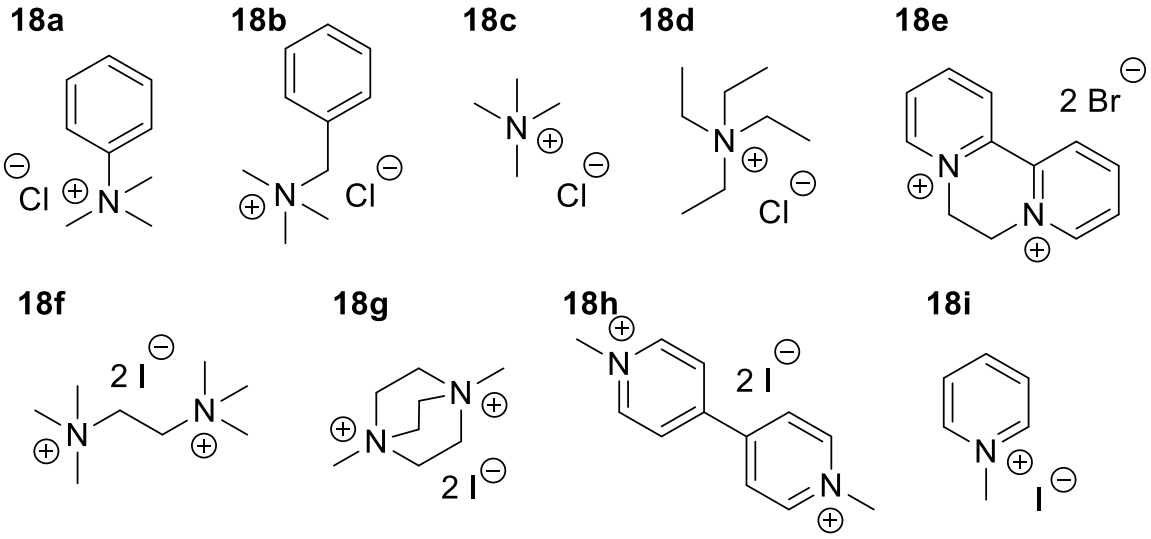

Figure 14. Quarternary cations used in the study of a sulfonato-resorcinarene.

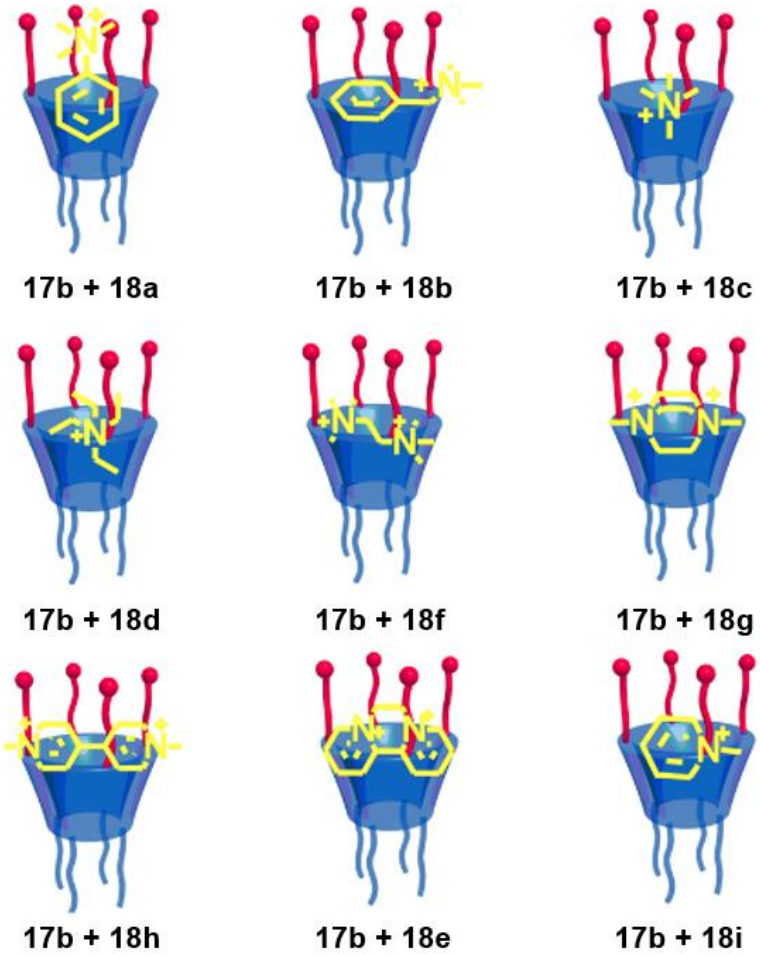

Figure 15. Bindings modes of **17b** and guests **18a-i**. Reprinted with permission from Hong, M et. al, Journal of Organic Chemistry, 2015, 80, 1849–1855. Copyright 2015 American Chemical Society.

The stability constants between the host and the guests were also recorded using competitive binding studies. It was shown that the highest stability constant is between **18h** and the host, with a stability constant of $3.18 \bullet 10^6$ M^{-1}. The guests **18a**, **18b**, **18c**, **18d** and **18i** have four orders of magnitude smaller stability constants with the host than **18h** and the host.[43]

Clark *et al.*[45] have synthesized phosphonated C4As (**19c**-**19e**) by functionalization after cyclization (Scheme 17). The resulting C4A **19e** is water-soluble at a high pH.[46]

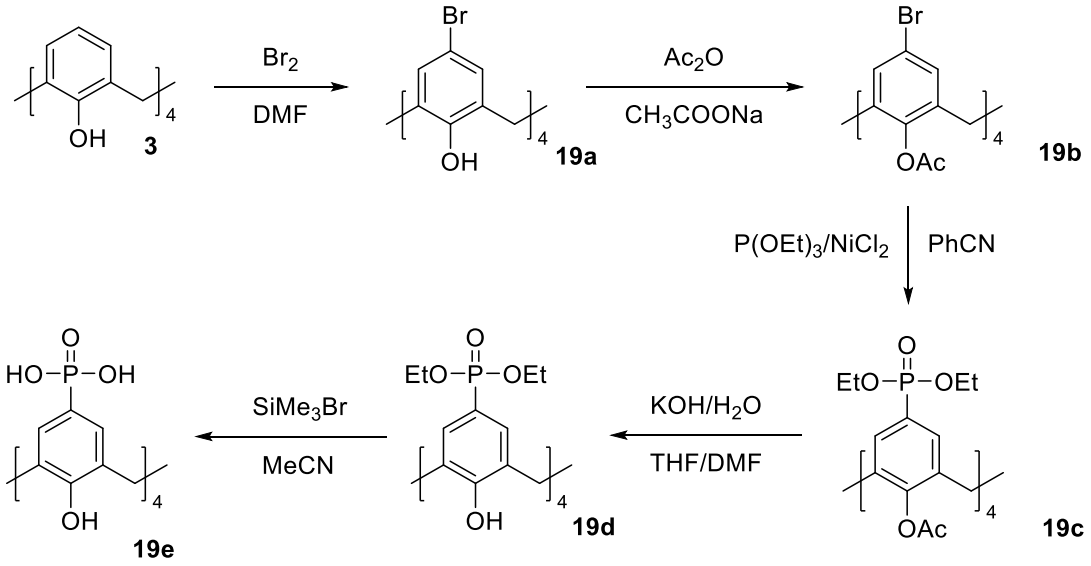

Scheme 17. Synthesis of phosphonated C4A.

19e can be used to construct nanorafts using a spinning disk method. A solution of the macrocycle in 1 M NaOH was fed onto a spinning disk alongside another stream of HCl. **19e** self-assembles into bilayers which are stabilized by the hydrogen bonding between molecules, seen in Figure 16. [45]

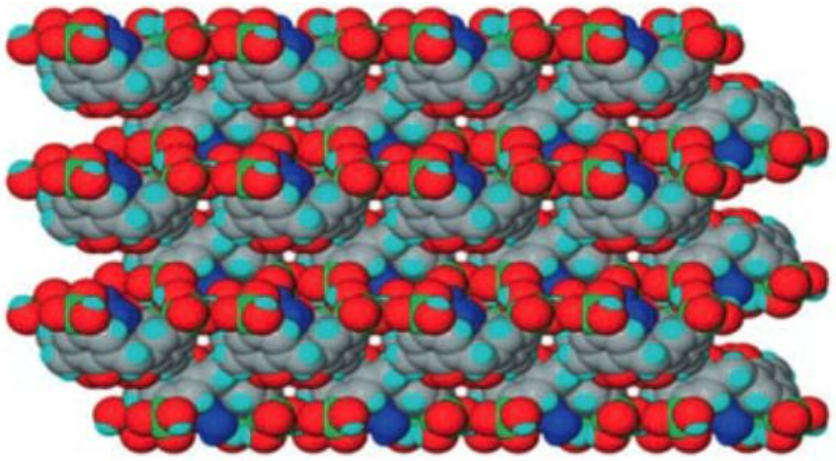

Figure 16. The bilayer formed by phosphonated C4A.

Collin *et al.*[47] have also investigated the water solubility of resorcinarenes. A bridged resorcinarene was functionalized with pyridinium- and imidazolium-containing groups, resulting in the formation of a cavitand **20** (Scheme 18). It is soluble in water over a range of pH-values due to the ionized pyridinium groups. **20** readily binds zinc(II).

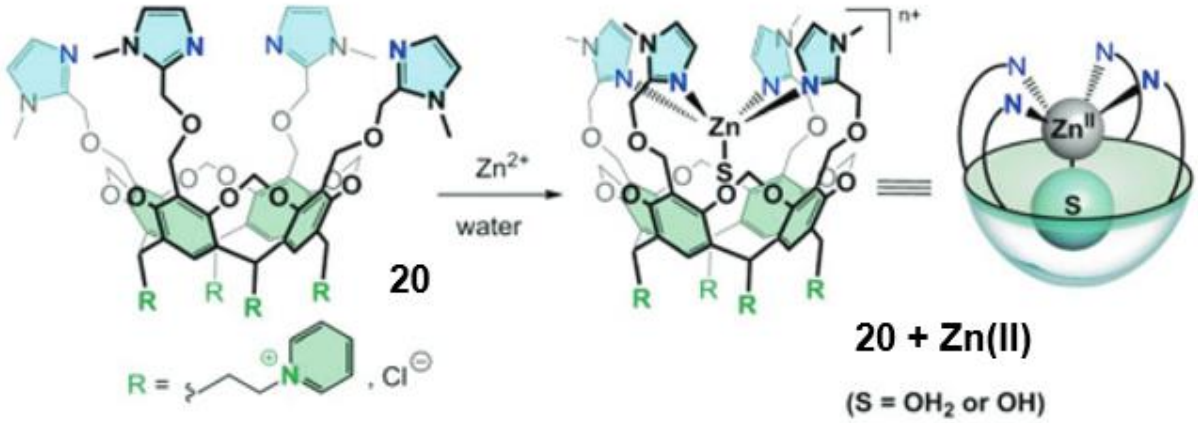

Scheme 18. Pyridiunium-resorcinarene **20** binding zinc. Reproduced from ref. 47 with permission from the Chinese Chemical Society (CCS), Shanghai Institute of Organic Chemistry (SIOC), and the Royal Society of Chemistry.

Phosphates are very important to life due to them participating in many biological functions, most importantly in energy transport in the form of adenosine triphosphate. The system between **20** and zinc(II) has been used in the binding of phosphates (Scheme 19). Linear alkylated phosphates (n = 1-8, Figure 17) and regular phosphate were tested. The resorcinarene-zinc complex **20**-Zn binds un-alkylated phosphates and alkylated phosphates n = 3-6 well, and for n = 6 the binding constant is the highest $3.6 \bullet 10^4$ M^{-1} at neutral pH. **20**-Zn binds n = 0-2 and 7 poorly and with n = 8 no binding is observed. A closer look at n = 6 was taken. NMR studies showed that when the alkylated phosphates are bound, their alkyl chain goes into the resorcinarene cavity, seen in Scheme 19.[47]

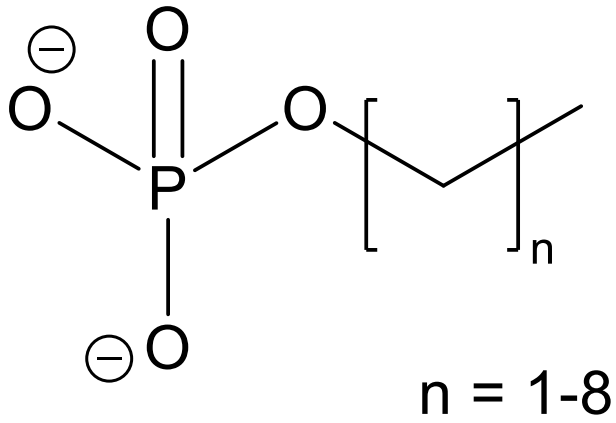

Figure 17. Alkylated phosphates tested.

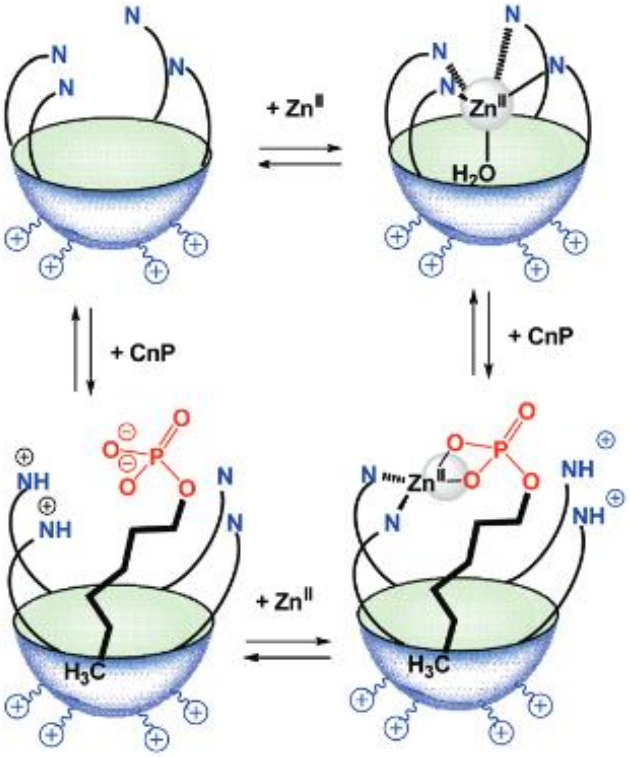

Scheme 19. Binding of n = 6 phosphate by **20**-Zn and **20**. Reproduced from ref. 47 with permission from the Chinese Chemical Society (CCS), Shanghai Institute of Organic Chemistry (SIOC), and the Royal Society of Chemistry.

In addition to solubilization by functionalization, co-micellization has been used to make C4As water-soluble. An amphiphilic C4A **21** was synthesized (Figure 18). **21** contains hydrophobic areas (R_1), hydrophilic areas (PEG-550 arms) and the biologically active secondary amides (R_2). The amide (*N*-(2-hydroxyethyl)-group) is a carcinoma-fighting group.[48]

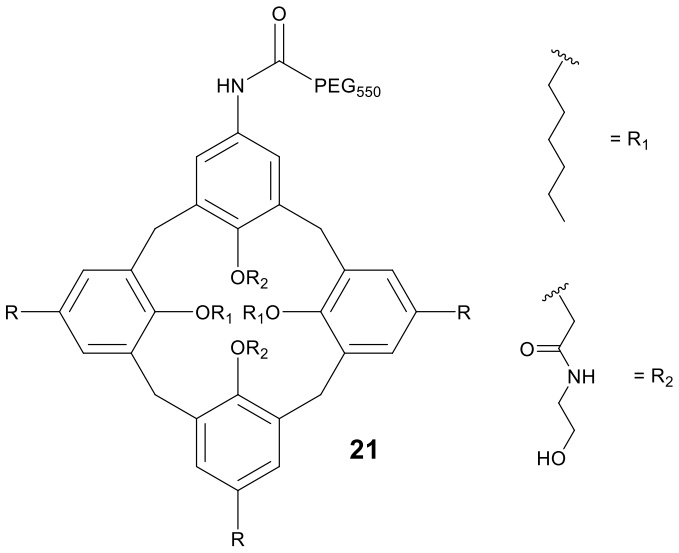

Figure 18. Anti-tumor C4A **21**.

Since folate is an important vitamin to cell proliferation, cancer cells often present an increased number of folate receptors on their surface compared to normal tissue. A folate derivative called DSPE-PEG_{2000}-FA can co-micellize with various other amphiphiles and can be used to selectively transport cancer fighting agents to the site of the tumor by targeting the receptors on the tumor cell membranes.[49]

21 (Figure 18) is an amphiphile which can be included into micelles with DSPE-PEG_{2000}-FA. In addition to **21** and the DSPE-PEG_{2000}-FA, a cancer drug known as Doxorubicin (DOX) was included into some micelles. The cytotoxicity of the micelle system with and without DOX was tested on seven different cell cultures.[48]

The inclusion of DOX increases the cytotoxicity of the micelles significantly compared to the micelles without DOX. This could be due to the PEG_{550} chains on **21** hindering the micelles' ability to go through the cell membrane which in turn lowered the amount of N-(2-hydroxyethyl)-group being supplied to the cell. However, there is an advantage in using **21** and DSPE-PEG_{2000}-FA in conjunction with DOX; DOX is not water-soluble, so solubilizing it within the co-micelle increased the cytotoxicity of DOX on cancer cells without increasing its toxicity to normal tissues (Figure 19). It can be seen in the figure, that the inclusion of DSPE-PEG_{2000}-FA has negligible effect on the inhibitory action of the system, so its utility is on the targeting of the cancerous site.[48]

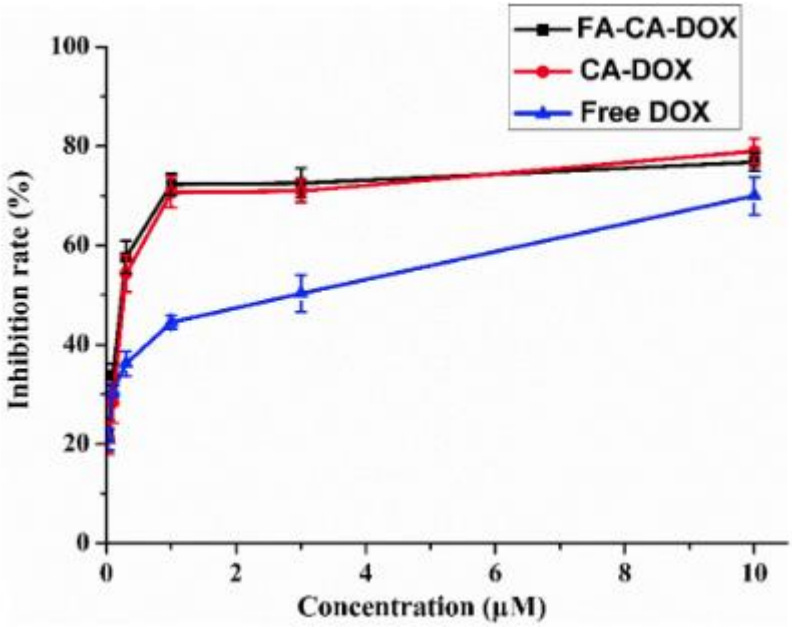

Figure 19. Cytotoxicities of the **21**/DSPE-PEG_{2000}-FA/DOX -system (black), **21**/DOX system (red) and free DOX (blue).[48]

5.2 Solubilization of C4Ps and their applications

The introduction of ionizable groups into C4Ps allows the host to be water-soluble. Hernández-Alonso *et al.*[50] have synthesized a C4P with an aromatic cavity and a triazole-containing ionizable group (Scheme 20). An alkyne-containing C4P **22** was first constructed with acid-catalyzed macrocyclization. The αααα-isomer was isolated using chromatography which was possible due to the ionizable group being introduced to the compound post-macrocyclization.

A copper-catalyzed alkyne-azide cycloaddition introduced a triazole bearing a carboxylic acid onto the C4P, resulting in **23**. The inclusion of the carboxylic acid group in the *meso*-position opposite to the phenyl ring of the C4P allows to simultaneously solubilize the compound into an aqueous environment while retaining integrity of the highly hydrophobic cavity of the macrocycle.[50]

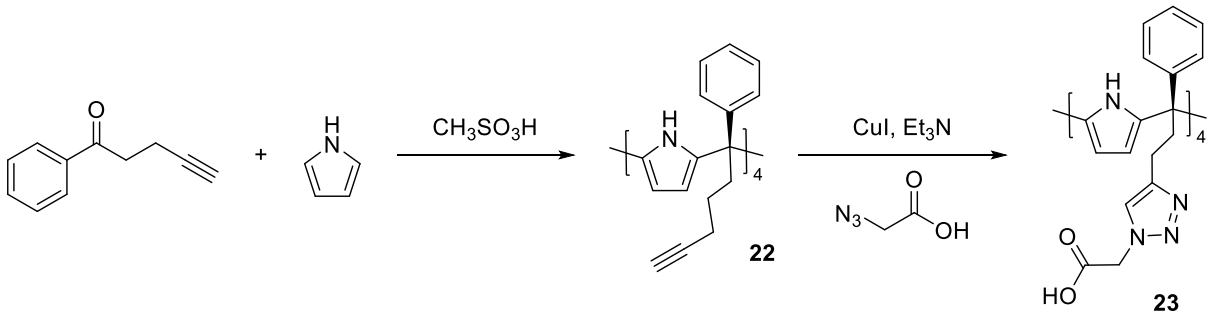

Scheme 20. Synthesis of a water-soluble C4P **23**.

23 was used to bind pyridine *N*-oxide in its hydrophobic cavity in basified water (Figure 20). The carboxylic acid ends of **23** are deprotonated, and the host is dissolved into water. During the binding the C4P adopts the cone conformation (changing its conformation from 1,3-alternate), and the negatively charged oxygen of the guest forms hydrogen bonds with the hydrogens on the pyrrole units. In addition to the hydrogen binding, the aromatic walls of **23** interact with the aromatic part of the pyridine creating a stable host-guest system with an association constant of $4.3 \bullet 10^4$ M^{-1} at pH 7.2.[50]

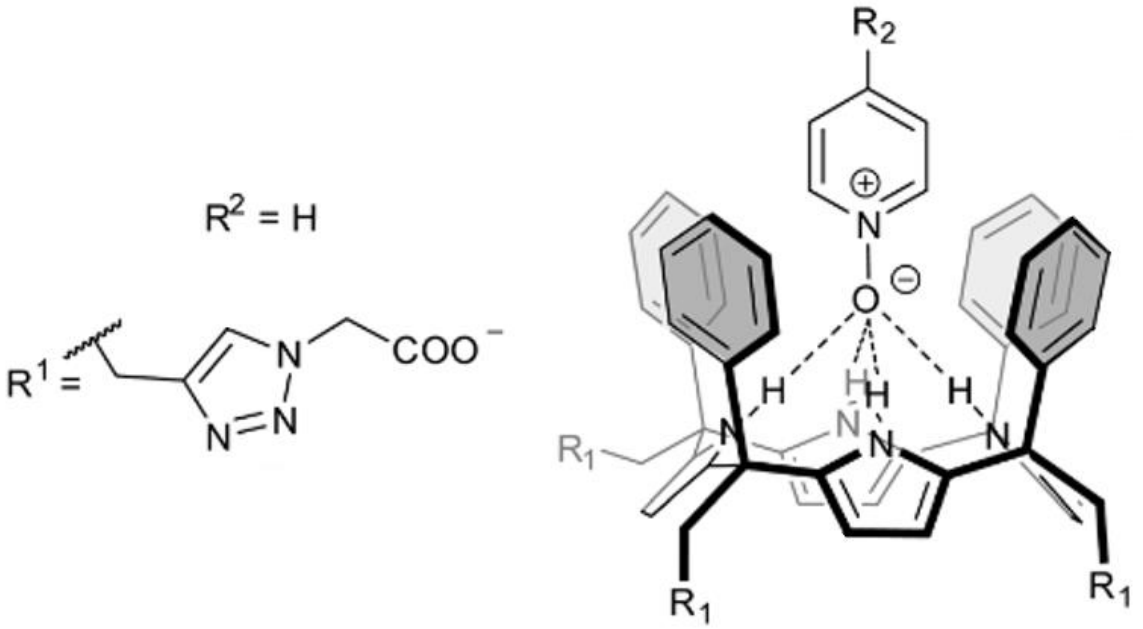

Figure 20. The binding of pyridine *N*-oxide by water soluble C4P **23**. Reproduced from ref. 50 with permission from the Royal Society of Chemistry.

In order to investigate biological applications, there was a need to synthesize C4Ps which are water-soluble at a lower pH. The chloride-functionalized calixpyrrole **24** was synthesized first with the aid of methyltributylammonium chloride according to Scheme 21.[51] The resulting C4A was then functionalized with pyridinium in its *meso*-positions which afforded C4P **25** which is water-soluble in up to 15 mM concentration. Since the compound is always ionized the water-solubility is independent of the pH of the environment.[52]

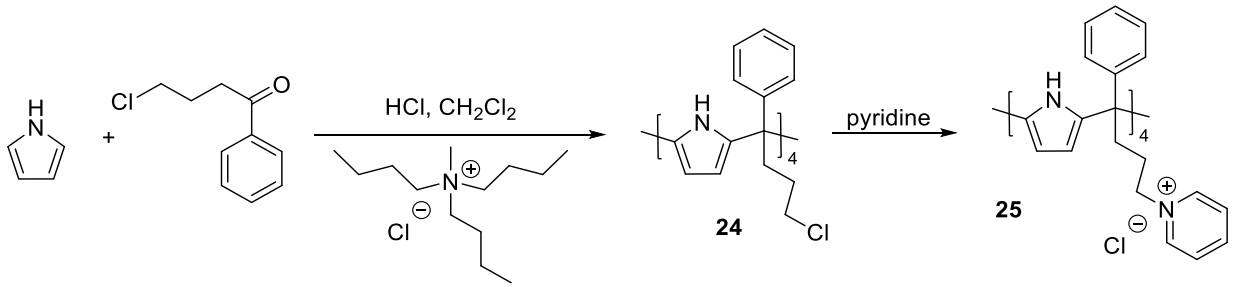

Scheme 21. The synthesis of pyridinium containing water soluble C4P.

The host-guest interactions between **25** and *cis*- and *trans*-rotamers of *N*-phenyl formamide were investigated. **25** favors the binding of the *cis*-rotamer of *N*-phenyl-formamide over its *trans*-rotamer. This is due to the *trans*-rotamer forming less favorable interactions with the C4P. The formamide binds to **25** from its oxygen atom, which in the case of the *trans*-rotamer brings the phenyl group too close to the aromatic walls of the cavity (Figure 21).[52]

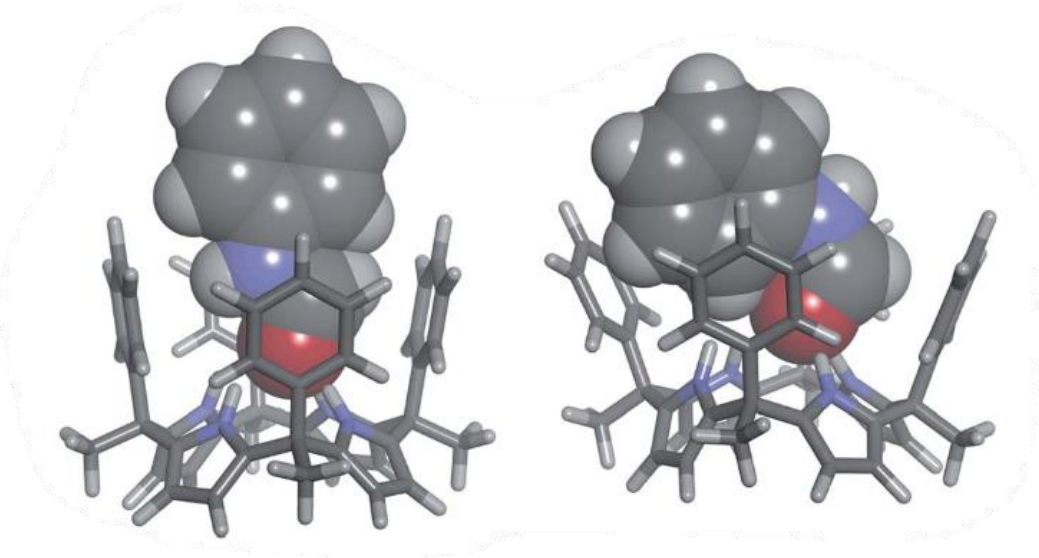

Figure 21. **25** binding *N*-phenyl-formamide (*cis* on the left, *trans* on the right). Reproduced from ref. 52 with permission from the Royal Society of Chemistry.

In addition to the *meso*-position across the aromatic moiety being functionalized, the aromatic part on the C4P has also been extended further. Verdejo *et al.*[53] treated a hydroxyl-C4P formed by the condensation reaction between acetophenone and pyrrole with bromoacetate in basic conditions. The resulting ester **26** was demethylated with the aid of LiOH, forming ionizable groups on all of the *meso*-positions of the C4P in **27**. The same hydroxyl-C4P was also made into an amine by first introducing a phthalimide-group which was then changed into the amino-group resulting in **28**. Compounds **27** and **28** are water-soluble but **26** is not. Both synthetic routes can be seen in Scheme 22.

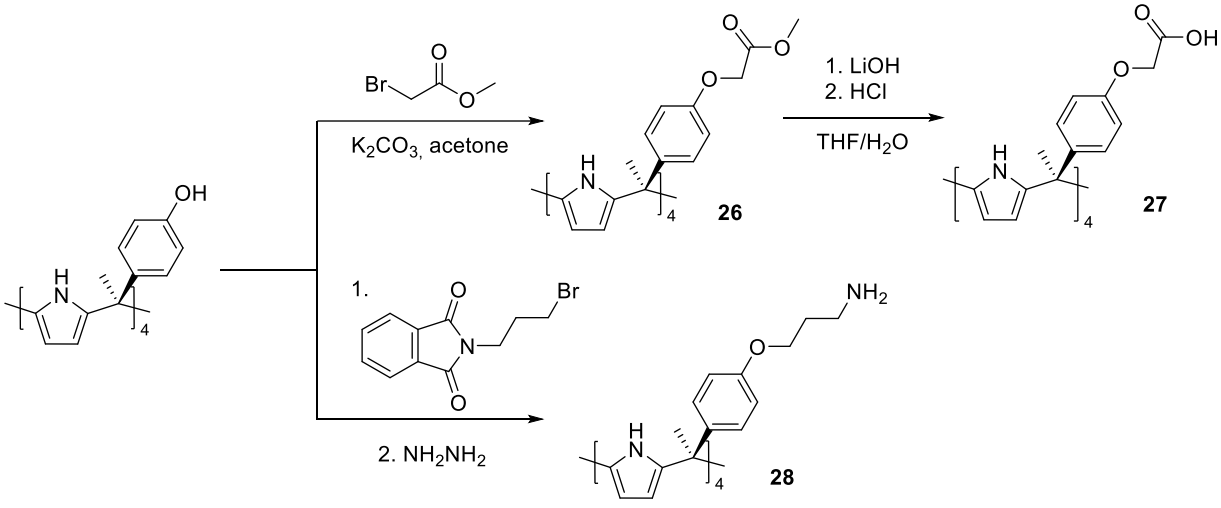

Scheme 22. Synthesis of two water-soluble C4Ps.

The *N*-oxide-binding abilities of these C4Ps were tested. The hosts were used to bind pyridine *N*-oxide and 4-phenyl-pyridine *N*-oxide (**e** and **a**, respectively, in Figure 23). The binding constants (Table 4) were determined using ^{1}H NMR titration and ultraviolet-visible light titration (UV-vis titration). The hosts **26** and **27** bind guests **a** and **e** well in aqueous media in the order of 10^3-10^4. All the hosts bind the guests in 1:1 ratio.[53]

Table 4. The binding constants (M^{-1}) between hosts **26-28** and guests **a** and **e**

Host / Guest	**a**		**e**	
Solvent	**CD_3CN**	**D_2O**	**CD_3CN**	**D_2O**
26	$1 \cdot 10^4$ *a*	-	$2.9 \cdot 10^4$ *a*	-
27	$2.9 \cdot 10^3$ *b*	$2.4 \cdot 10^3$ *b*	$2.5 \cdot 10^4$ *a*	$1.6 \cdot 10^4$ *a*
28	-	$1.5 \cdot 10^3$ *b*	-	$2.0 \cdot 10^4$ *a*

a. UV-vis titration data
b. ^{1}H NMR titration data

The C4P **27** was used by Chi *et al.*[54] in the construction of a supra-amphiphile by adding a guest **29** which contains pyridine *N*-oxide-groups in both of its ends (Figure 22). **28** and **29** form a 2:1 (host:guest) complex, where the C4Ps are bound to the aromatic ends of the guest. In aqueous environment the complex forms layers which can self-assemble to form a multilamellar (multilayered) micelle (Scheme 23). The size and morphology of the vesicles were studies using scanning electron microscopy (SEM), transmission electron microscopy (TEM) and DLS. These large vesicles are formed at neutral to high pH, and lowering the pH causes **27** to precipitate, freeing **29** which can form smaller micelles on its own. The micelles can further encapsulate water-soluble molecules.

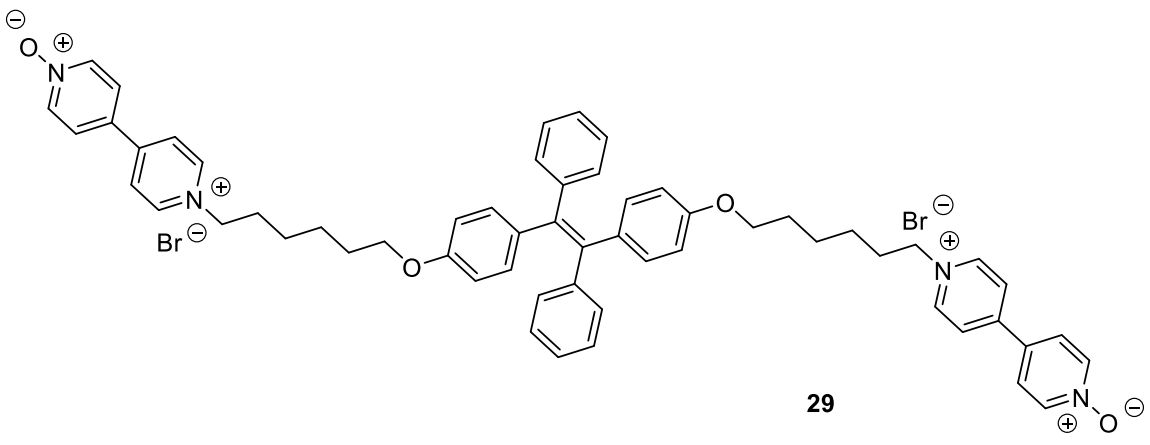

29

Figure 22. The guest **29** used in the construction of the amphiphile.

The molecule-carrying properties of the vesicles were investigated by introducing the chemotherapy drug gemcitabine into the vesicle. The drug was shown to go inside of the vesicle via fluorescent studies. Lowering the pH of this drug-**27**-**29** -solution disassembled the vesicle resulting in the drug being freed.[54] This kind of a controlled release of the drug could be beneficial in the delivery in the human body.

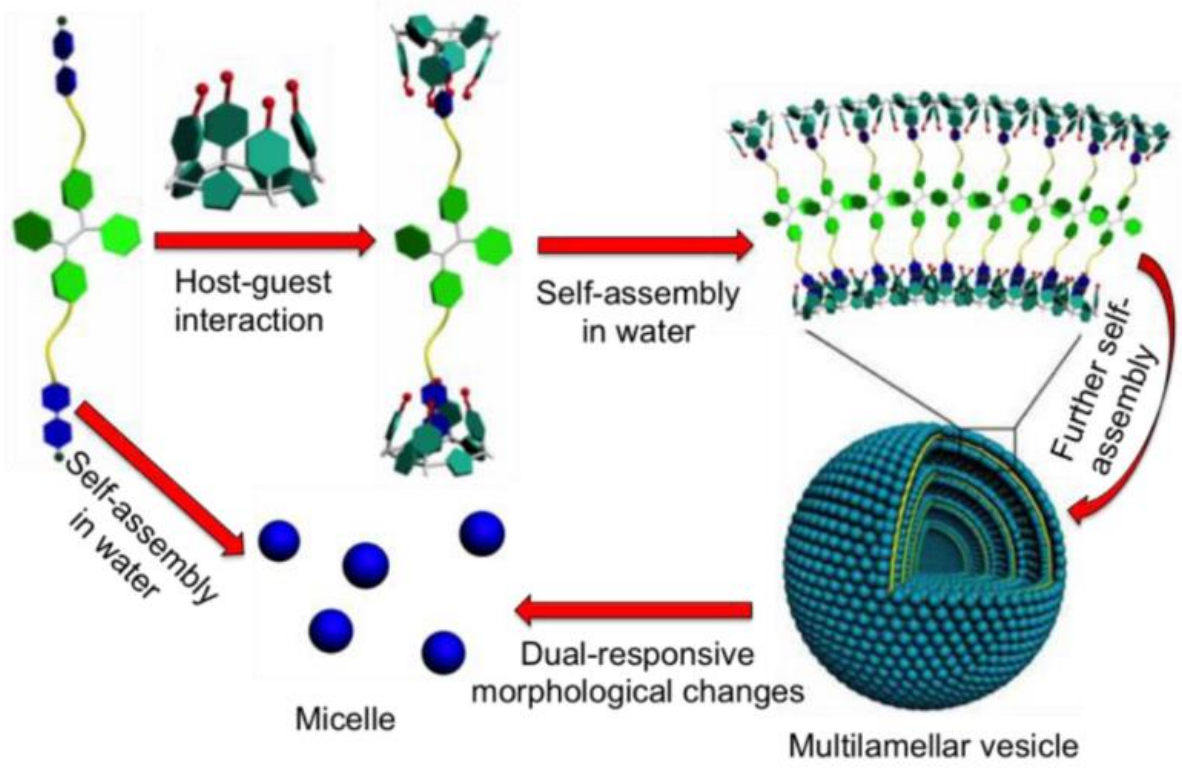

Scheme 23. The micelles formed by **27** and the guest.

The Ballester group has continued the quest to water-soluble C4Ps by further extending the aromatic cavity of aryl-extended C4Ps, seen in Scheme 24. A phenyl-C4P **30** formed by the standard acid-catalyzed condensation of pyrrole and 5-chloro-1-(4-iodophenyl)pentan-1-one was extended via Sonogashira coupling resulting in **31**. After that either 1-methylimidazole or a pyridine was introduced to the alkylated *meso*-position, creating **32** and **33**. In a similar manner to Scheme 21 the ends of the C4Ps were outfitted with eight ionic groups in total, which facilitate good water-solubility for the compound at any pH.[55]

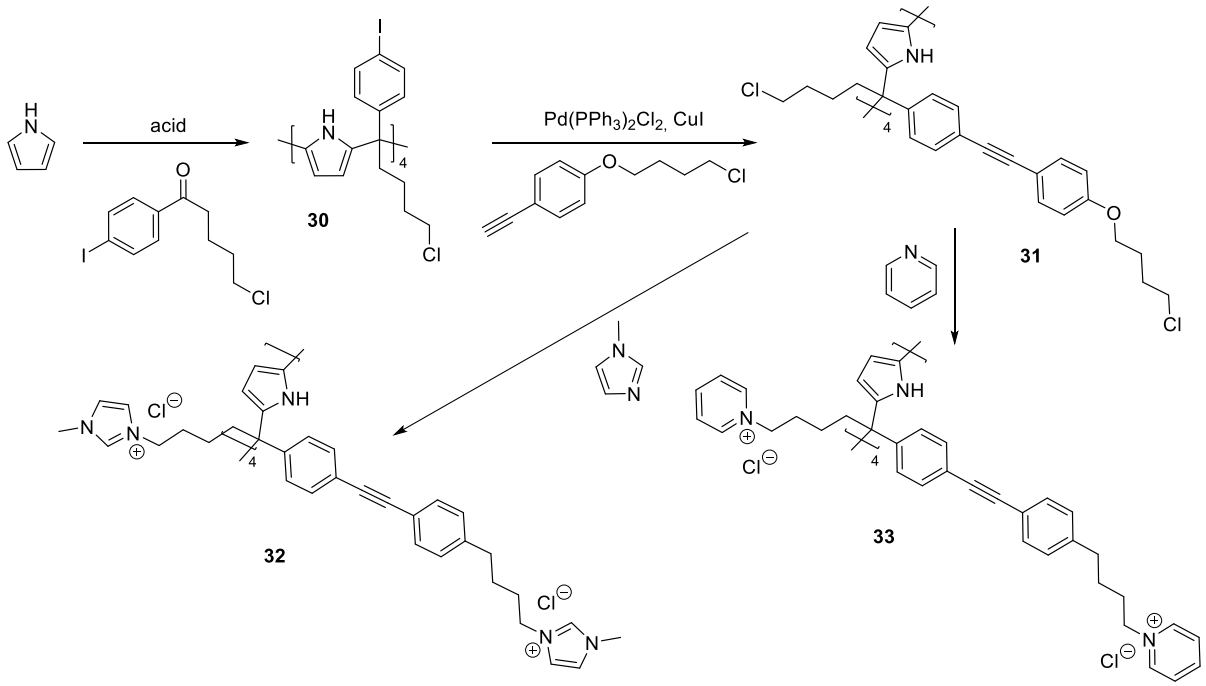

Scheme 24. Synthesis of super aryl-extended C4Ps **32** and **33**.

The host-guest binding between the super aryl-extended C4P **33** and various pyridine *N*-oxides (Figure 23) were investigated. **33** binds **34e** in neutral water with association constant $2.6 \bullet 10^9$ M^{-1} which is a lot higher than for the aryl-extended C4P **23**.[55] The binding constants between host **33** and guests **34a-c** can be seen in Table 5.

In water **33** binds larger *N*-oxides **34a-c** especially well, with binding constants in the order of 10^7-10^9 M^{-1}. This can be attributed to favorable interactions between the very deep and hydrophobic cavity of the C4P and the larger hydrophobic area of the guests. While guest **34f** has a comparable binding area to guest **34a** the association constant between it and the host is multiple orders of magnitude less. This is due to steric hindrances caused by the shape of the dual ring.[55] The group was thus successful in simultaneously enhancing the water-solubility and pyridine *N*-oxide binding of C4Ps by introducing a deeper cavity with multiple ionized groups.

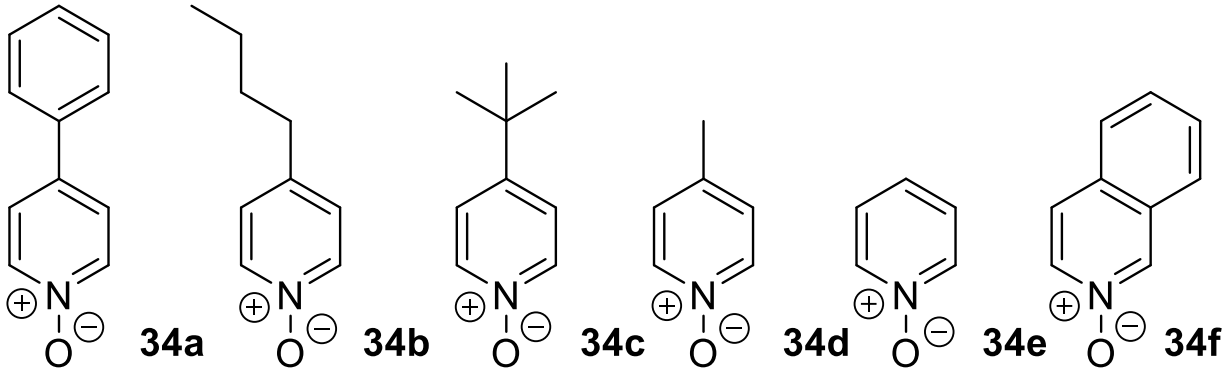

Figure 23. The investigated pyridine *N*-oxides.

Table 5. Binding constants between host **33** and guests **34a-f**

Guest	Binding constant / M^{-1}
34a	$> 10^{7a}$, $2.6 \cdot 10^{9b}$
34b	$> 10^{7a}$, $3.7 \cdot 10^{8b}$
34c	$3.7 \cdot 10^{7b}$
34d	$6.1 \cdot 10^{6c}$
34e	$1.9 \cdot 10^{6c}$
34f	$7.1 \cdot 10^{6c}$

a. ITC estimation
b. pair-wise ^{1}H NMR competitive experiments
c. ITC determination

Sun *et al.*[56] started with the same C4P **30** and added a similar extension to the *p*-position of the phenyl of the *meso*-position resulting in **35**. Finally, to the alkylated *meso*-position a pyridinium group was added in the same way yielding the final C4P **36** (Scheme 25). **36** was used to bind Pd(II) with the aid of a ditopic pyridine *N*-oxide. One end of the *N*-oxide binds to the N-H of the cavity of **36**. The pyridyl-arms of the C4P are pointed away from the negatively charged *N*-oxide due to charge repulsion. When one equivalent of Pd(II) is added to the solution, it coordinates to both the other O-terminal of the *N*-oxide and the pyridyl **36** causing the pyridyl groups to close in on the top (Scheme 26). Thus, a 1:1:1 (**36**/*N*-oxide/Pd(II)) complex is formed.

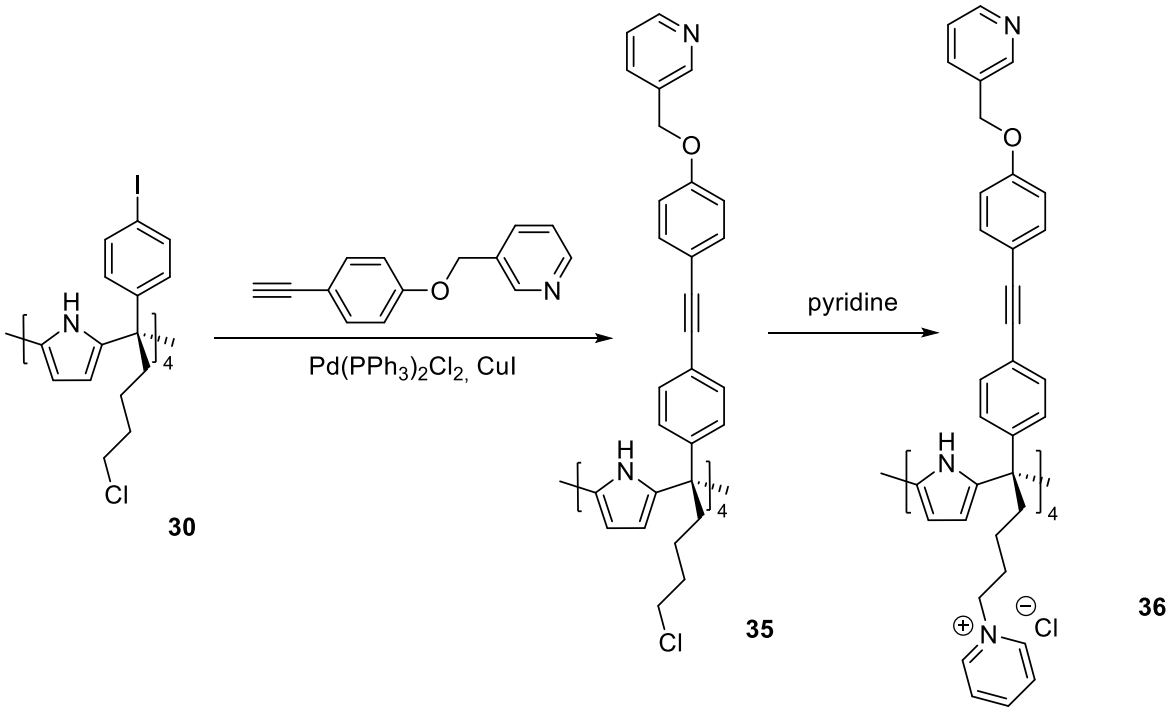

Scheme 25. Synthesis of super aryl-extended C4P **35**.

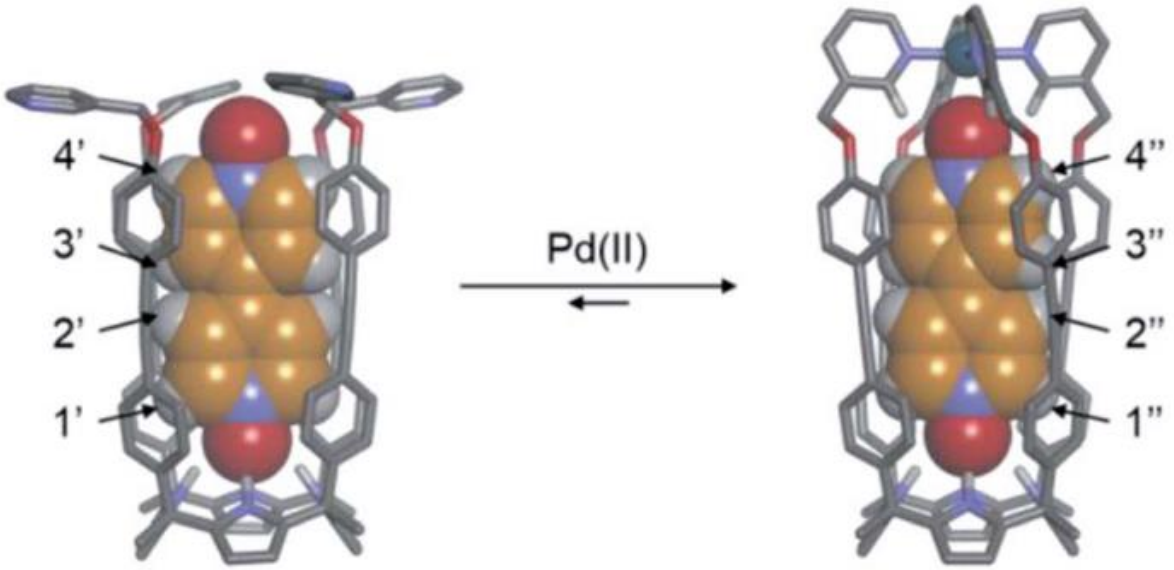

Scheme 26. The self-assembly of the **36**/*N*-oxide/Pd(II)-system. Reproduced from Ref. 56 with permission from the Royal Society of Chemistry.

6 Conclusions

C4As, resorcinarenes and C4Ps are versatile supramolecular hosts for different guests ranging from inorganic ions to more complex, biologically significant organic molecules like acetylcholine. They have easy syntheses which require only a catalytic amount of acid or base, and all have a huge range of possibilities for synthetic modifications either via the choice of their constituents (like the ketone in the case of C4P) or functionalization post-cyclization.

The synthesis of water-soluble C4As goes back nearly 40 years with the carboxylic acid-groups and their derivatives being added to the lower rim. These compounds were used in some early studies for cation extraction from one phase to another.

The development of water-soluble C4As grew in conjunction with the general research of the compound class. Sulfonation is an important way to achieve water-soluble C4As and resorcinarenes. Especially calixarenes sulfonated on the upper rim have been studied extensively. The sulfonated C4As bind many biologically significant molecules and their cytotoxicity has been studied somewhat. The compounds were shown to not be cytotoxic. Covalently joined C4A-dimers have been used in the formation of supramolecular polymers.

In addition to sulfonation and carboxylation the addition of other negatively charged groups has been used to solubilize C4As. Phosphonation creates water-soluble C4As, which have been used to create nanorafts. The charge-bearing groups are affected by the pH of the solution, which may limit their solubility at a lower pH.

Synthetic methods are not the only methods used to solubilize compounds. Amphiphilic C4As have been co-micellized with acyclic amphiphiles resulting in solubilization of the C4A. The use of host molecules in micelles have potential, since supramolecular assemblies can be used to carry drugs within the human body. Like C4As, resorcinarenes have also been included into micelles. A carboxylic acid-containing resorcinarene was co-micellized with CPC, which can form nanosized assemblies through aggregation.

The utility of the co-micellization between an amphiphile and a resorcinarene has also been investigated. The lanthanoid-binding ability of a resorcinarene was used in a micelle. A sulfonated resorcinarene was co-micellized with Triton X-100 and the cloud point extraction of lanthanoids (La(III), Gd(III) and Yb(III)) by the micelles were investigated using

spectrophotometry. Including the compound into a Triton X-100 micelle improved the La(III) and Gd(III) extraction by the micelle from water significantly.

Resorcinarenes are unique in that they have three distinct positions (upper rim, lower rim and the OH-groups on the resorcinol) from which they can be functionalized. Researchers have added sulfonato-groups into all three of these positions. Sulfonation in any of the three positions results in water-soluble compounds.

Chiral sulfonated resorcinarenes were used in resolving enantiomers of chiral compounds from aqueous solution using NMR. To a lower rim-sulfonated resorcinarene different proline-derivatives and pipecolic acid were added on its upper rim. The enantiomeric discrimination of all of resorcinarenes were investigated. The pipecolic acid-functionalized resorcinarene was shown to be the best at resolving enantiomers from a mixture for the majority of the investigated guests.

Resorcinarenes bind cations of different sizes and they can be modified to be selective for a specific cation, for example heavy metal cations that must be removed from environments due to their toxicity to aquatic life. A resorcinarene that was selective for mercury (out of mercury, cadmium, lead and copper) was synthesized.

In stark contrast to C4As, the chemistry of the C4P is significantly younger. The efforts to solubilize them in water dates back only just over 10 years. The use of ionizable groups (namely, acidic groups) in the solubilization of C4Ps initially suffered from restrictions concerning the pH of the aqueous solution, as at low pH the groups protonate, and the compound precipitates out. This is a problem with applications, as usually environments of interest (waterways, the human body) are acidic. Researchers overcame this hurdle with the use of permanently ionized groups like pyridinium-groups in the *meso*-position of C4Ps, which allow for water-solubility in any pH. The same has been done to resorcinarenes with the same result.

Meso-aryl-extended C4Ps are good hosts to investigate due to many different reasons. Firstly, the aromatic moiety can easily be functionalized further due to the functional groups which are introduced with the choice of ketone in the macrocyclization-step. The late introduction of the ionizable groups means that chromatographic resolution of the isomers of C4Ps as organic soluble derivatives is possible, yielding specific isomers.

Secondly, because of the deeper cavities, aryl-extended C4Ps have NH-groups which are very shielded from solvation by water molecules. The binding of polar guests in the cavity is enhanced since there is less competition by water on the binding sites of the host.

Finally, hydrophobic, or aromatic guests enjoy the deep cavity, which offers a large concentration of π-electrons. Due to this, aryl-extended C4Ps like **25** are great at binding pyridine *N*-oxide and its derivatives. The combined binding of the *O*-terminus and hydrogens on the pyrrole subunits in addition to the association between π-electrons on the aromatic cavity and the aromatic body of the guest result in high binding constants in the order of 10^4-10^6 M^{-1}.

EXPERIMENTAL PART

1 Introduction and aim of work

Calix[4]pyrroles (C4Ps) are macrocyclic molecules which are made of pyrrole units joined by alkyl bridges, and they can act as hosts for anionic and neutral guests. Through the years of investigation, C4Ps have been outfitted with many different functional groups.[12] Aryl-extended C4Ps have been functionalized with aryl groups and they can interact with guests through π-π-interactions.[57]

Polyethylene glycol (PEG) are a class of polyether molecules, with the general formula $C_{2n}H_{4n+2}O_{n+1}$. PEGs often exist as a mixture of different length polymers, where *n* is the average length of the chain. For example, for PEG900 the average *n* is 22. PEGs are water soluble. Functionalizing C4Ps with oligoethylene glycol or polyethylene glycol arms could increase their solubility and allow them to form micelles and to partake in co-micellization with other amphiphiles.

The widely used non-ionic detergent family Triton X (Figure 24) forms micelles and can be used to solubilize poorly water-soluble compounds. Triton X has the formula $C_{14}H_{22}O(C_2H_4O)_n$. The number of oxyethylene subunits (8 for Triton X-114 and 9-10 for Triton X-100) affect the properties of the detergents.[58] For example the aggregation numbers are also different for the detergents; 142 for Triton X-100 and 220 for Triton X-114.[59]

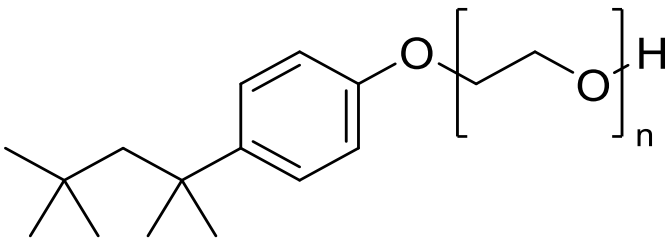

Figure 24. The general formula of Triton X.

Many micelle-forming nonionic detergents, including Triton X, have a property called cloud point. When the temperature of the solution is raised, at a specific temperature (unique to the solution) the micelles in solution start to aggregate. This can be due to the hydrophilic ends of the amphiphiles getting dehydrated, which promotes the micelles to join. The aggregates become so large that they become insoluble, and they separate into their own phase.[44] The

cloud point of Triton X -solutions are affected by additives in the solutions. An example of an additive is cetyltrimethylammonium bromide (CTAB). It is a cationic quaternary ammonium salt, which increases the cloud point of both Triton X-100 and X-114 solutions.[58]

The phase separation of an amphiphilic system can be utilized in a cloud point extraction. The analyte is bound to the micelles and the solution is heated to cloud point temperature. It is then centrifuged, which causes the micelles or their aggregates to lay in the bottom and the supernatant can be removed giving access to the analyte.[41]

The aim of the work was to synthesize an aryl-extended C4P (**1**) and use it to make potentially water-soluble C4Ps (**2-4**) utilizing two low molecular weight PEG monomethyl ethers (mPEG4 and mPEG2) and one higher molecular weight PEG, PEG900 (Scheme 27). They were characterized with various methods; infrared spectroscopy (IR), nuclear magnetic spectroscopy (NMR) and electrospray ionization mass spectrometry (ESI-MS).

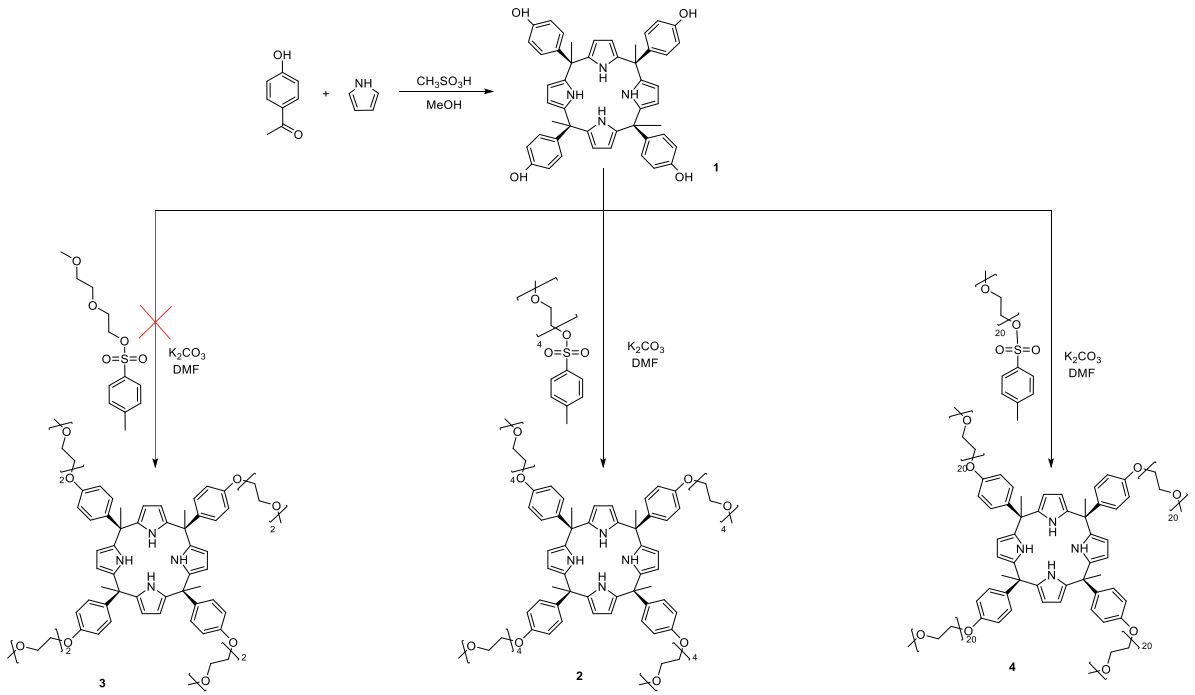

Scheme 27. The syntheses performed or attempted in the work.

1 and **2** were solubilized in aqueous solutions with the detergents Triton X-100 and Triton X-114. The effect of C4Ps on the size and clouding of micelles were studied using different methods, including cloud point temperature observations, atomic force microscopy (AFM) and dynamic light scattering (DLS). **4** was partially soluble in water. The micelle sizes of it in aqueous solutions were measured using DLS with no added Triton X.

DLS takes advantage of the random movement of particles in a suspension diffusing randomly due to Brownian motion. The diffusion coefficient *D* of this motion for a particle of a fixed hydrodynamic diameter *d* can be solved from the Stokes-Einstein-equation (3). The hydrodynamic diameter is the diameter of a sphere which experiences the same force (drag) when moving through a solution as the particle in question. Consequently, the diameter of a particle can be solved when the diffusion coefficient, temperature, and the viscosity η of the solvent are known.[60]

$$D = \frac{k_B T}{3\pi\eta d} \tag{2}$$

During a DLS measurement the sample of micelles is irradiated with a monochromatic laser. The particles in the solution scatter the light and interfere with each other creating an intensity reading. The machine measures the similarity between the interference pattern at different points in time using a digital correlator by comparing the correlation of the intensity to the beginning of the measurement. Since smaller particles move faster the intensity pattern changes faster and vice versa for large particles. When enough time passes, the readings do not correlate at all. The rate of change of the correlation is used to calculate the diffusion coefficient and other variables are used to solve the diameters of the particles in the solution.[60,61]

When Triton X co-micellizes with some compound, there may be a range of different sized micelles. A value that illustrates this is the polydispersity index (PDI), also known as dispersity. The dispersity is an indication of the homogeneity of the size of the micelles. Oftentimes, a monodisperse solution of micelles (meaning lower PDI) is more desirable for applications.

Since DLS gives the hydrodynamic diameter of a particle with diameter *d*, the machine approximates the micelles as spheres. This however is not always the case, because Triton X has been seen to have non-spherical micelles.[62] The morphology of the micelles was studied with AFM.

2 Materials and instrumental methods

2.1 Reagents, solvents, and instruments used

The reagents and solvents used in the work are in Table 6 and Table 7. The instruments used are in

Table 8.

Glassware and K_2CO_3 were dried in a 120 ºC oven for at least 2 hours before use. For reactions in dry conditions the N_2 atmosphere was established with a balloon. Pyrrole was distilled before use.

Table 6. Reagents used in the work

Reagent	**Supplier**	**Purity / %**
CTAB	Sigma	≥99
4-hydroxyacetophenone	Merck	-
K_2CO_3	VWR	99.8
methane sulfonic acid	Sigma-Aldrich	≥99.0
mPEG4-OH	Fluorochem	-
NaOH	VWR	> 98.5
Na_2SO_4	Fischer	≥99
PEG900-Ts	Aldrich	-
p-toluenesulfonyl chloride	Aldrich	98
pyrrole	TCI	>99
triethyl amine	Sigma-Aldrich	99.5
Triton X-100	Sigma-Aldrich	-
Triton X-114	Sigma-Aldrich	-

Table 7. Solvents used

Solvent	Supplier	Purity / %
acetic acid	VWR	99.9
acetonitrile	From MBraun MB-SPS-800	-
chloroform	Fischer	≥ 99.8
dichloromethane	VWR	100.0
diethyl ether	VWR	> 99.7
dimethyl formamide, anhydrous	Acros Organics	99.8
ethanol	ETAX	99.5
methanol, anhydrous	Sigma-Aldrich	99.8
methanol		
tetrahydrofuran	Honeywell	≥ 99.9
toluene	VWR	100.0

Table 8. Instruments used

Method	Instrument
atomic force microscopy	Bruker Dimension Icon AFM
block heater	Thermo Scientific Dry Bath
flash chromatography	Teledyne ISCO CombiFlash NextGen 300
dynamic light scattering	Malvern Panalytical Zetasizer Ultra
infrared spectroscopy	Bruker Alpha II
mass spectrometry	Agilent 6560, ESITOF
nuclear magnetic resonance	Bruker Avance III 500 MHz

2.2 Micelle solution preparations

Stock solution of Triton X-100 was prepared by dissolving 0.9965 g into 100 ml of ultrapure water (1.00 w/V %).

Stock solution of Triton X-114 was prepared by dissolving 1.0662 g into 100 ml of ultrapure water (1.07 w/V %). Since the cloud point of Triton X-114 is below room temperature, CTAB had to be added to raise it. 50 ml of the stock was moved to an Erlenmeyer and 5.19 mg of CTAB was added.

Stock solution of **1** was prepared by dissolving 48.39 mg into 1 ml of methanol. Stock solution of **2** was prepared by dissolving 54.50 mg into 1 ml of methanol.

Sample solutions were prepared by pipetting different amounts (**Error! Reference source not found.**) of C4P solutions to 3 ml of aqueous Triton solution and adding methanol until the total volume of the samples were 3.1 ml.

A solution of **3** for DLS measurements was made by adding 4.68 mg into 1 ml of ultrapure deionized water. The oil was not completely soluble, so the mixture was filtered using a syringe filter with 0.22 µm pore size. A dilution series of **3** was made by measuring the prepared solution using DLS and diluting with ultrapure water incrementally.

2.3 Cloud point method, DLS measurements and AFM sample preparation

In cloud point observations, the prepared sample vials were heated in one-degree increments using a block heater. The vials were allowed to equilibrate for about two minutes at each temperature. The cloud point was determined to be the temperature at which turbidity in a vial was observed.

The hydrodynamic diameters and particle concentrations of the prepared samples were measured with DLS. Experimental details of all DLS measurements are in Table 9.

For AFM measurements the sample with 2.43 % of **1** in Triton X-100 was diluted 50 times with 3.33 % Methanol in ultrapure water. Silica and mica were used as the substrate for the AFM measurements and micelle deposition. 30 µl of the solution was pipetted on a mica plate and 10 µl was pipetted onto a silica plate. The plates were left in a chamber saturated with water vapor for an hour. Two of the plates (mica and silica) were then rinsed gently two times with 500 µl of ultrapure water and one plate (mica) was left unrinsed.

Table 9. Parameters for DLS-measurements

Parameter	Value
Temperature	25 °C
Equilibration time	30 seconds
Cuvette	Malvern Panalytical DTS0012
Beam angle, size measurement	Backscatter
Beam angle, particle concentration	Multi-angle
Absorbance	0.01
Refractive index, Triton-containing samples	1.49
Refractive index, samples of **3**	1.458

3 Synthetic methods and reaction schemes

C4Ps are synthesized by a one-pot condensation reaction between a ketone and pyrrole in acidic conditions. As is often the case in macrocyclization reactions, the formation of the C4P competes with the formation of a polymer, in which the pyrrole and alkyl bridge units alternate indefinitely without the macrocycle closing. The formation of the C4P can be promoted by slowing the reaction down. Adding the acid slowly and/or diluting it can limit the amount of polymers forming.

A four-walled *αααα*-4-hydroxyphenyl-C4P **1** was synthesized using a methanesulphonic acid-catalyzed condensation reaction between 4-hydroxyacetophenone and pyrrole (Scheme 28).[63] Different configurational isomers of C4Ps have different chemical properties. The solubility of the isomers varies which allows separation of isomers using recrystallization from solution. In this work, two recrystallizations were used to purify the product into pure *αααα*-isomer. Recrystallization from acetic acid results in the *αααα*-isomer to crystallize and the other isomers to remain in solution. Recrystallization from ethanol/water-solution was used to remove the excess acetic acid.

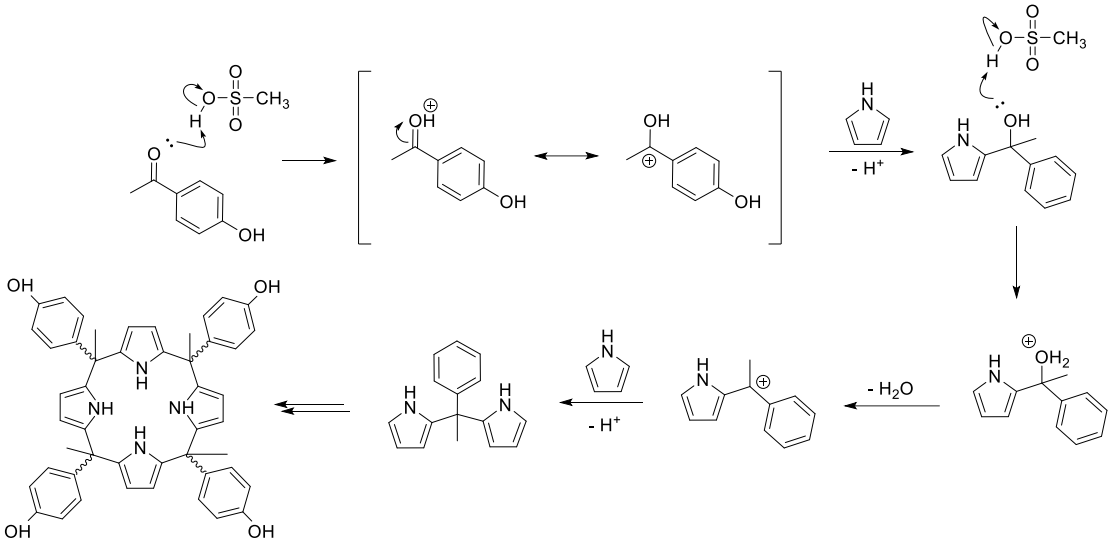

Scheme 28. Proposed reaction mechanism of the condensation reaction to form **1**.

After the recrystallizations **1** was functionalized using ether-forming reactions in basic conditions. Three different PEGs (two of which were short chain low-molecular weight and one heavier) were used during the work: mPEG4, mPEG2 and PEG900 (Scheme 29).

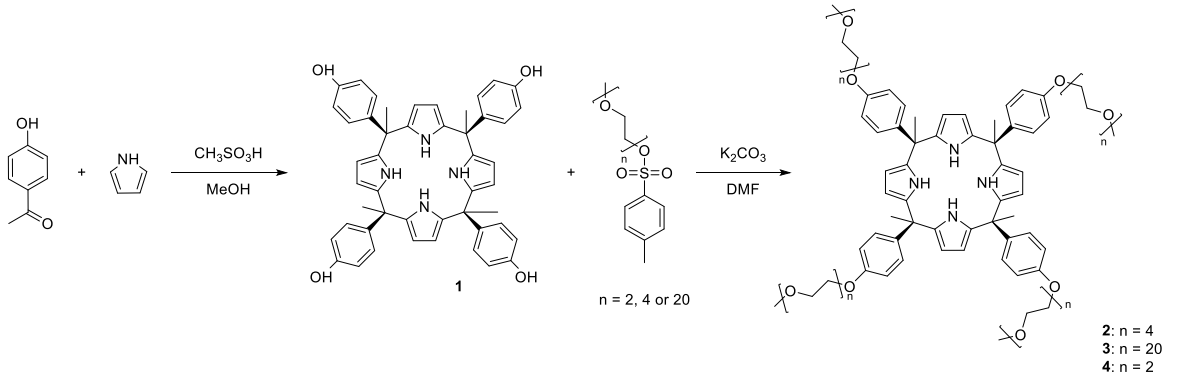

Scheme 29. Synthesis of 1 and its functionalization with three PEGs.[64]

The PEGylation of the C4P **1** is an S_N2 reaction, where the potassium carbonate deprotonates the OH groups of **1** which can then perform a nucleophilic attack on the tosylated PEG. In Scheme 30 is the reaction mechanism of the PEGylation of one position on **1** by mPEG2.

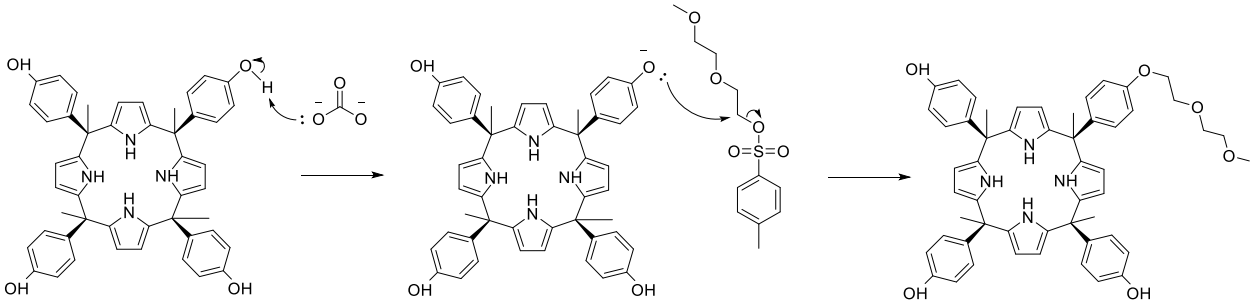

Scheme 30. Reaction mechanism of the PEGylation of one arm of **1** with mPEG2.

Tosylation of mPEG4-OH was performed (Scheme 31). The tosylation was done in basic conditions.

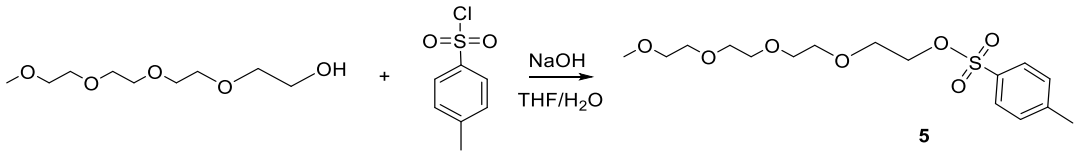

Scheme 31. Tosylation of mPEG4-Ts.

The PEGylation with mPEG2-Ts was attempted on a two-armed calix[4]pyrrole **7** (Scheme 32).

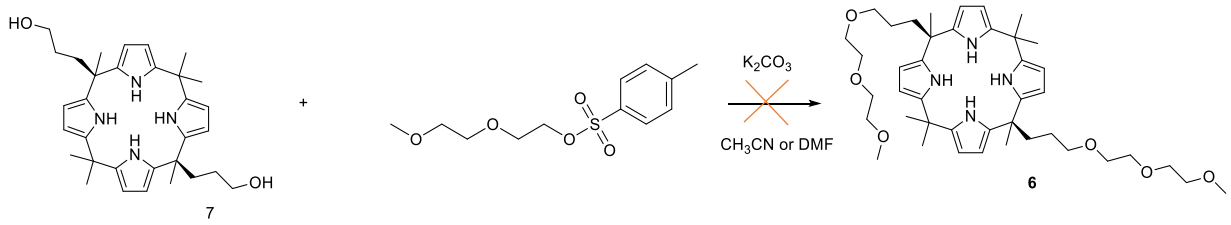

Scheme 32. The PEGylation of a two-armed C4P **7** with mPEG-2-Ts.

4 Syntheses

4.1 Four-walled *αααα*-4-hydroxyphenyl-C4P, 1[63]

Details per synthesis are in Table 10. General synthetic procedure:

p-Hydroxyacetophenone (1.1-2.5 g, 1 eq.) was added to an oven dried two-necked round bottom flask and N_2 atmosphere was established. Dry methanol (22 ml per 1 g ketone) was added. To the flask, freshly distilled pyrrole (1.1-1.2 eq.) was added. Methanesulphonic acid (0.5 eq.) was added dropwise within 5 minutes. Reaction was stirred at room temperature overnight. Reaction was quenched with triethyl amine (0.5 eq.) and diluted to half concentration with chloroform.

An initial purification to remove unreacted material was done with manual column with 50/50 methanol/chloroform as eluent and 30 g of silica per 1 g of crude. Product-containing fractions were recognized with thin-layer chromatography and combined, the solvent was evaporated, and residue dried in vacuum.

Product was recrystallized from acetic acid (6 – 15 ml per 1 g of crude) at 85 °C. Mixture was cooled to room temperature, covered with parafilm with holes and put to fridge (4 °C) for a few hours. The mixture was filtered with suction and precipitate which formed upon cooling was dried in a round bottom flask.

Product was recrystallized from 21/79 water/ethanol (10 ml per 1 g of crude) at 67 °C. Solution was cooled to room temperature and put to fridge to cool down. Precipitate was filtered with suction and washed with cold solvent mixture. Product was transferred to a vial and dried in vacuum overnight.

Table 10. Syntheses of **1**.

Entry	**Ketone (g / mmol)**	**Pyrrole (ml / mmol)**	**Acid (ml / mmol)**	**Yield 1 (g / %)[a]**	**Yield 2 (g / %)[b]**	**Yield 3 (g / %)[c]**
1	1.1829 / 8.7	0.65 / 9.4	0.3 / 4.6	1.6967 / 105	0.5620 / 35	0.022 / 1
2	2.5159 / 18.5	1.5 / 21	0.6 / 9.2	3.4835 / 102	0.4662 / 14	- [d]
3	2.4043 / 17.6	1.4 / 20	0.6 / 9.2	3.1738 / 97	0.8914 / 27	0.1845 / 6
4	2.3627 / 17.4	1.4 / 20	0.6 / 9.2	3.2977 / 103	1.3891/ 43	0.3384/ 11

a. after precolumn
b. after first recrystallization
c. after second recrystallization
d. no product recovered.

^{1}H NMR (DMSO-d6, 500 MHz, 30 °C)

δ (ppm): 1.71 (s, 12H), 5.92 (d, *J* = 2.51 Hz, 8H), 6.62 (d, *J* = 8.7 Hz, 8H), 6.69 (d, *J* = 8.7 Hz, 8H), 9.23 (s, 4H), 9.43 (s, 4H)*

*Solvent peaks (ppm): 1.06 (ethanol), 1.91 (acetic acid), 3.32 (water), 3.44 (ethanol)

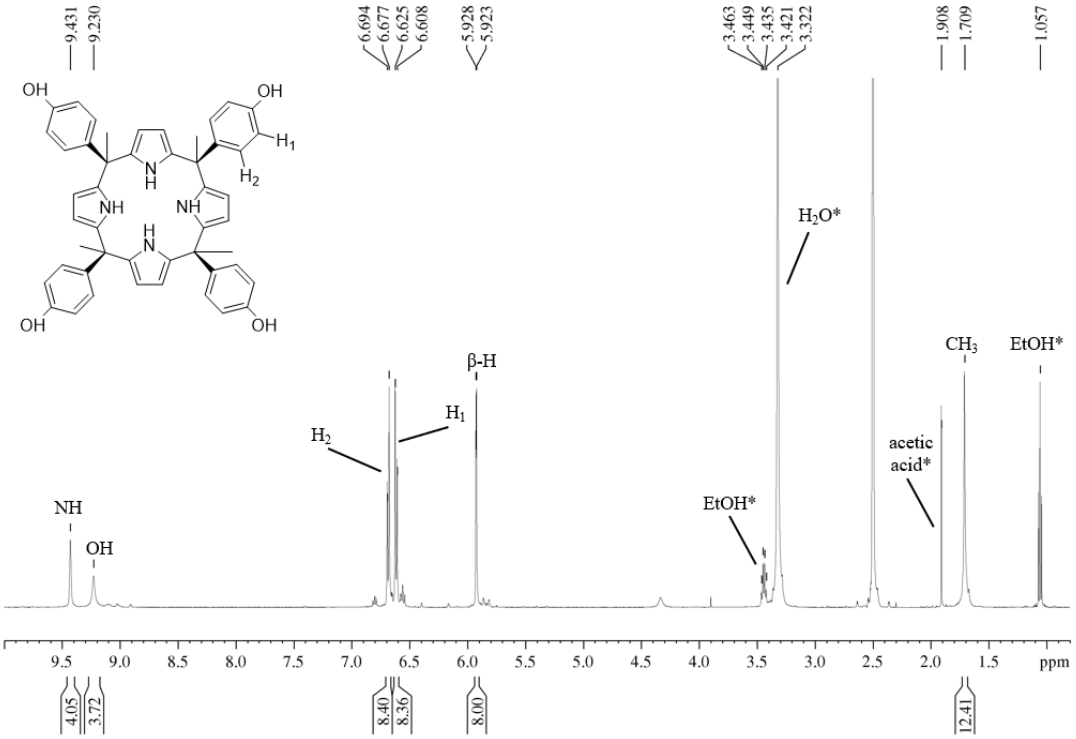

^{13}C NMR (DMSO-d6, 125 MHz, 30 °C)

δ (ppm): 31.5, 43.3, 104.2, 114.8, 127.9, 137.4, 140.4, 155.9*

*Solvent peaks (ppm): 18.5 (ethanol), 21.0 (acetic acid), 56.00 (ethanol)

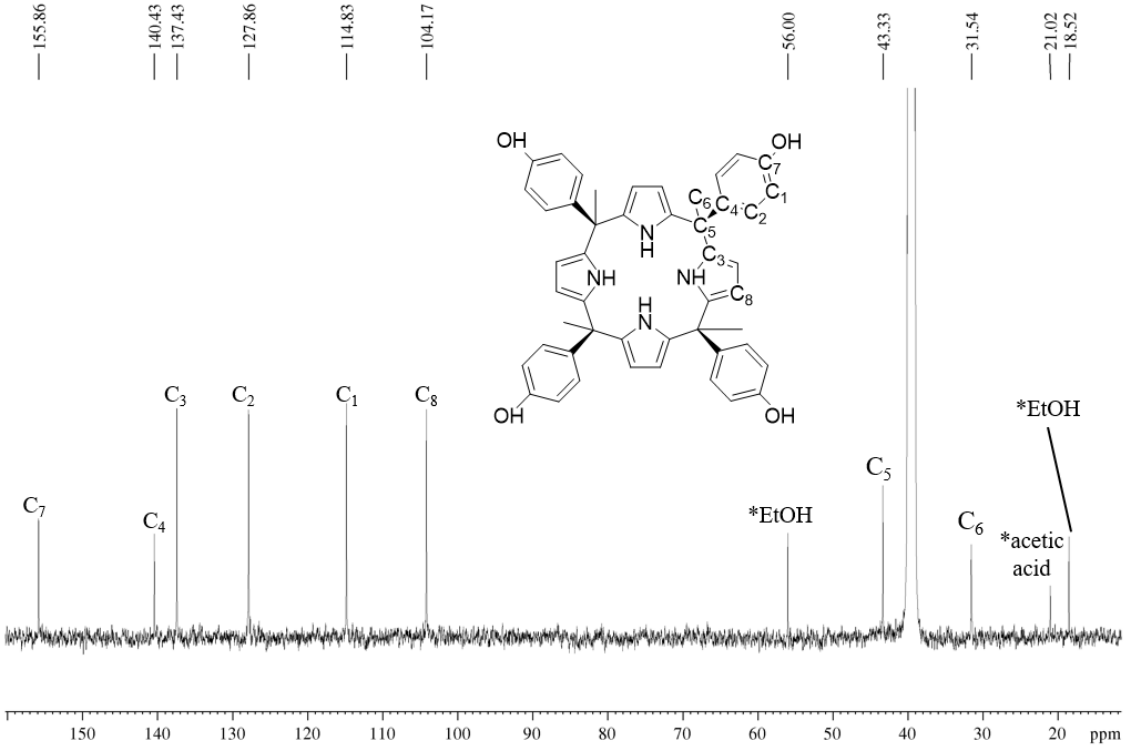

IR (cm^{-1}): 3370 (O-H stretch), 1684 (C=C), 1592 (N-H bend), 1361 (O-H bend)

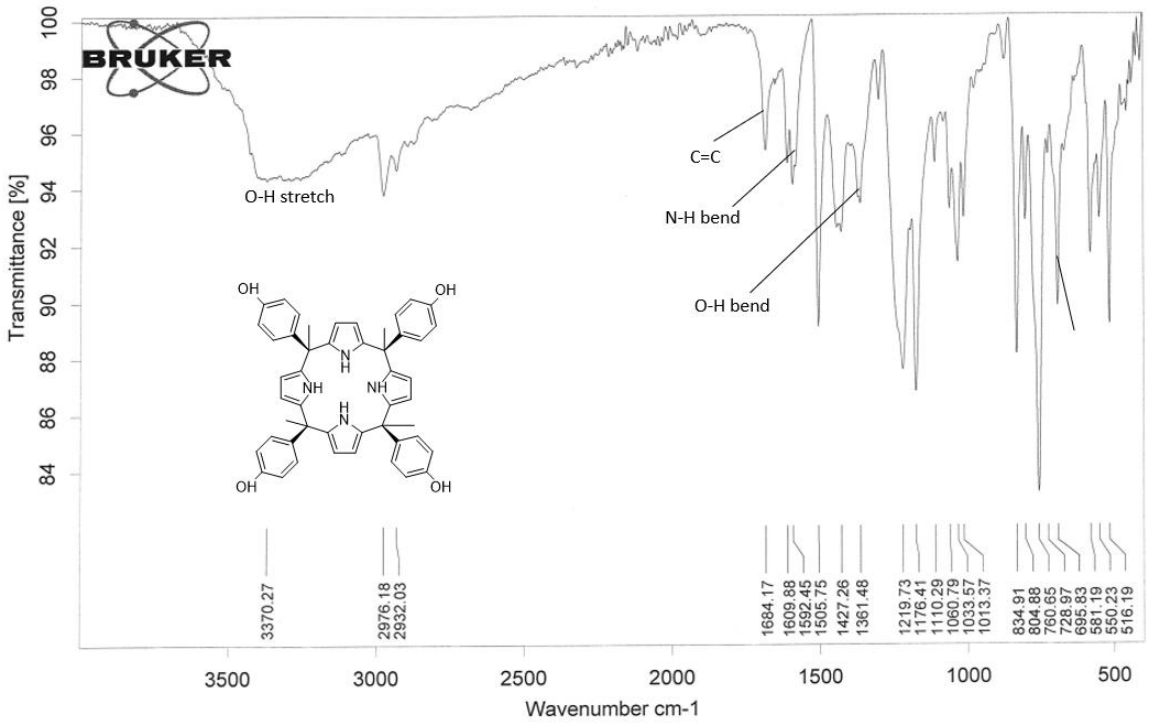

4.2 mPEG4-Ts, 5[65]

mPEG4-OH (5 ml, 5.35 g, 25.7 mmol, 1 eq.) was dissolved into 9 ml of tetrahydrofuran in a 250 ml round bottom flask. The flask was cooled to 0 °C and N_2 atmosphere was established. NaOH (1.7122 g, 42.8 mmol, 1.7 eq.) was dissolved into 9 ml of deionized water and added via a dropping funnel. Solution was stirred for 30 minutes at 0 °C. *p*-Toluenesulphonyl chloride (5.4090 g, 28.4 mmol, 1.1 eq.) was dissolved into 9 ml of tetrahydrofuran and added via a dropping funnel. Solution was warmed to room temperature and stirred for 18 hours. Reaction was diluted with 70 ml of diethyl ether.

Solution was washed in separatory funnel: three times with 10 ml of 1 M NaOH, two times with 20 ml of deionized water and once with 10 ml of brine. The organic phase was collected into an Erlenmeyer flask and dried over Na_2SO_4 while stirring. Solvent was evaporated with rotary evaporator and the residue was dried in vacuum overnight.

Mass of clear oil 5.1990 g (56 %).

^{1}H NMR (MeOD, 500 MHz, 30 °C)

δ (ppm): 2.45 (s, 3H), 3.35 (s, 3H), 3.52-3.56 (m, 6H), 3.59-3.62 (m, 6H), 3.65 (m, 2H), 4.14 (m, 2H), 7.44 (d, *J* = 8.2, 2H), 7.79 (d, *J* = 8.2 Hz, 2H)*

*Solvent peaks (ppm): 2.33 (tetrahydrofuran), 4.23 (water)

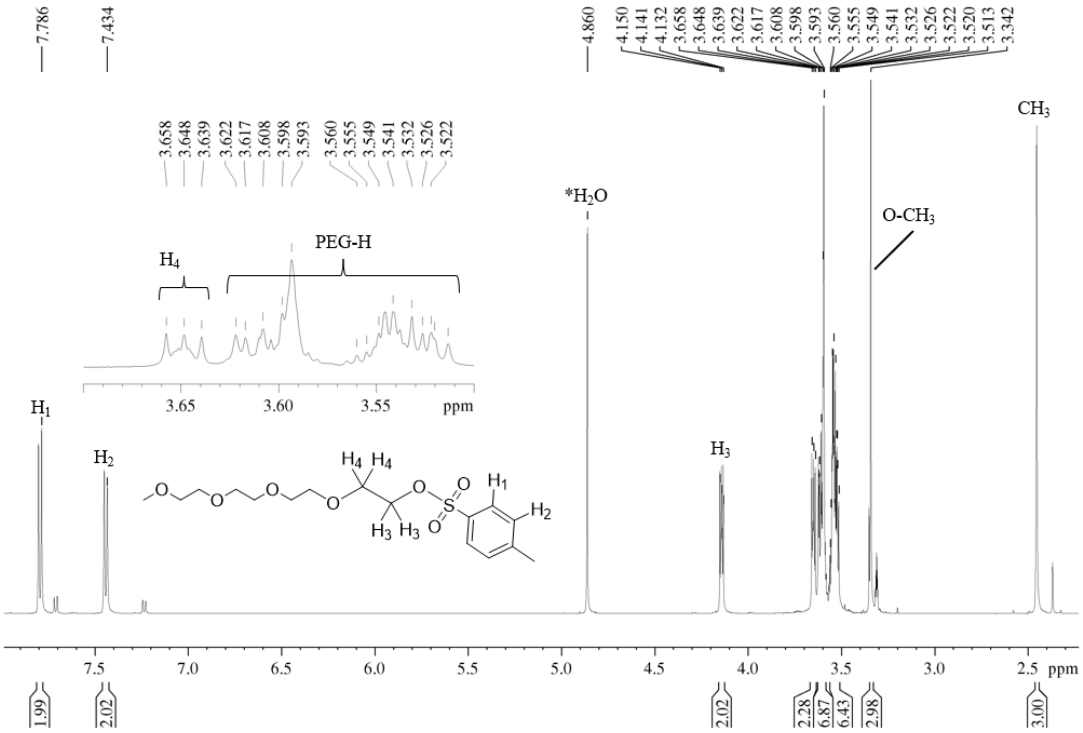

^{13}C NMR (MeOD, 500 MHz, 30 °C)

δ (ppm): 21.6, 59.1, 69.7, 70.9, 71.3, 71.5, 72.9, 126.9, 129.0, 129.8, 131.0, 134.4, 146.4

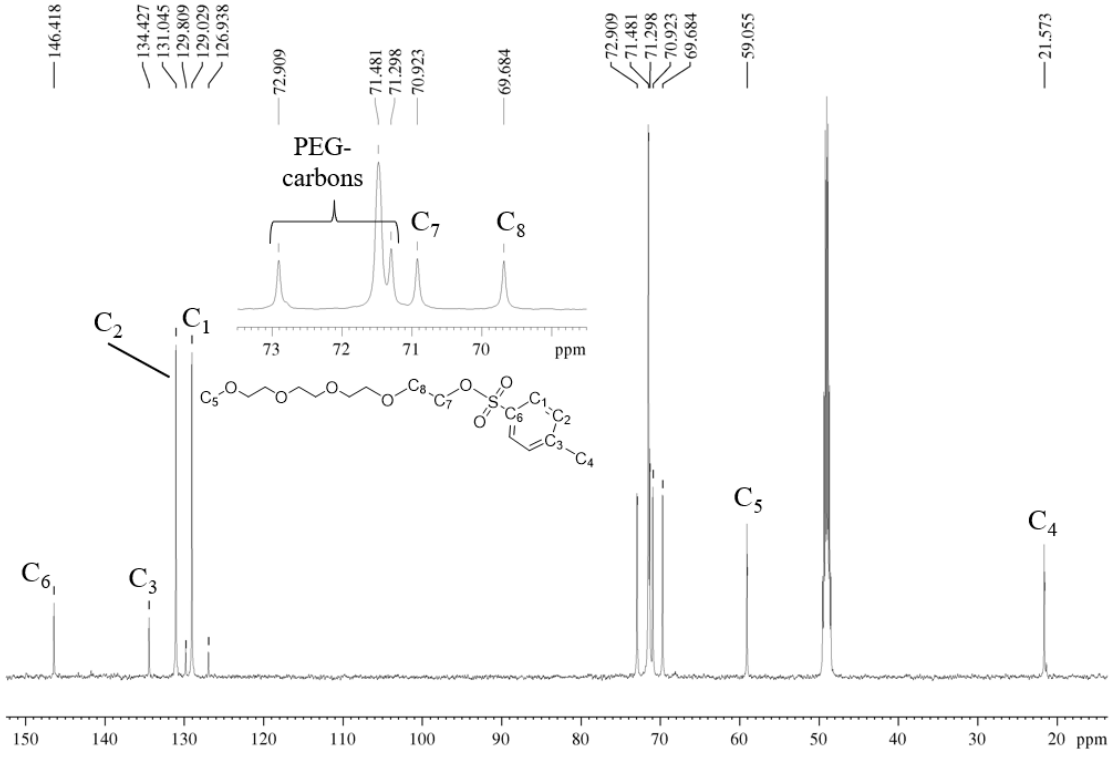

IR (cm^{-1}): 1353 (S=O stretch)

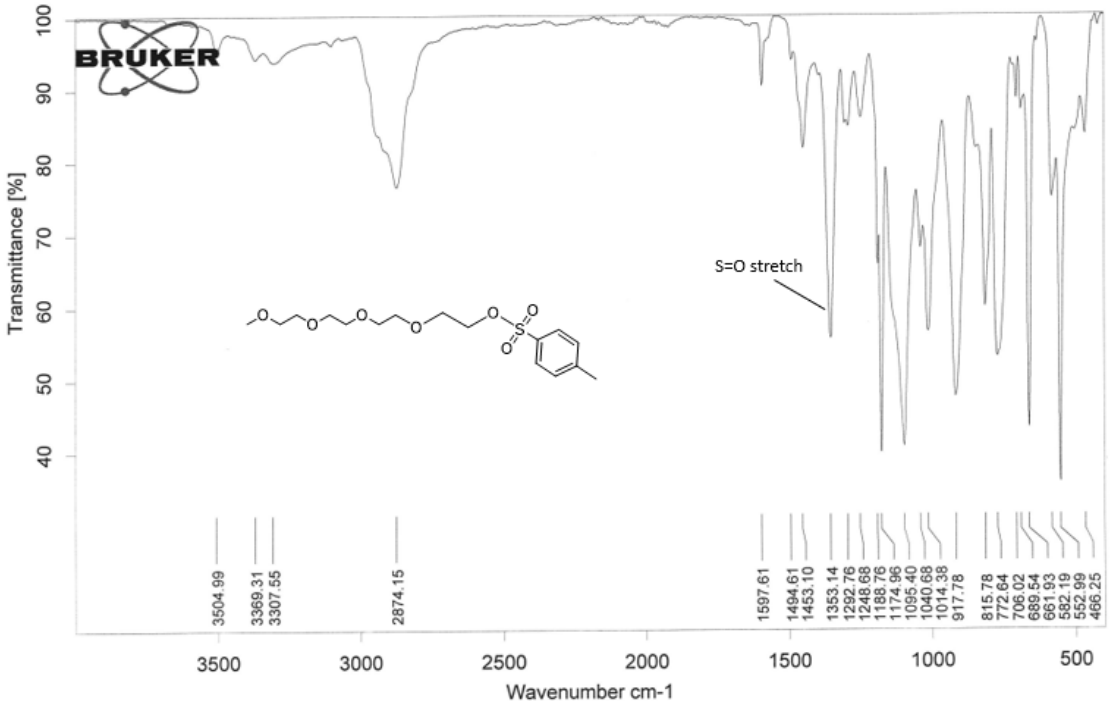

4.3 mPEG4-ylated C4P, 2

4.3.1 First synthesis

C4P **1** (38.7 mg, 52.2 µmol, 1 eq.) was added to a 25 ml two-necked flask. Dry K_2CO_3 (92.2 mg, 667.1 µmol, 12.8 eq.) was added. 1.7 ml dry dimethyl formamide was added. N_2 atmosphere was established, and the mixture was stirred for 35 minutes. mPEG4-Ts **5** (93.1 mg, 256.9 µmol, 4.9 eq.) was dissolved into 1.6 ml of dry dimethyl formamide and added to the flask. Reaction was stirred at 87 °C for 19 hours 25 minutes. Liquid from the flask was decanted to a 10 ml flask using a pipette, concentrated and co-evaporated with toluene. Residue was dried in vacuum overnight.

Residue was dissolved into methanol. Column purification was performed, with 30 g silica per 1 g of crude and eluent 8 % methanol in dichloromethane. Fractions were combined, solvent was evaporated and residue dried under vacuum. Mass of waxy residue 63.8 mg (81 %).

4.3.2 Second synthesis

C4P **1** (78.5 mg, 0.105 mmol, 1 eq.) was added to a 25 ml two-necked flask. K_2CO_3 (196.2 mg, 1.420 mmol, 13 eq.) was added. 3.4 ml dry dimethyl formamide was added. N_2 atmosphere was established, and the mixture was stirred for 30 minutes. Previously prepared mPEG4-Ts **5** (199.2 mg, 0.550 mmol, 5 eq.) was dissolved into 3.2 ml dry dimethyl formamide and added to the flask. Reaction was refluxed at 87 °C for 19 hours. Liquid from the flask was decanted to a 10 ml flask using a pipette. Dimethyl formamide was evaporated off using a rotary evaporator, doing co-evaporation with toluene. Residue was dried in vacuum overnight.

Residue was dissolved into methanol. Column purification was performed, with 30 g silica per 1 g of crude and eluent 8 % methanol in dichloromethane. Fractions were combined, solvent evaporated, and residue dried under vacuum.

Residue was dissolved into 4 ml methanol. 0.7 g of silica was added, and the solvent was evaporated with rotary evaporator. Flash chromatography was performed using 24 g R_f Gold column. Fractions were collected, solvent evaporated, and residue dried in vacuum.
Mass of waxy residue 67.6 mg (42 %).

^{1}H NMR (DMSO-d6, 500 MHz, 30 °C)
δ (ppm): 1.74 (m, 12H), 3.23 (s, 9H), 3.42-3.43 (m, 6H), 3.50-3.55 (m, 30H), 3.68 (m, 6H), 3.99 (m, 6H), 5.93 (d, *J* = 2.3 Hz, 8H), 6.64-6.92 (m, 16H), 9.20 (s, 1H), 9.40 (m, 4H)*
*Solvents: 3.23 (water)

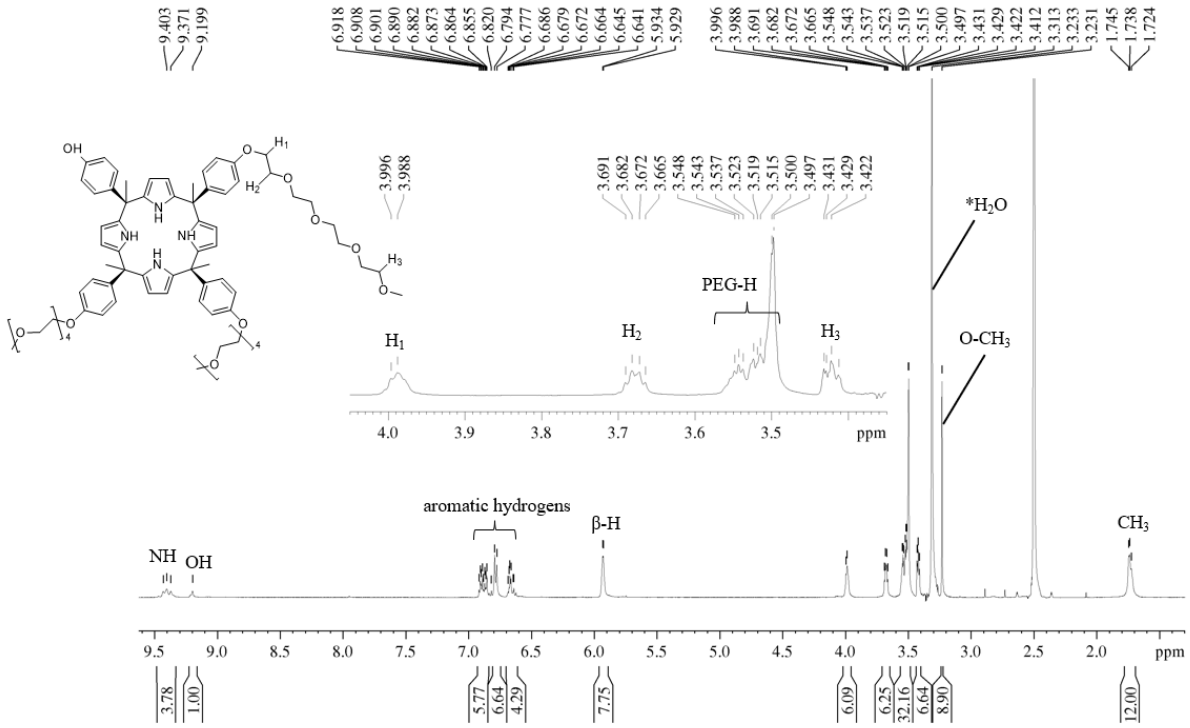

^{13}C NMR (DMSO-d6, 125 MHz, 30 °C)

δ (ppm): 31.3, 43.4, 58.0, 67.2, 68.8, 69.6, 69.8, 69.8, 71.3, 104.5, 114.3, 114.8, 127.9, 137.3, 142.2, 157.1

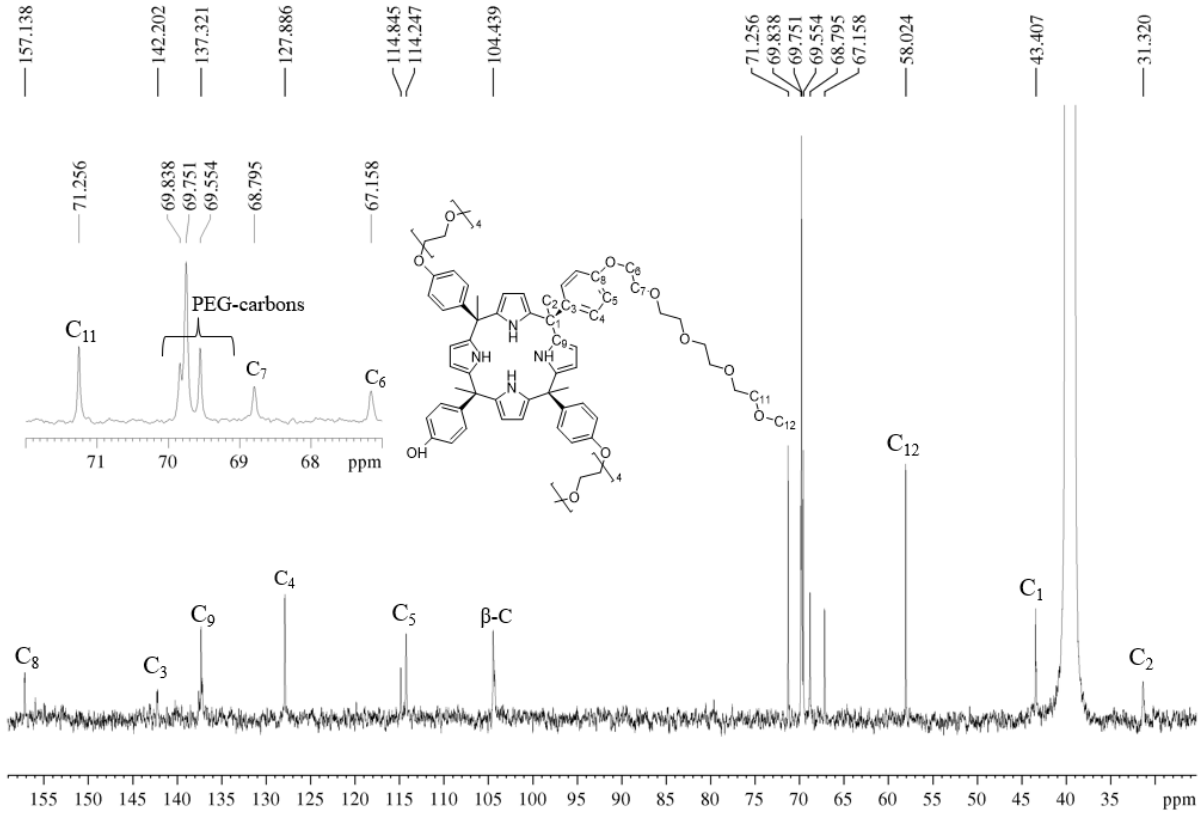

ESI-: *m/z* $[M-H]^-$ 1119.5678, $[M+Cl]^-$ 1535.7825

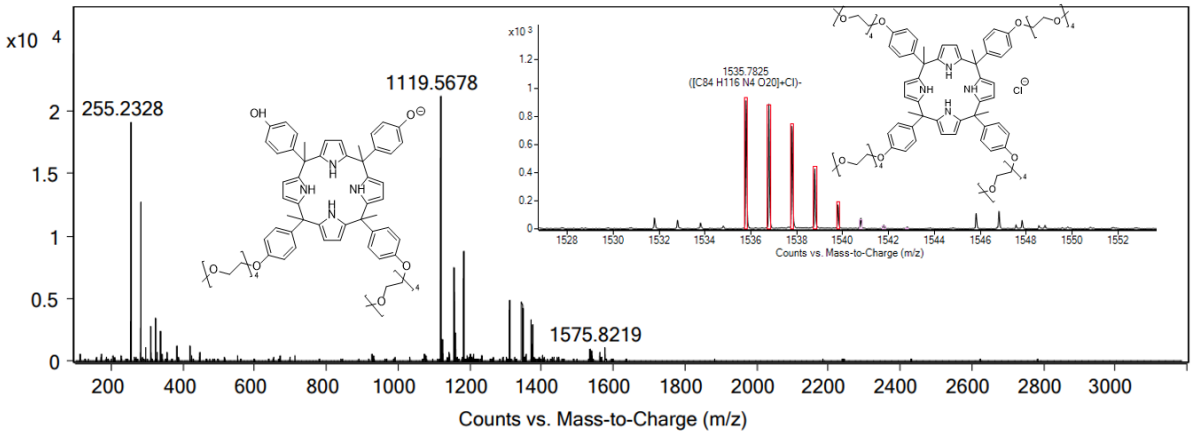

4.4 PEGylated C4P, 3

C4P **1** (38.9 mg, 52.5 µmol, 1 eq.) was added to a 25 ml two-necked flask. N_2 atmosphere was established. Dry K_2CO_3 (80.3 mg, 0.581 mmol, 12.1 eq.) and 1.6 ml of dry dimethyl formamide was added and the mixture was stirred at room temperature for 30 minutes. PEG900-Ts (0.2231 g, 0.248 mmol, 4.7 eq.) was dissolved into 1.7 ml of dimethyl formamide and added to the reaction. Solution was stirred at 87 °C for 18 hours. Solution was decanted out of the flask with a pipette and transferred to a 10 ml round bottom flask. dimethyl formamide was evaporated out by co-evaporation with toluene using rotary evaporator. Residue was dried under vacuum overnight.

Mass 0.2004 g (104 %).

Residue was dissolved into methanol. Flash chromatography was performed, with methanol in dichloromethane (column: 12 g R_f Gold). Product containing fractions were combined, solvent evaporated using rotary evaporator and residue dried in vacuum.

Mass of yellow oil 64.2 mg (33 %).

^{1}H NMR (DMSO-d6, 500 MHz, 30 °C)

δ (ppm): 1.72 (s, 12H), 3.24 (s, 16H), 3.40-3.44 (m, 14H), 3.46-3.57 (m, 292H), 3.59 (m, 2H), 3.64-3.72 (m, 12H), 3.96-4.02 (m, 4H), 4.10 (m, 2H), 5.97 (d, 8H), 6.60-6.69 (m, 11H), 6.77-6.90 (m, 8H), 9.50 (s, 2H), 9.38-9.45 (m, 4H)*

*Solvents: 2.01 (acetic acid), 2.89, 2.74 (dimethyl formamide), 3.31 (water), 7.95 (dimethyl formamide)

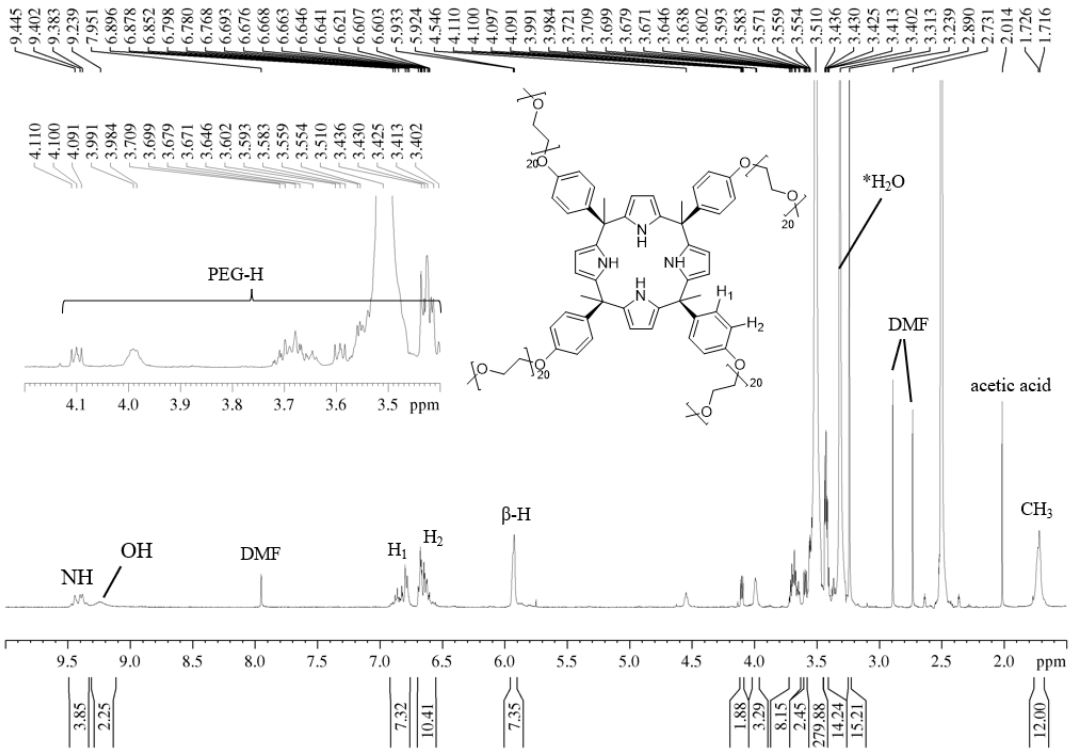

^{13}C NMR (DMSO-d6, 125 MHz, 30 °C)

δ (ppm): 31.4, 35.8, 43.3, 58.0, 60.2, 63.2, 67.1, 68.2, 68.8, 69.6, 69.8, 70.5, 71.3, 72.3, 104.2, 114.3, 114.8, 127.9, 137.5, 140.4, 142.5, 156.2, 157.6*

*Solvents: 20.8, 170.8 (acetic acid), 30.7, 35.8 (dimethyl formamide)

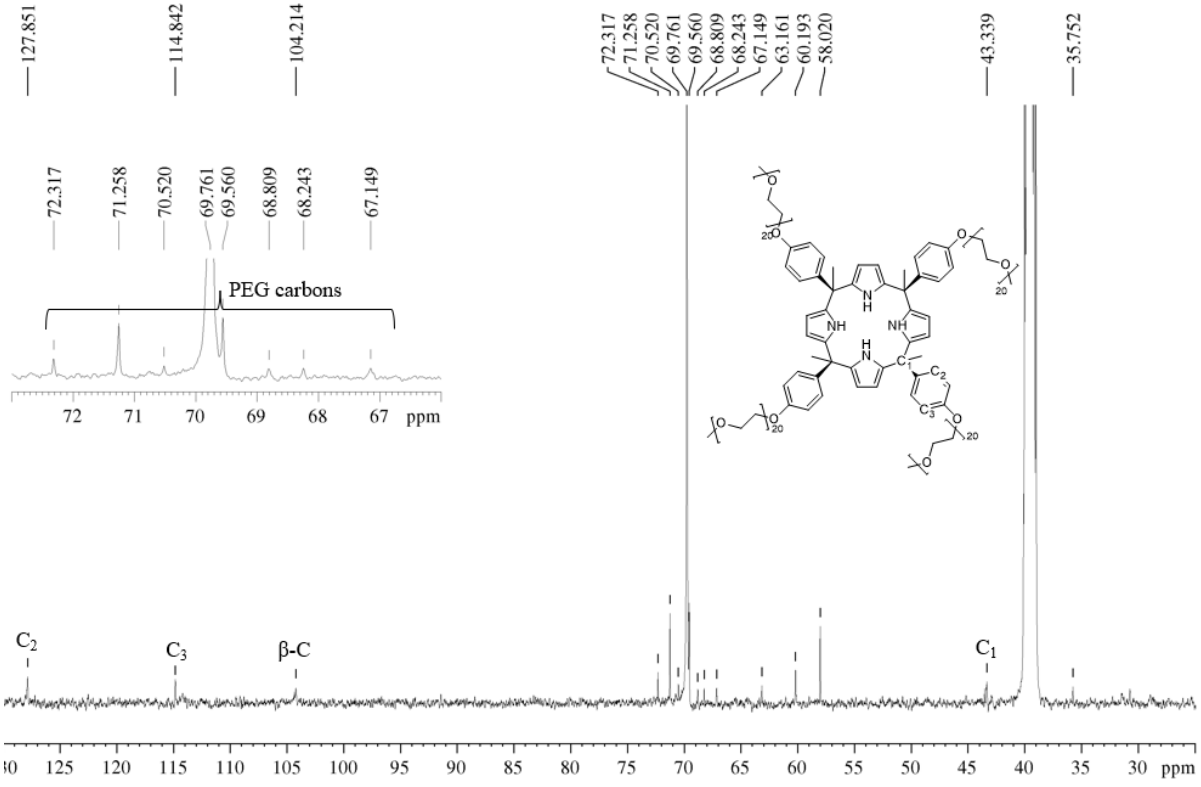

4.5 mPEG2-ylated C4P, 4

C4P **1** (80.0 mg, 108 µmol, 1 eq.) was added to a 25 ml two-necked flask. Dry K_2CO_3 (173.1 mg, 1.25 mmol, 11.6 eq.) and 3.2 ml dry dimethyl formamide were added. N_2 atmosphere was established, and the mixture was stirred for 30 minutes. Previously prepared mPEG2-Ts (121.2 mg, 442 µmol, 4.1 eq.) was dissolved into 3.2 ml dry dimethyl formamide and added to the flask. Reaction was stirred at 87 °C for 17 hours. Liquid from the flask was decanted to a 10 ml flask using a pipette. Dimethyl formamide was evaporated off using a rotary evaporator, doing co-evaporation with toluene. Residue was dried in vacuum overnight.

Mass of white solid 0.2495 g (201 %).
Solid was not soluble in toluene, methanol, dichloromethane, acetonitrile, tetrahydrofuran, ethanol, water or hexane. Product was added to deuterated methanol and filtered, which allowed ^{1}H NMR to be performed (**Error! Reference source not found.**). Due to the low solubility, purification of product was not performed.

4.6 mPEG2-ylated two-armed C4P, 6

4.6.1 In dimethyl formamide

C4P **7** (31.1 mg, 60.2 µmol, 1 eq.) was added to a 25 ml two-necked flask. N_2 atmosphere was established. Dry K_2CO_3 (96.4 mg, 697.5 µmol, 11.6 eq.) was added. 1.7 ml of dry dimethyl formamide was added and the mixture was stirred at room temperature for 30 minutes. mPEG2-Ts (38.5 mg, 140.3 µmol, 2.3 eq.) was dissolved into 1.7 ml of dimethyl formamide and added to the reaction. Solution was stirred at 86 °C for 40 hours 30 minutes. Solution was decanted out of the flask with a pipette and transferred to a 10 ml round bottom flask. dimethyl formamide was evaporated out by co-evaporation with toluene using rotary evaporator. Residue was dried under vacuum for two nights.

Residue was dissolved into 8 ml of ethanol. Silica column chromatography was performed, with 8 % methanol in dichloromethane. Fractions 7-15 were combined, solvent was evaporated, and residue dried in vacuum. Mass 63.3 mg.

Residue was dissolved into 1.5 ml of methanol. Column was performed, with 8 % methanol in dichloromethane and silica that was neutralized with triethyl amine. Fractions 5-15 were combined, solvent was evaporated, and residue dried in vacuum. Mass 21.2 mg.

Residue was dissolved into 1 ml of methanol. Column was performed, with 8 % methanol in dichloromethane. Product containing fractions were combined, solvent was evaporated, and residue dried in vacuum.

Mass of yellow solid 5.5 mg.

Based on mass spectrometry (**Error! Reference source not found.**), no product formed.

4.6.2 In acetonitrile

C4P **7** (28.7 mg, 55.5 µmol, 1 eq.) was added to a 25 ml two-necked flask. N_2 atmosphere was established. Dry K_2CO_3 (82.3 mg, 595.5 µmol, 10.7 eq.) was added. 3 ml of dry acetonitrile was added, and the mixture was stirred at room temperature for 30 minutes. mPEG2-Ts (59.3 mg, 216.2 µmol, 3.9 eq.) was dissolved into 3 ml of dry acetonitrile and added to the reaction. Solution was refluxed at 80 °C for 65. Solution was decanted out of the flask with a pipette and transferred to a 100 ml round bottom flask. Solution was diluted with 90 ml of ether.

Solution was washed in a 250 ml separatory funnel: three times with 10 ml of 1M NaOH and two times with 20 ml of water. Organic phase was transferred to an Erlenmeyer flask and dried over Na_2SO_4 while stirring. Solution was filtered, solvent was evaporated, and residue dried in vacuum.

Mass of yellow, thick oil 41.8 mg.

Based on ^{1}H NMR (**Error! Reference source not found.**), no product formed.

5 Cloud point observations

The successfully synthesized C4Ps **1** and **2** were chosen for the co-micellization with Triton X-100 and Triton X-114. They had to be added to the samples in methanol, since they were not soluble in water. Methanol is toxic and itself influences the cloud point of Triton.[66] Cloud point observations are in **Error! Reference source not found.**.

An attempt to make control solutions of **1** and **2** without Triton were unsuccessful since the compounds precipitated out of the methanol-water solvent. There is thus no knowledge if either **1** or **2** form micelles on their own.

Addition of **1** to solution of Triton X-100 lowered the cloud point of the solution (Figure 25). The cloud point was lowered down to room temperature, when the percentage of C4P **1** was raised to 16 %.

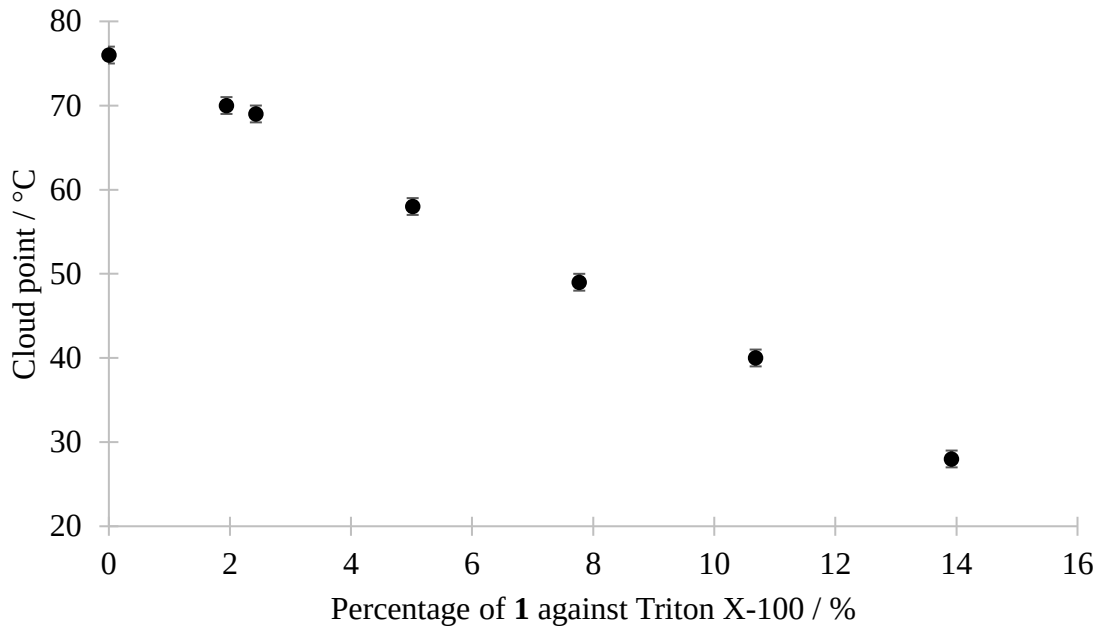

Figure 25. The cloud point of Triton X-100 with added **1**.

Adding **2** to Triton X-100 lowered the cloud point of the solution a lot less (Figure 26).

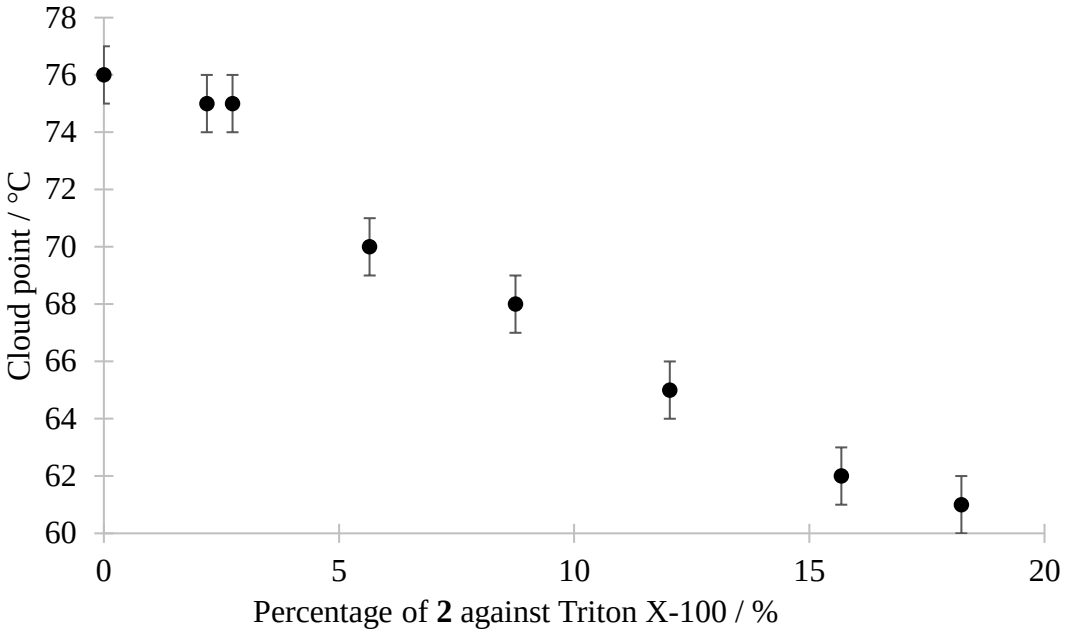

Figure 26. The cloud point of Triton X-100 with added **2**.

Interestingly, when **1** was added to Triton X-114 the cloud point was lower for a solution with 9 % C4P than it was for a solution with 11 % of **1** (Figure 27).

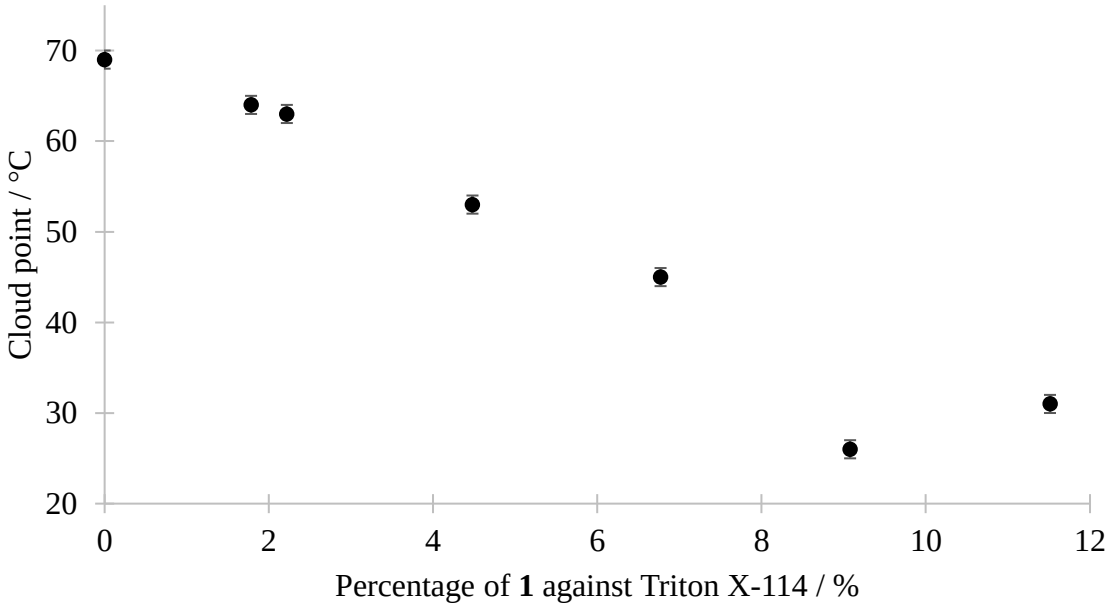

Figure 27. The cloud point of Triton X-114 with added **1** and CTAB.

Adding **2** to Triton X-114 caused the cloud point of the detergent solution to lower to near room temperature almost linearly (Figure 28).

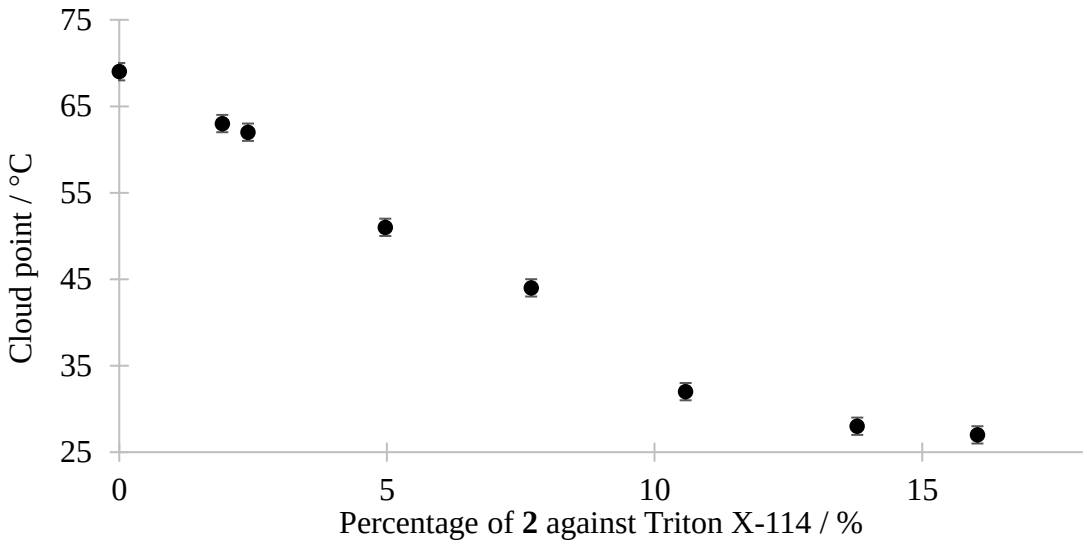

Figure 28. The cloud point of Triton X-114 with added **2** and CTAB.

Like **2**, PEG200 has been shown to raise the cloud point of both Triton X-100 and Triton X-114.[58] The average *n* for PEG200 is 4, so it is close to mPEG4. Thus, there is a difference in the addition of PEG-compounds versus PEG-functionalized C4Ps in the effect on the cloud point of the detergents.

Unlike in the case of the attempted control solutions, **1** and **2** did not precipitate out of any of the Triton X -containing solutions which means it is likely that the C4Ps are included within the micelles. The inclusion of the compounds into the micelles (either within or as a part of the micelle wall) protects the C4P from the aqueous environment.

6 DLS measurements

The prepared C4P-Triton samples were measured using DLS. Samples that were cloudy or close to cloud point at room temperature were not measured. The micelle sizes alongside their PDIs of all the measurements are in appendices**Error! Reference source not found.** and **Error! Reference source not found.**. Particle sizes from particle concentration measurements are in appendices**Error! Reference source not found.** and**Error! Reference source not found.**.

Adding **1** to Triton X-100 caused the diameter of the micelles to become significantly larger (Figure 29), from 6 nm to 32 nm. The peaks also got broader.

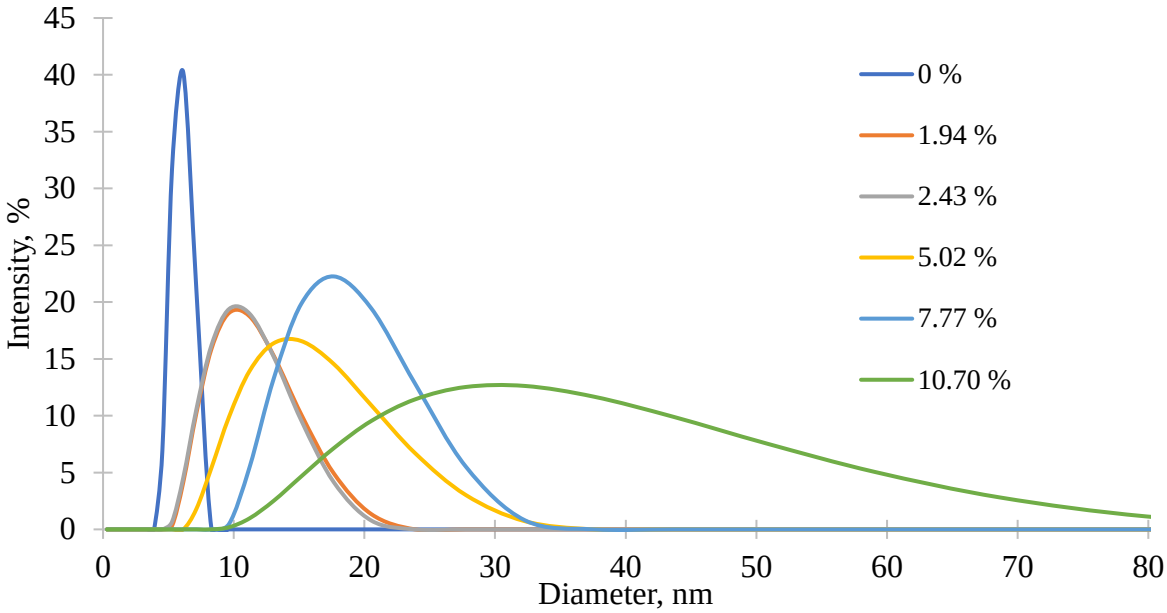

Figure 29. Micelle diameter of 1 w/v% solution of Triton X-100 with added **1**, with the percentage of C4P against Triton.

Adding **2** to Triton X-100 did not affect the size of the micelles of Triton (Figure 30). The sizes of the micelles seem to stay consistent in diameter. The size distribution of the micelles is discreet and composed of size bins. When the sizes of the micelles are similar to each other they land in the same size bin which causes the diameters of the micelles to be measured as 9.655 nm in diameter.

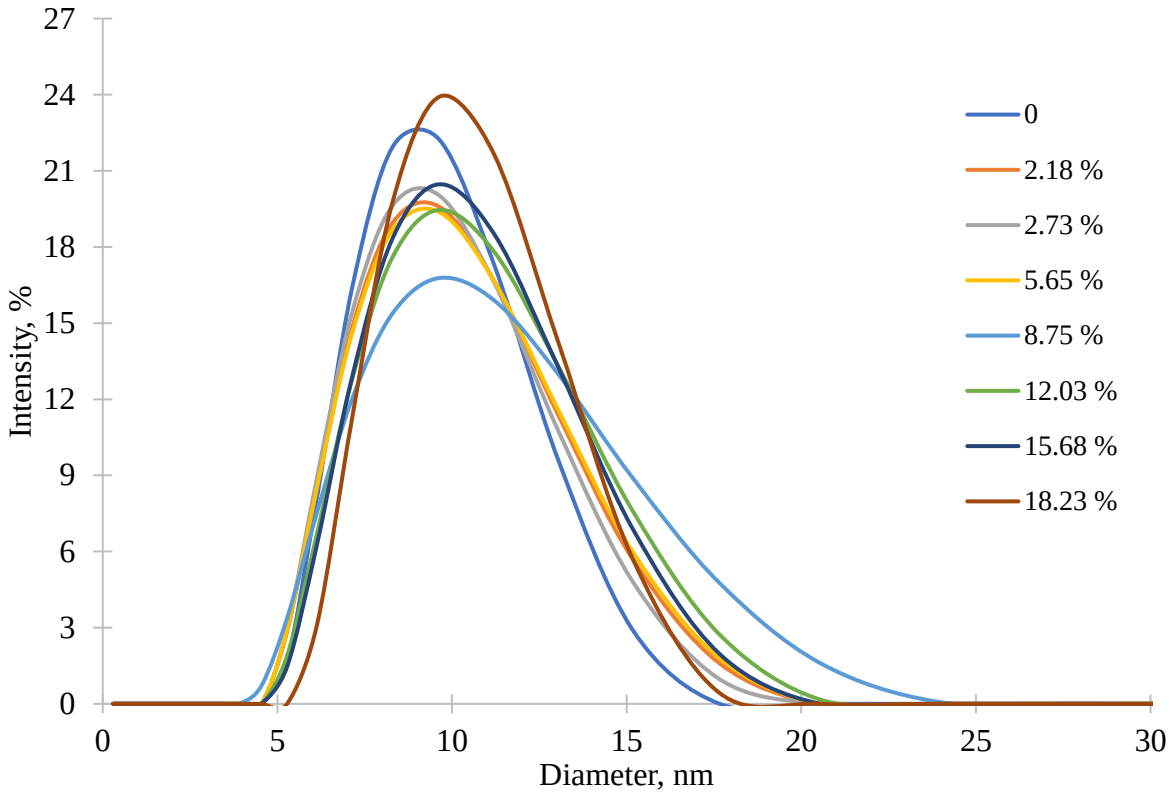

Figure 30. Micelle diameter of 1 w/v% solution of Triton X-100 with added **2**, with the percentage of C4P against Triton.

Adding **1** to Triton X-114 did not cause as significant change in the size of the micelles as in Triton X-100 (Figure 31). However, some bigger particles with diameter of 50-100 nm start to form with rising C4P concentration.

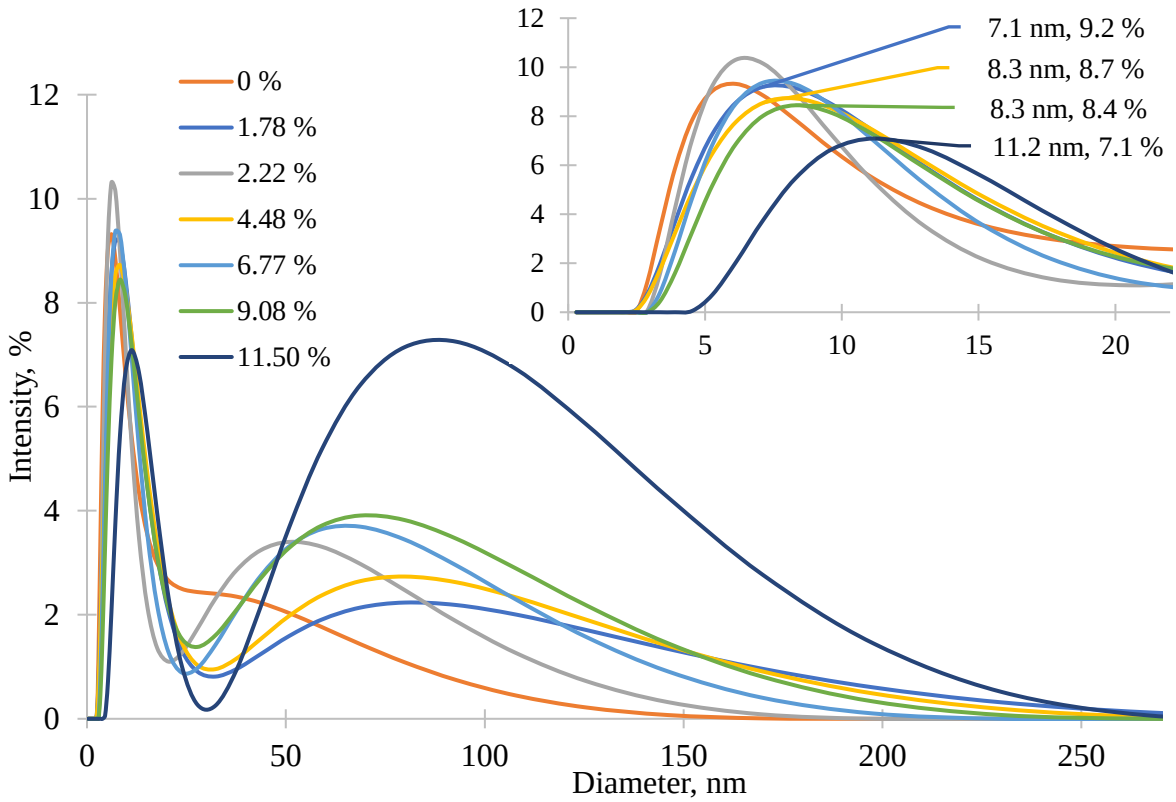

Figure 31. Micelle diameter of 1 w/v% solution of Triton X-114 with added **1**, with the percentage of C4P against Triton.

Like with **1**, adding **2** to Triton X-114 caused the formation of large particles (Figure 32). The size of micelles also quickly got bigger with rising percentage of **2** in the solution.

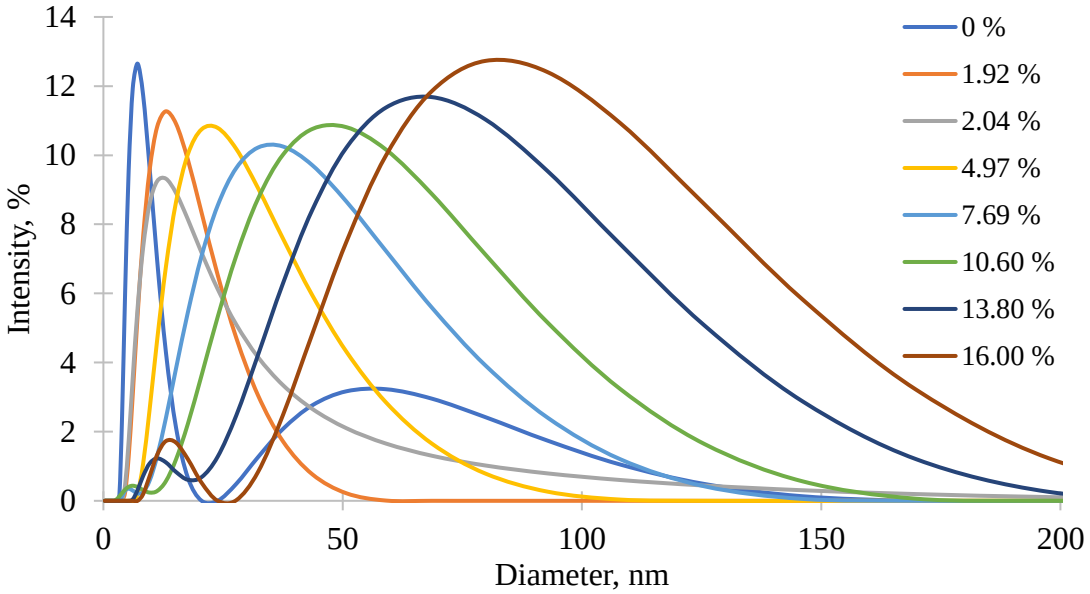

Figure 32. Micelle diameter of 1 w/v% solution of Triton X-114 with added **2**, with the percentage of C4P against Triton.

The DLS measurements of **3** revealed that it does form some sort of particles (Figure 33). The size, around 30 nm, does not strongly depend on the molarity of the solution at the 0.1-1 mM range. There are also some bigger particles, with diameters around in the hundreds of nanometers. These could be agglomerates of micelles, the size of which get larger with rising molarity.

The PDI for solutions of **3** (**Error! Reference source not found.**) are larger (> 0.5) than for any of the other solutions (< 0.2) (**Error! Reference source not found.**). This indicates that the solutions are polydisperse, which is also predictable from the diameters. There are quite small and also very big particles in the solutions.

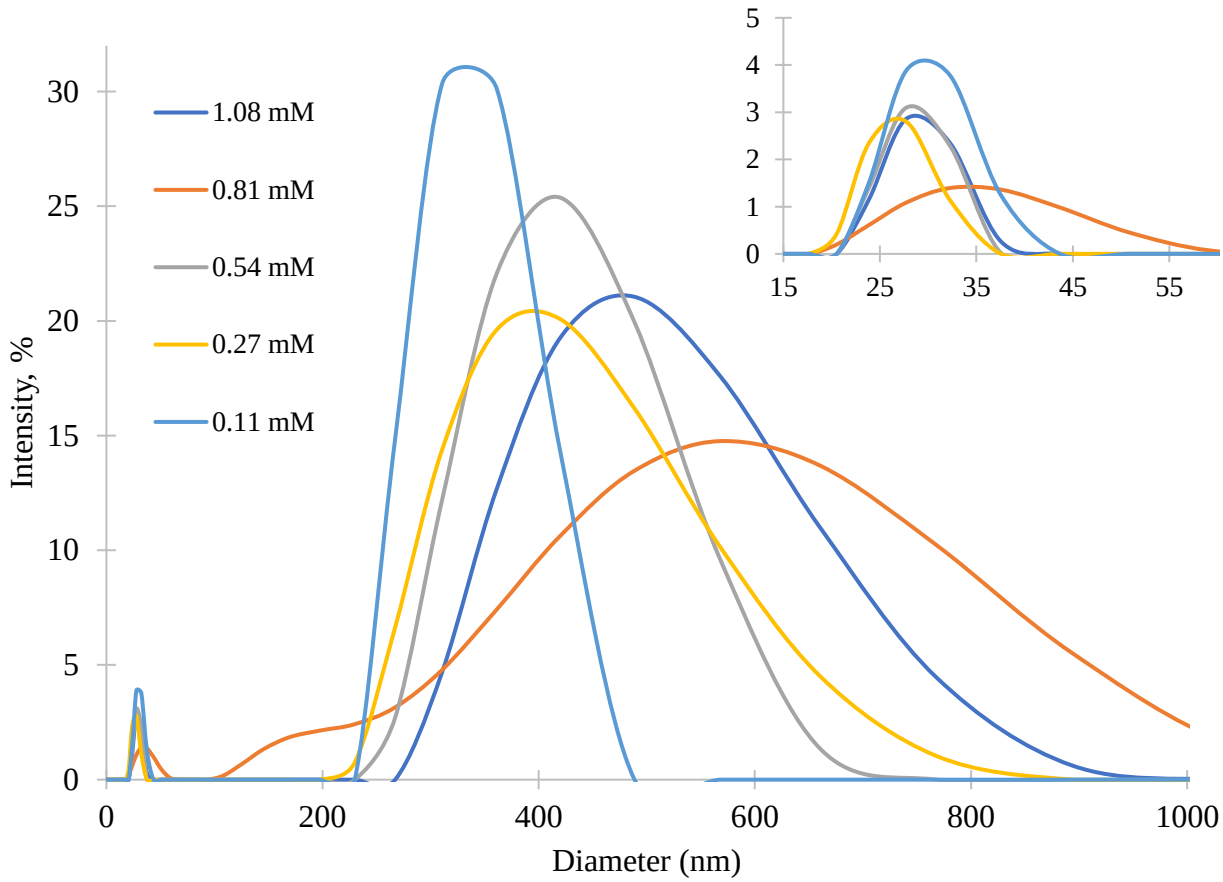

Figure 33. Micelle diameter of solutions of **3** with different molarities.

The particle concentrations of the different sized particles in the solutions were measured (**Error! Reference source not found.** and **Error! Reference source not found.**). The sizes of the micelles and bigger particles are roughly the same as in the intensity measurements of the particles.

7 Atomic force microscopy

The sample of Triton X-100 with 2.43 % of **1** against Triton was chosen for the studies with AFM due to it having a suitable number of particles per milliliter. Two substrates were chosen in order to compare the adhesion of the particles on the plates.

In Figure 34 and Figure 35 the AFM images of **1** and Triton X-100 (on mica and silica, respectively) at 5 nm resolution can be seen. These samples underwent rinsing with water. The particles seen on the images seem irregular in shape and large (~ 70-130 nm) in diameter. Since the diameters are so big, the particles are most probably some sort of aggregates of the micelles. They are also quite short vertically, which means that they got flattened during the deposition onto the mica or silica.

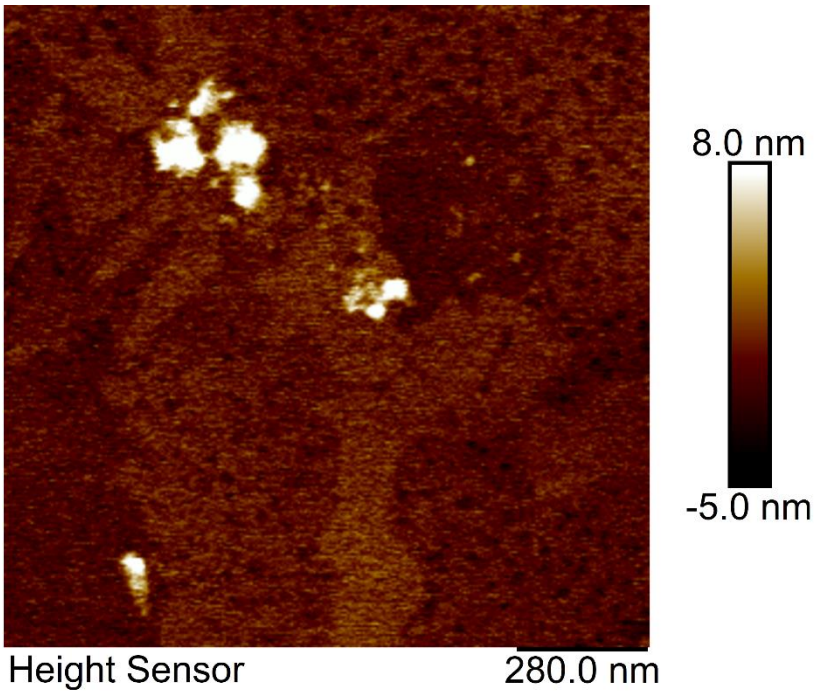

Figure 34. AFM image of Triton and C4P **1** micelles at 5 nm resolution on mica.

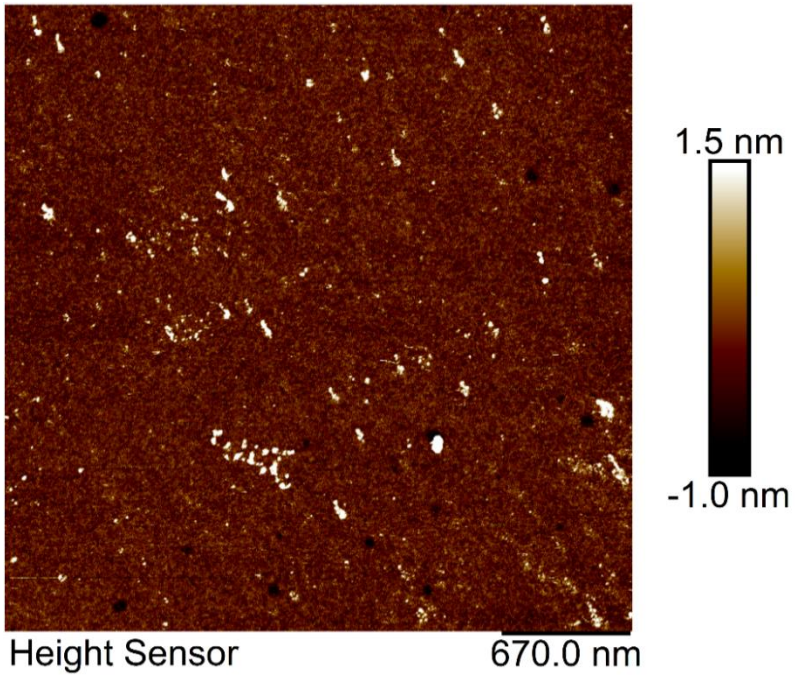

Figure 35. AFM image of Triton and C4P **1** micelles at 5 nm resolution on silica.

More images of **1** and Triton X-100 on mica were taken (Figure 36). The plate was not rinsed with water after deposition. In the images the aggregates at about 60 nm in diameter can be seen. They seem spherical in shape.

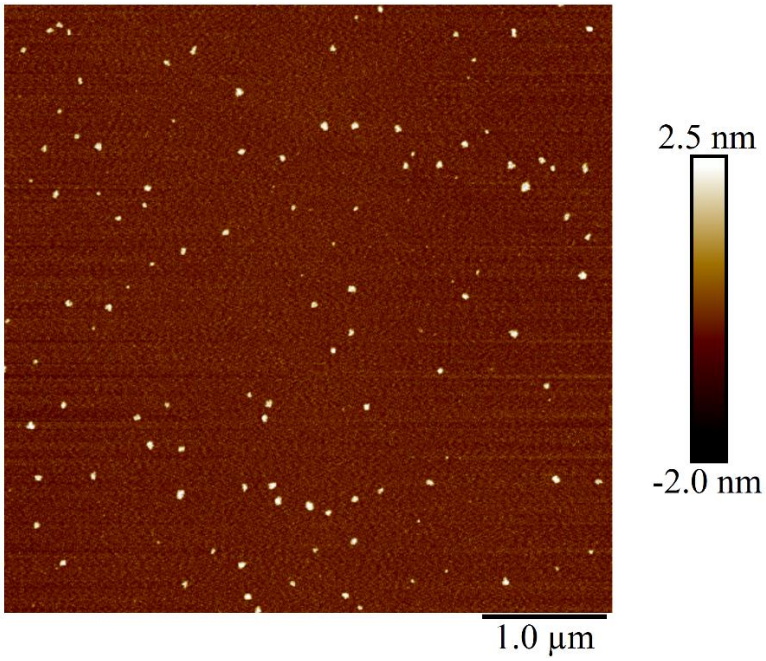

Figure 36. AFM image of Triton X-100 with **1** at resolution 10 nm on mica.

8 Conclusions

8.1 Syntheses

The synthesis and purification of **1** initially suffered from low yields. The recrystallization was extremely sensitive to the amount of either acetic acid or ethanol/water solvent mixture. The yields of the reactions improved when greater care was taken so that not too much solvent was added. In addition to that, the yield improved due to washing the residue from recrystallization in ethanol/water with a smaller amount of the solvent. In the last synthesis, the yield of 11 % of pure *αααα*-isomer was very good.

The tosylation of mPEG4-OH was successful with a yield and purity that it was sufficient for use in following reactions. The reaction was easy to perform, but the yield of 56 % was a lot lower than what is recorded in literature.[65] Based on ^{1}H NMR, the product also contains some amount of free *p*-toluenesulphonyl chloride. However, for this specific use the purity is sufficient, and the lack of complex purification results the synthesis in being very viable to quickly tosylate PEGs for similar uses.

A problem with synthesis of **2** was that the tosyl-group remained in the product after purification with a manual column in the first synthesis. The use of flash chromatography was successful in removing the excess tosyl from the product in the purification steps of the second synthesis and was also much faster. In further syntheses flash should be used, when possible, instead of a manual column.

Another problem with syntheses of both **2** and **3** was that not all the phenol groups were functionalized. This is seen in the ^{1}H spectrum of **2**, where the number of hydrogen atoms match the three-armed C4P. MS spectrum of **2** also shows a prominent peak at *m/z* 1119, which corresponds to **1** that has been functionalized with two arms. The MS spectrum shows that there is only a small contribution of fully PEGylated C4P. The incomplete functionalization is also seen in the NH and aromatic proton peaks of the ^{1}H NMR spectrum of both **2** and **3**. They are split into complex patterns, which indicate that some of the phenols have undergone the reaction, and some have not. If there was full PEGylation, there would also be no OH peaks. The reaction is quite tricky, since the four tosylated-PEGs must react with four individual sites of the C4P. The reaction time may be too short, which means that not all of the phenols have time to react. The base also might not be strong enough to deprotonate the OH of the C4P.

The success of PEGylation of four-walled C4P with mPEG2-Ts was indeterminate, due to the product being insoluble in most solvents. The residue was soluble in DMSO, but it was not possible to continue to purification using DMSO. The product contained some amount of dimethyl formamide, which could cause the solid to be insoluble. The NH peaks of the C4P were also not visible, which was unexpected. The decision to not continue with the purification in some other manner was due to time running out.

The ether synthesis between mPEG2-Ts and two-armed C4P was not successful in either dimethyl formamide or acetonitrile. The hydroxyl group of the aliphatic chain on the two-armed C4P does not deprotonate as easily as the aromatic hydroxyl group of the four-walled C4P. This could be solved with the use of a stronger base. Such PEGylations to aliphatic hydroxy groups have been done with sodium hydride.[67]

8.2 Cloud point and micelle studies

Addition of **1** and **2** in methanol to aqueous solutions of Triton X-100 and 114 had an effect on the cloud point of the solutions. The cloud point temperature generally got lower when the percentage of C4P in the solution was raised.
Use of block heater in cloud point observing was a very efficient way. All the vials were inserted at the same time and experienced the same temperature changes. Observing cloud point is subjective. Some samples (like Triton X-100 with 13.9 % of **1**) were almost indeterminate as they were so close to cloud point at room temperature. For that reason, the error in the observations is approximated at 1 °C. A machine that would detect the change in light transmission would be a more reliable and repeatable method to record cloud point.
While **1** affected the cloud point and micelle size of Triton X-100 solution, **2** did not have a significant effect. Adding **1** to Triton X-114 did not have a big impact on the size of the micelles but did cause the agglomerates of the micelles to become bigger. **2** had a complex effect on Triton X-114. What all these effects are due to, cannot be determined using these methods. The C4Ps probably were included in the micelles either in the micelle core or its surface.

The blanks (0 % of **1** or **2** added to the Triton X-100 or X-114) used in the DLS measurements did not match. The size distributions are different, and the peaks are at different points. For example, 0 % **1** added to Triton X-114 has only one peak at 6.1 nm while 0 % of **2** added to Triton X-114 has two peaks at different diameters. These samples should be identical,

containing only the Triton, the solvents and CTAB. This means that there is some uncertainty to the DLS measurements.

3 was seen to form some sort of particles in the solution, the size of which do not seem to be affected by the concentration of the solution (at this range of molarities). Some bigger agglomerates of the micelles were also seen, and the size of them rose with the rising molarity of the solution.

The particle counts of the different sized micelles in the solutions were also measured (seen in **Error! Reference source not found.** and **Error! Reference source not found.**). In general, for all samples (Triton-containing or not) there were many orders of magnitude more of the individual micelles, than there were of the bigger particles. The blanks in these measurements also seemed to correspond to each other better than in the size measurements.

While the measurements of the diameters of the micelles per intensity and per particle concentration did land in the same ballpark, the micelle hydrodynamic diameters were ultimately different in the two measurements. This discrepancy in the sizes can be explained by the technique differences in the measurements. The machine uses backscattering detection to measure the size of the micelles, while in the particle concentration a changing angle of detection is used.

While the water used in the sample preparation was purified, the methanol was not. It contained water and probably other impurities which may have affected the samples. Further purification of the solvent system could give better samples. Overall, the inclusion of methanol in the Triton-co-micellization studies was problematic, since a third (or in the case of Triton X-114 and CTAB, fourth) variable was brought into the samples alongside Triton and C4P. A fully water-soluble C4P could be a better candidate for these studies. Obtaining **3** as a pure compound, fully PEGylated, would be a good step into that direction. Obtaining a water-soluble batch of **3** would also make the DLS measurements more reproducible and reliable. The sample was filtered which removed some of the analyte, so there is uncertainty in the reported concentrations.

The refractive indices used in the DLS measurements were approximations. Especially for measurements on solutions of **3** more reliable measurements could be obtained if the index of the C4P was measured. Unfortunately, there was not enough product to perform the

measurement. In order to continue with studies with DLS, more of the product should be synthesized to obtain the refractive index for accurate measurements.

Unfortunately, in the AFM studies of **1** and Triton X-100 individual micelles were not seen. Much longer measurements with a higher resolution and magnification would be needed for that. Thus, no information on the shape of individual micelles was obtained.

9 References

1. Zaretsky, S. and Yudin, A. K., Contemporary Macrocyclization Technologies. In: Marsault, E. and Peterson, M. L. (eds.), *Practical Medicinal Chemistry with Macrocycles: Design, Synthesis, and Case Studies*, 1st edition, John Wiley & Sons, Inc., 2017, pp. 3–4.
2. Talotta, C.; Gaeta, C.; Rosa, M. De; Soriente, A.; Neri, P. and Salerno, U., Calixarenes. In: *Comprehensive Supramolecular Chemistry II*, 2017, vol. 3, pp. 49–53.
3. Wishard, A. and Gibb, B. C., A Chronology of Cavitands. In: Neri, P.; Sessler, J. L. and Wang, M.-X. (eds.), *Calixarenes and Beyond*, 1st edition, Springer, 2016.
4. Gale, P. A.; Sessler, J. L. and Král, V., Calixpyrroles, *Chemical Communications*, **1998**, 1–8.
5. Steed, J. W. and Atwood, J. L., *Supramolecular Chemistry*, 2nd edition, Wiley, 2009. a: p. 197-206; b: p. 311-312; c: 2-28.
6. Mustafina, A.; Elistratova, J.; Burilov, A.; Knyazeva, I.; Zairov, R.; Amirov, R.; Solovieva, S. and Konovalov, A., Cloud point extraction of lanthanide(III) ions via use of Triton X-100 without and with water-soluble calixarenes as added chelating agents, *Talanta*, **2006**, *68*, 863–868.
7. Cafeo, G.; Carbotti, G.; Cuzzola, A.; Fabbi, M.; Ferrini, S.; Kohnke, F. H.; Papanikolaou, G.; Plutino, M. R.; Rosano, C. and White, A. J. P., Drug Delivery with a Calixpyrrole– *trans* -Pt(II) Complex, *J Am Chem Soc*, **2013**, *135*, 2544–2551.
8. Sokkalingam, P.; Kim, D. S.; Hwang, H.; Sessler, J. L. and Lee, C. H., A dicationic calix[4]pyrrole derivative and its use for the selective recognition and displacement-based sensing of pyrophosphate, *Chem Sci*, **2012**, *3*, 1819–1824.
9. Reinhoundt, D. N., Introduction and History. In: Neri, P.; Sessler, J. L. and Wang, M.-X. (eds.), *Calixarenes and Beyond*, 1st edition, Springer, 2016, pp. 6–8.

10. Fischer, C.; Seichter, W. and Weber, E., Structural conditions required for the bridge lithiation and substitution of a basic calix[4]arene, *Beilstein Journal of Organic Chemistry*, **2011**, *7*, 1602–1608.
11. Dvořáková, H.; Štursa, J.; Čajan, M. and Moravcová, J., Synthesis and conformational properties of partially alkylated methylene-bridged resorc[4]arenes - Study of the 'flip-flop' inversion, *European J Org Chem*, **2006**, 4519–4527.
12. Gale, P. A.; Anzenbacher, P. and Sessler, J. L., Calixpyrroles II, *Coord Chem Rev*, **2001**, 222, 57–102.
13. Gutsche, C. D. and Iqbal, M., p-tert-BUTYLCALIX[4]ARENE, *Organic Syntheses*, **1993**, *8*, 75.
14. Stewart, D. R. and Gutsche, C. D., The one-step synthesis of p-tert-butylcalix[5]arene, *Org Prep Proced Int*, **1993**, *25*, 137–139.
15. Gutsche, C. D.; Dhawan, B.; Leonis, M. and Stewart, D., p-tert-BUTYLCALIX[6]ARENE, *Organic Syntheses*, **1990**, *68*, 238.
16. Ferchichi, M.; Jeanneau, E.; Sollier, J.-C.; Meganem, F.; Darbost, U. and Bonnamour, I., The first inexpensive, simplified and large scale synthesis of p-tert-butylcalix[7] and [9]arenes, *Chem*, **2011**, *1*, 27–35.
17. Munch, J. H. and Gutsche, C. D., p-tert-BUTYLCALIX[8]ARENE, *Organic Syntheses*, **1990**, *68*, 243.
18. Gutsche, C. D. and Levine, J. A., Calixarenes. 6. Synthesis of a Funtionalizable Calix[4]arene in a Conformationally Rigid Cone Conformation, *J Am Chem Soc*, **1982**, *104*, 2652–2653.
19. Balasubramanian, R.; Kwon, Y. G. and Wei, A., Encapsulation and functionalization of nanoparticles in crosslinked resorcinarene shells, *J Mater Chem*, **2007**, *17*, 105–112.
20. Jain, V. K. and Mandalia, H. C., Azocalix[4]pyrroles: One-pot microwave and one drop water assisted synthesis, spectroscopic characterization and preliminary investigation of its complexation with copper (II), *J Incl Phenom Macrocycl Chem*, **2009**, *63*, 27–35.
21. Custelcean, R.; Delmau, L. H.; Moyer, B. A.; Sessler, J. L.; Cho, W. S.; Gross, D.; Bates, G. W.; Brooks, S. J.; Light, M. E. and Gale, P. A., Calix[4]pyrrole: An old yet new ion-pair receptor, *Angewandte Chemie - International Edition*, **2005**, *44*, 2537–2542.
22. Bott, S. G.; Coleman, A. W. and Atwood, J. L., Inclusion of both cation and neutral molecule by a calixarene. Structure of the [p-tert-butylmethoxycalix[4]arene-sodium-toluene]cation, *Journal of American Chemical Society*, **1986**, *108*, 1709–1710.

23. Davydova, E. I.; Sevastianova, T. N.; Timoshkin, A. Y.; Suvorov, A. V. and Frenking, G., Chelate effect: The importance of reorganization energy, *Int J Quantum Chem*, 2004, pp. 419–425.
24. Cram, D. J., Preorganization - From solvents to spherands, *Angewandte Chemie*, **1986**, *25*, 1039–1040.
25. Smithrud, D. B.; Sanford, E. M.; Chao, I.; Ferguson, S. B.; Carcanague, D. R.; Evanseck, J. D.; Houk, K. N. and Diederich, F., Solvent effects in molecular recognition, 62, 1990.
26. Sessler, J. L.; Gross, D. E.; Cho, W. S.; Lynch, V. M.; Schmidtchen, F. P.; Bates, G. W.; Light, M. E. and Gale, P. A., Calix[4]pyrrole as a chloride anion receptor: Solvent and countercation effects, *J Am Chem Soc*, **2006**, *128*, 12281–12288.
27. Peñuelas-Haro, G. and Ballester, P., Efficient hydrogen bonding recognition in water using aryl-extended calix[4]pyrrole receptors, *Chem Sci*, **2019**, *10*, 2413–2423.
28. Arduini, A.; Pochini, A.; Reverberi, S. and Ungaro, R., p-t-Butyl-calix[4]arene tetracarboxylic acid. A water soluble calixarene in a cone structure, *J Chem Soc Chem Commun*, **1984**, 981–982.
29. Arnaud-Neu, F.; Barrett, G.; Cremin, S.; Deasy, M.; Ferguson, G.; Harris, S. J.; Lough, A. J.; Guerra, L.; McKervey, M. A.; Schwing-Weill, M. J. and Schwinte, P., Selective alkali-metal cation complexation by chemically modified calixarenes. Part 4. Effect of substituent variation on the Na+/K+ selectivity in the ester series and X-ray crystal structure of the trifluoroethyl ester, *Journal of the Chemical Society, Perkin Transactions 2*, **1992**, 1119–1125.
30. Morozova, J. E.; Syakaev, V. V.; Shalaeva, Y. V.; Ermakova, A. M.; Nizameev, I. R.; Kadirov, M. K.; Voloshina, A. D.; Zobov, V. V.; Antipin, I. S. and Konovalov, A. I., Unusual nanosized associates of carboxy-calix[4]resorcinarene and cetylpyridinium chloride: the macrocycle as a glue for surfactant micelles, *Soft Matter*, **2017**, *13*, 2004–2013.
31. Perret, F.; Lazar, A. N. and Coleman, A. W., Biochemistry of the para-sulfonato-calix[n]arenes, *Chemical Communications*, **2006**, 2425–2438.
32. Dalgarno, S. J.; Atwood, J. L. and Raston, C. L., Sulfonatocalixarenes: Molecular capsule and 'Russian doll' arrays to structures mimicking viral geometry, *Chemical Communications*, **2006**, 4567–4574.
33. Lehn, J. M.; Meric, R.; Vigneron, J. P.; Cesario, C. M.; Guilhem, J.; Pascard, C.; Asfari, Z. and Vicens, J., Binding of acetylcholine and other quaternary ammonium cations by sulfonated calixarenes. Crystal structure of a [choline-tetrasulfonated calix[4]arene] complex, *Supramol Chem*, **1995**, *5*, 97–103.

34. Da Silva, E.; Shahgaldian, P. and Coleman, A. W., Haemolytic properties of some water-soluble para-sulphonato-calix[n]arenes, *Int J Pharm*, **2004**, *273*, 57–62.
35. Da Silva, E. and Coleman, A. W., Synthesis and complexation properties towards amino acids of mono-substituted p-sulphonato-calix-[n]-arenes, *Tetrahedron*, **2003**, *59*, 7357–7364.
36. Zhao, H. X.; Guo, D. S.; Wang, L. H.; Qian, H. and Liu, Y., A novel supramolecular ternary polymer with two orthogonal host–guest interactions, *Chemical Communications*, **2012**, *48*, 11319–11321.
37. Guo, D. S.; Chen, K.; Zhang, H. Q. and Liu, Y., Nano-supramolecular assemblies constructed from water-soluble bis(calix[5]arenes) with porphyrins and their photoinduced electron transfer properties, *Chem Asian J*, **2009**, *4*, 436–445.
38. Pham, N. H. and Wenzel, T. J., A water-soluble calix 4 resorcinarene with L-pipecolinic acid groups as a chiral NMR solvating, *Chirality*, **2012**, *24*, 193–200.
39. Wenzel, T. J., *Differentiation of Chiral Compounds Using NMR Spectroscopy*, 1st edition, John Wiley & Sons, Incorporated, 2018.
40. Kazakova, E. K.; Makarova, N. A.; Ziganshina, A. U.; Muslinkina, L. A.; Muslinkin, A. A. and Habicher, W. D., Novel water-soluble tetrasulfonatomethylcalix[4]resorcinarenes, 41, 2000.
41. Arya, S. S.; Kaimal, A. M.; Chib, M.; Sonawane, S. K. and Show, P. L., Novel, energy efficient and green cloud point extraction: technology and applications in food processing, *J Food Sci Technol*, **2019**, 56, 524–534.
42. Sanabria, E.; Esteso, M. A. and Vargas, E. F., Recognition of heavy metals by using resorcin[4]arenes soluble in water, *Toxics*, **2022**, *10*.
43. Hong, M.; Zhang, Y. M. and Liu, Y., Selective binding affinity between quaternary ammonium cations and water-soluble calix[4]resorcinarene, *Journal of Organic Chemistry*, **2015**, *80*, 1849–1855.
44. Naqvi, A. Z. and Kabir-ud-Din, Clouding phenomenon in amphiphilic systems: A review of five decades, *Colloids Surf B Biointerfaces*, **2018**, *165*, 325–344.
45. Clark, T. E.; Makha, M.; Sobolev, A. N.; Rohrs, H.; Atwood, J. L. and Raston, C. L., Engineering nanorafts of calixarene polyphosphonates, *Chemistry - A European Journal*, **2008**, *14*, 3931–3938.
46. Martin, A. D. and Raston, C. L., Multifunctional p-phosphonated calixarenes, *Chemical Communications*, **2011**, *47*, 9764–9772.
47. Collin, S.; Giraud, N.; Dumont, E. and Reinaud, O., A biomimetic strategy for the selective recognition of organophosphates in 100% water: Synergies of electrostatic

interactions, cavity embedment and metal coordination, *Organic Chemistry Frontiers*, **2019**, *6*, 1627–1636.

48. An, L.; Wang, J. W.; Liu, J. D.; Zhao, Z. M. and Song, Y. J., Design, preparation, and characterization of novel calix[4]arene bioactive carrier for ntitumor drug delivery, *Front Chem*, **2019**, *7*.
49. Hilgenbrink, A. R. and Low, P. S., Folate receptor-mediated drug targeting: From therapeutics to diagnostics, *J Pharm Sci*, **2005**, 94, 2135–2146.
50. Hernández-Alonso, D.; Zankowski, S.; Adriaenssens, L. and Ballester, P., Water-soluble aryl-extended calix[4]pyrroles with unperturbed aromatic cavities: synthesis and binding studies, *Org Biomol Chem*, **2015**, *13*, 1022–1029.
51. Díaz-Moscoso, A.; Hernández-Alonso, D.; Escobar, L.; Arroyave, F. A. and Ballester, P., Stereoselective synthesis of lower and upper rim functionalized tetra-α isomers of calix[4]pyrroles, *Org Lett*, **2017**, *19*, 226–229.
52. Escobar, L.; Díaz-Moscoso, A. and Ballester, P., Conformational selectivity and high-affinity binding in the complexation of N-phenyl amides in water by a phenyl extended calix[4]pyrrole, *Chem Sci*, **2018**, *9*, 7186–7192.
53. Verdejo, B.; Gil-Ramírez, G. and Ballester, P., Molecular recognition of pyridine N-oxides in water using calix[4]pyrrole receptors, *J Am Chem Soc*, **2009**, *131*, 3178–3179.
54. Chi, X.; Zhang, H.; Vargas-Zúniga, G. I.; Peters, G. M. and Sessler, J. L., A dual-responsive bola-type supra-amphiphile constructed from a water-soluble calix[4]pyrrole and a tetraphenylethene-containing pyridine bis-N-oxide, *J Am Chem Soc*, **2016**, *138*, 5829–5832.
55. Escobar, L. and Ballester, P., Quantification of the hydrophobic effect using water-soluble super aryl-extended calix[4]pyrroles, *Organic Chemistry Frontiers*, **2019**, *6*, 1738–1748.
56. Sun, Q.; Escobar, L.; de Jong, J. and Ballester, P., Self-assembly of a water-soluble endohedrally functionalized coordination cage including polar guests, *Chem Sci*, **2021**, *12*, 13469–13476.
57. Escobar, L.; Aragay, G. and Ballester, P., Super Aryl-Extended Calix[4]pyrroles: Synthesis, Binding Studies, and Attempts To Gain Water Solubility, *Chemistry - A European Journal*, **2016**, *22*, 13682–13689.
58. Koshy, L.; Saiyad, A. H. and Rakshit, A. K., The effects of various foreign substances on the cloud point of Triton X 100 and Triton X 114, 274, Steinkopff Verlag, 1996.
59. Stubiear, N. and Petres, J. J., Micelle Formation by Tritons in Aqueous Solutions, *Croatica Chemica Acta* , **1981**, *54*, 255–266.

60. Stetefeld, J.; McKenna, S. A. and Patel, T. R., Dynamic light scattering: a practical guide and applications in biomedical sciences, *Biophys Rev*, **2016**, 8, 409–427.
61. Zetasizer advance series, User guide, **2022**.
62. Dharaiya, N.; Aswal, V. K. and Bahadur, P., Characterization of Triton X-100 and its oligomer (Tyloxapol) micelles vis-à-vis solubilization of bisphenol A by spectral and scattering techniques, *Colloids Surf A Physicochem Eng Asp*, **2015**, *470*, 230–239.
63. Anzenbacher, P.; Jursíková, K.; Lynch, V. M.; Gale, P. A. and Sessler, J. L., Calix[4]pyrroles containing deep cavities and fixed walls. Synthesis, structural studies, and anion binding properties of the isomeric products derived from the condensation of p-hydroxyacetophenone and pyrrole [10], *J Am Chem Soc*, **1999**, *121*, 11020–11021.
64. Clayden, J.; Greeves, N.; Warren, S. and Wothers, P., *Organic chemistry*, Oxford University Press, 2001.
65. Ding, Z.; Li, H.; Gao, W.; Zhang, Y.; Liu, C. and Zhu, Y., Detection of Picric Acid by Terpy-Based Metallo-Supramolecular Fluorescent Coordination Polymers in Aqueous Media, *Chin J Chem*, **2017**, *35*, 447–456.
66. Mahajan, R. K.; Vohra, K. K.; Kaur, N. and Aswal, V. K., Organic additives and electrolytes as cloud point modifiers in octylphenol ethoxylate solutions, *J Surfactants Deterg*, **2008**, *11*, 243–250.
67. Wu, X.; Boz, E.; Sirkis, A. M.; Chang, A. Y. and Williams, T. J., Synthesis and phosphonate binding of guanidine-functionalized fluorinated amphiphiles, *J Fluor Chem*, **2012**, *135*, 292–302.

10 Appendices

APPENDIX 1. Detergent solution preparations and cloud point observations of all samples.

APPENDIX 2. 1H NMR spectrum of mPEG2-ylation of 1.

APPENDIX 3. ESI-MS + spectrum of attempted mPEG2-ylation of 7.

APPENDIX 4. 1H NMR spectrum of attempted mPEG2-ylation of 7.

APPENDIX 5. Micelle sizes and PDIs of DLS measurements of Triton-containing samples.

APPENDIX 6. Micelle sizes and PDIs of DLS measurements of 3.

APPENDIX 7. Particle counts of Triton samples.

APPENDIX 8. Particle concentrations of 3.

Series	Volume of C4P stock / µl	Percentage of C4P / %	Cloud point / °C
Triton X-100 with **1**	0	0	76
	12	1.9	70
	15	2.4	69
	31	5.0	58
	48	7.8	49
	66	10.7	40
	86	13.9	28
	100	16	room temperature
Triton X-100 with **2**	0	0	76
	12	2.2	75
	15	2.7	75
	31	5.7	70
	48	8.8	68
	66	12.0	65
	86	15.7	62
	100	18	61
Triton X-114 with **1**	0	0	69
	12	1.8	64
	15	2.2	63
	31	4.5	53
	48	6.8	45
	66	9.1	26
	86	11.5	31
	100	13.1	room temperature
Triton X-114 with **2**	0	0	69
	12	1.9	63
	15	2.4	62
	31	5.0	51
	48	7.7	44
	66	10.6	32
	86	13.8	28
	100	16.0	27

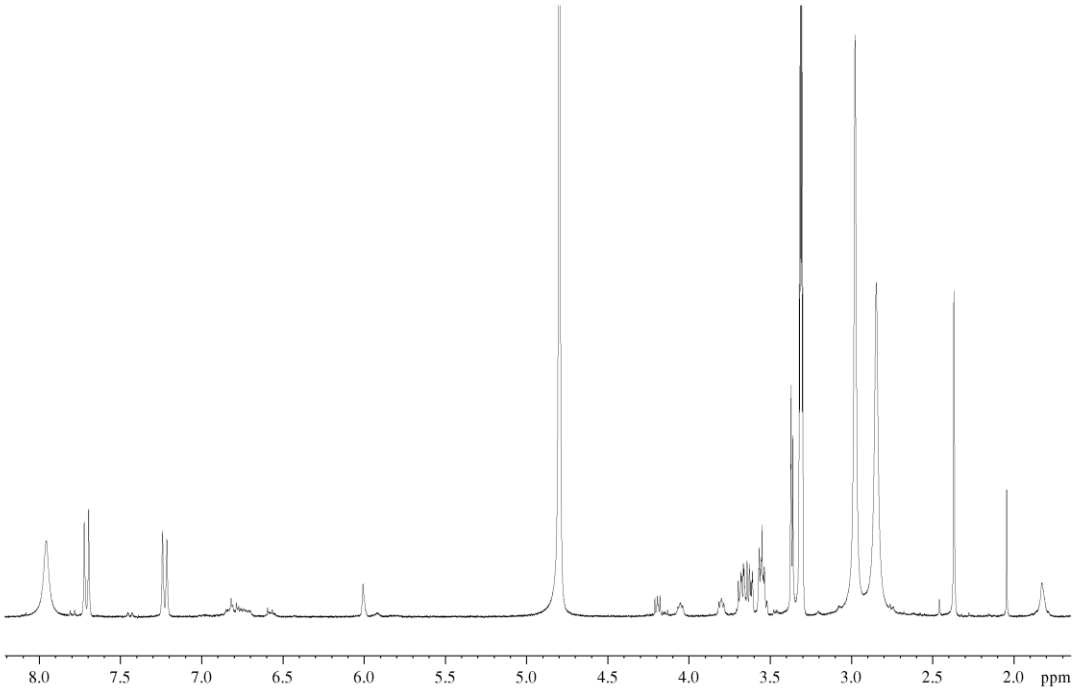
8.0
7.5
7.0
6.5
6.0
5.5
5.0
4.5
4.0
3.5
3.0
2.5
2.0
ppm

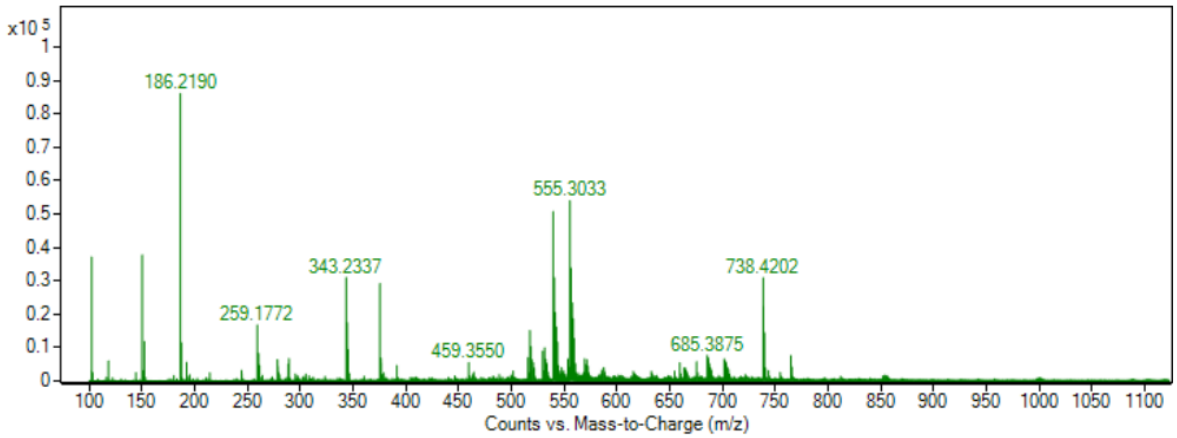
x10 5
1
0.9
0.8
0.7
0.6
0.5
0.4
0.3
0.2
0.1
0
186.2190
555.3033
343.2337
738.4202
259.1772
459.3550
685.3875
100 150 200 250 300 350 400 450 500 550 600 650 700 750 800 850 900 950 1000 1050 1100
Counts vs. Mass-to-Charge (m/z)

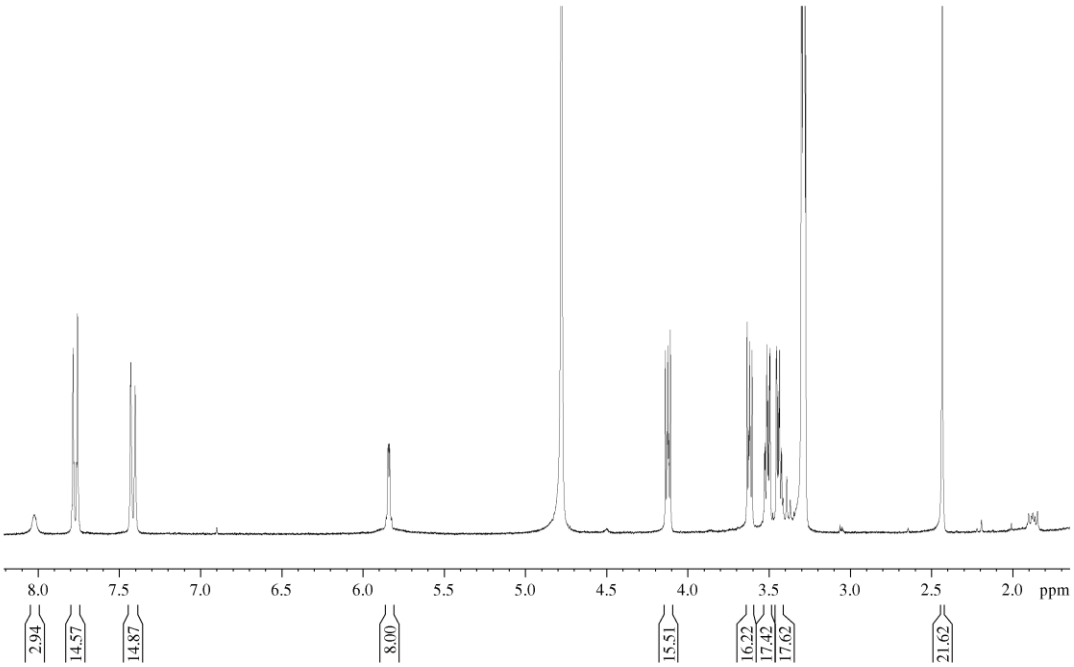
8.0
7.5
7.0
6.5
6.0
5.5
5.0
4.5
4.0
3.5
3.0
2.5
2.0
ppm
2.94
14.57
14.87
8.00
15.51
16.22
17.42
17.62
21.62

Series	Percentage of C4P / %	Size of micelle / nm		PDI
Triton X-100 with **1**	0	6.1		0.385
	1.9	9.7		0.0977
	2.4	9.7		0.130
	5.0	15.2		0.0980
	7.8	17.7		0.213
	10.7	32.3		0.158
Triton X-100 with **2**	0	9.7		0.0340
	2.2	9.7		0.878
	2.7	9.7		0.0574
	5.7	9.7		0.132
	8.8	9.7		0.0923
	12.0	9.7		0.138
	15.7	9.7		0.213
	18	9.7		0.176
Triton X-114 with **1**	0	6.1		0.330
	1.8	7.1	79.9	0.363
	2.2	6.1	50.8	0.368
	4.5	8.3	70.9	0.132
	6.8	7.1	68.7	0.383
	9.1	8.3	79.9	0.427
	11.5	11.2	92.9	0.518
Triton X-114 with **2**	0	7.1	59.1	0.279
	1.9	13.1		0.235
	2.4	13.1		0.250
	5.0	23.9		0.238
	7.7	5.3	37.6	0.230
	10.6	6.1	50.8	0.242
	13.8	11.2	68.7	0.267
	16.0	13.1	79.9	0.280

Molarity / mM	Size / nm		PDI
1.078	27.8	488.7	0.542
0.809	32.3	568.3	0.513
0.539	27.8	420.2	0.580
0.270	27.8	420.2	0.556
0.108	27.8	310.7	0.676

Series	**Percentage of C4P / %**	**Size of micelle / nm**	**Particle count / particles ml^{-1}**
Triton X-100 with **1**	0	8.6	$1.1 \cdot 10^{16}$
	1.9	9.2	$7.2 \cdot 10^{15}$
	2.4	9.9	$6.5 \cdot 10^{15}$
	5.0	14.0	$1.9 \cdot 10^{15}$
	7.8	18.5	$4.7 \cdot 10^{14}$
	10.7	28.2	$8.2 \cdot 10^{13}$
Triton X-100 with **2**	0	8.0	$1.0 \cdot 10^{16}$
	2.2	8.6	$1.1 \cdot 10^{16}$
	2.7	8.6	$1.3 \cdot 10^{16}$
	5.7	8.6	$1.1 \cdot 10^{16}$
	8.8	9.2	$1.2 \cdot 10^{16}$
	12.0	9.2	$8.6 \cdot 10^{15}$
		495.2	$1.6 \cdot 10^{6}$
	15.7	9.9	$8.5 \cdot 10^{15}$
		461.7	$1.4 \cdot 10^{6}$
	18	9.2	$9.3 \cdot 10^{15}$
		495.2	$1.7 \cdot 10^{6}$

Triton X-114 with **1**	0	5.3	$2.4 \cdot 10^{17}$
		26.3	$1.3 \cdot 10^{13}$
	1.8	6.1	$9.8 \cdot 10^{16}$
		32.4	$3.7 \cdot 10^{12}$
	2.2	5.65	$1.4 \cdot 10^{17}$
		30.24	$5.7 \cdot 10^{12}$
	4.5	6.5	$1.0 \cdot 10^{17}$
		40.0	$2.6 \cdot 10^{12}$
	6.8	6.5	$1.4 \cdot 10^{17}$
		40.0	$3.0 \cdot 10^{12}$
	9.1	6.5	$2.3 \cdot 10^{17}$
		34.8	$9.1 \cdot 10^{12}$
		430.6	$3.3 \cdot 10^{6}$
	11.5	8.6	$7.6 \cdot 10^{16}$
		60.1	$8.3 \cdot 10^{11}$
Triton X-114 with **2**	0	5.7	$1.7 \cdot 10^{17}$
		21.3	$3.0 \cdot 10^{13}$
	1.9	8.6	$1.6 \cdot 10^{16}$
		22.9	$2.2 \cdot 10^{13}$
	2.4	6.1	$7.1 \cdot 10^{16}$
		16.1	$3.3 \cdot 10^{15}$
	5.0	7.0	$1.4 \cdot 10^{16}$
		24.5	$8.3 \cdot 10^{13}$
	7.7	8.0	$4.3 \cdot 10^{15}$
		34.8	$2.4 \cdot 10^{13}$
	10.6	49.2	$5.7 \cdot 10^{12}$
	13.8	8.6	$5.5 \cdot 10^{15}$
		65.2	$1.4 \cdot 10^{12}$
	16.0	80.5	$2.5 \cdot 10^{11}$
		229.5	$5.0 \cdot 10^{7}$

Molarity / mM	**Size / nm**	**PDI**
1.078	199.6	$1.4 \cdot 10^{7}$
	430.6	$1.6 \cdot 10^{7}$
	807.7	$1.2 \cdot 10^{8}$
0.809	264.0	$1.6 \cdot 10^{8}$
	753.1	$2.3 \cdot 10^{8}$
0.539	49.3	$1.6 \cdot 10^{10}$
	430.6	$7.7 \cdot 10^{7}$
0.270	430.6	$2.1 \cdot 10^{7}$
	753.1	$4.0 \cdot 10^{6}$
0.108	131.2	$3.2 \cdot 10^{8}$